Ubiquitin-binding domains in polyubiquitin chain synthesis

DISSERTATION
zur Erlangung des akademischen Grades

Doctor rerum naturalium
(Dr. rer. nat.)

im Fach Biologie
eingereicht an der
Lebenswissenschaftlichen Fakultät der Humboldt-Universität zu Berlin

von
Diplom-Biochemiker Lukas Pluska

Präsidentin der Humboldt-Universität zu Berlin
Prof. Dr.-Ing. Dr. Sabine Kunst

Dekan der Lebenswissenschaftlichen Fakultät
der Humboldt-Universität zu Berlin
Prof. Dr. Bernhard Grimm

Gutachter

1. Prof. Dr. Oliver Daumke
2. Prof. Dr. Andreas Herrmann
3. Prof. Dr. Thomas Sommer

Tag der mündlichen Prüfung: 8.11.2019

Table of Contents

List of Figures

Abbreviations

Ub	ubiquitin
K48 chain	polyubiquitin chain linked through lysine 48 (K48)
K63 chain	polyubiquitin chain linked through lysine 63 (K63)
K48/K63 branched chain	polyubiquitin chain with a moiety ubiquitinated at K48 and K63
$^{63}Ub_2$	K63-linked diubiquitin

other abbreviations for polyubiquitin accordingly (see section 1.3)

6xHis	hexahistidine-tag
10xHis	decahistidine-tag
aa	amino acid(s)
AMP	adenosine monophosphate
APC/C	anaphase-promoting complex/cyclosome
AT2	2,2-dithiodipyridine (or aldrithiol-2)
ATP	adenosine triphosphate
AU	absorbance units
Bis-Tris propane	1,3-Bis[tris(hydroxymethyl)methylamino]propane
β-ME	β-mercaptoethanol
bp	base pair(s)
C. elegans	Caenorhabditis elegans
CSP	chemical shift perturbation
ddH_2O	Milli-Q water
DNA	deoxyribonucleic acid
dNTP	deoxynucleotide triphosphates
dsRNA	double-strand ribonucleic acid
DTT	dithiothreitol
DUB	deubiquitinating enzyme
E1 enzyme	E1 ubiquitin-activating enzyme
E2 enzyme	E2 ubiquitin-conjugating enzyme
E3 enzyme	E3 ubiquitin ligase
E. coli	Escherichia coli
EDT	ethane-dithiol
EDTA	ethylenediaminetetraacetic acid
ERAD	endoplasmic reticulum associated protein degradation
FMP Berlin	Leibniz-Forschungsinstitut für Molekulare Pharmakologie im Forschungsverbund Berlin e.V.
GSH	glutathione (reduced)
GST	glutathione S-transferase
h	hour(s)
HADDOCK	High Ambiguity Driven protein-protein DOCKing
HEPES	4-(2-hydroxyethyl)-1-piperazineethanesulfonic acid
Htt	Huntingtin
IEX	ion exchange chromatography
IPTG	Isopropyl β-D-1-thiogalactopyranoside
ITC	isothermal titration calorimetry
K_d	dissociation constant
kDa	kilo Dalton
LB	lysogeny broth
MDC, Berlin	Max-Delbrueck Center for Molecular Medicine (Helmholtz Association)
MeOH	Methanol
min	minute(s)

MPIB	Max-Planck-Institute for Biochemistry
MS	mass spectrometry
MST	microscale thermophoresis
MWCO	molecular weight cut-off
Ni-NTA	nickel-nitrilotriacetic acid
NMR	nuclear magnetic resonance
OD_{600}	optical density at 600 nm
PAGE	polyacrylamide gel electrophoresis
PBS	phosphate buffered saline
PCR	polymerase chain reaction
PDB	protein data bank
PELDOR	pulsed electron-electron double resonance
pH	potential of Hydrogen
PMSF	phenylmethylsulfonyl fluoride
PRM	parallel reaction monitoring
PTM	posttranslational modification
RT	room temperature
S. cerevisiae	Saccharomyces cerevisiae
SD medium	minimal synthetic defined medium
SDS	sodium dodecyl sulfate
SEC	size exclusion chromatography
sec	second(s)
SOC	super optimal broth with catabolite repression
SPR	surface plasmon resonance
Talon	cobalt(II)-carboxymethylaspartate
TB	terrific broth
Tris	tris(hydroxymethyl)aminomethane
U7BR	Ubc7 binding region
UBA	Ubiquitin-associated
UBC	Ubiquitin-conjugating enzyme catalytic core
UBD	Ubiquitin binding domain
UPR	unfolded protein response
wt	wild type
x g	relative centrifugal force
YFP	yellow fluorescent protein
YPD medium	yeast extract peptone dextrose medium

Summary

Ubiquitination is an essential posttranslational protein modification (PTM) that regulates widespread intracellular processes in eukaryotic cells. Ubiquitin (Ub) can be assembled into polymeric chains through its seven internal lysine residues and the N-terminus. Considering the high number of possible combinations, it becomes evident that the molecular machinery assembling this "Ubiquitin Code" needs to be tightly regulated. Often E2 ubiquitin-conjugating enzymes play a key role in defining the shape of a ubiquitin signal. However, factors that guide their activity remain poorly understood. In this study, I investigated the molecular underpinnings of Ub chain assembly by the E2 enzymes Ubc1 and Ubc7 through *in vitro* reconstitution of ubiquitination activity, biochemical assays, structural investigation and cell biological experiments. This study shows that associated ubiquitin bindings domains (UBDs) substantially contribute to the assembly of particular Ub chains by both E2 enzymes.

Uniquely among the eleven E2 enzymes of *S. cerevisiae* Ubc1 contains a ubiquitin binding UBA domain. Ubc1 exclusively modifies lysine 48 (K48) in Ub and has been implicated in protein quality control and cell cycle progression. However, the function of its UBA domain remained elusive. I identified Ubc1 to preferentially target specific Ub molecules in K63-linked polyubiquitin via its UBA domain. This activity results in the assembly of K48/K63 branched Ub chains. Based on existing structural information and my own X-ray crystallographic experiments, I propose a structure for the transition state of branched chain assembly by Ubc1. Although homotypic ubiquitin chains have been thoroughly studied, little is known about the prevalence and function of mixed or branched chains. My findings provide a basis for their study.

Ubc7 has previously been shown to be activated by its co-factor Cue1 to assemble Ub chains linked through lysine 48 (K48) in the context of endoplasmic reticulum associated protein degradation (ERAD). I studied Ubc7 and Cue1 in collaboration with Dr. Maximilian von Delbrück (AG Sommer - MDC, Berlin) and Dr. Andreas Kniss (AG Dötsch - Goethe University, Frankfurt). We identified the ubiquitin binding CUE domain in Cue1 to play a key role in aligning Ubc7 with the distal tip of a K48-linked Ub chain for rapid chain elongation. Furthermore, we showed how binding of Ub by the CUE domain is well adapted towards the chain elongation process and how its disruption impairs degradation of the ERAD substrate Ubc6.

Zusammenfassung

Ubiquitinierung ist eine essentielle posttranslationale Proteinmodifikation (PTM), die vielfältige Prozesse in eukaryotischen Zellen reguliert. Ubiquitin (Ub) wird sowohl durch sieben interne Lysin-Reste als auch durch den Amino-Terminus zu polymeren Ketten zusammengesetzt. Aus den zahlreichen Kombinationsmöglichkeiten ergeben sich komplexe intrazelluläre Signale, die durch spezialisierte Enzyme selektiv aufgebaut werden. Häufig sind hierbei E2-Ubiquitin-konjugierende Enzyme von entscheidender Bedeutung. Über Faktoren, die ihre Aktivität regulieren, war bisher jedoch wenig bekannt. Im Rahmen meines Promotionsstudiums habe ich die molekularen Grundlagen der Ub-Kettensynthese durch die E2-Enzyme Ubc1 und Ubc7 untersucht. Hierzu habe ich *in vitro* Ubiquitinierungs-Reaktionen, biochemische und strukturelle Untersuchungen sowie zellbiologische Experimente durchgeführt. Hierbei wurde deutlich, dass Ubiquitin-Binde-Domänen (UBDs), welche mit den E2-Enzymen assoziiert sind, wesentlich zum effizienten und spezifischen Aufbau von Ub-Ketten beitragen.

Als einziges unter elf E2-Enzymen in *S. cerevisiae* enthält Ubc1 eine Ubiquitin-bindende UBA-Domäne. Ubc1 modifiziert ausschließlich Lysin 48 (K48) in Ub und wurde mit Proteinqualitätskontrolle sowie der Regulation des Zellzyklus in Verbindung gebracht. Die Funktion der UBA-Domäne blieb hierbei jedoch unklar. Die Ergebnisse meiner Studie zeigen, dass Ubc1 mithilfe seiner UBA-Domäne vorzugsweise mit bestimmten Ub-Molekülen in K63-verknüpftem Polyubiquitin interagiert. Diese Aktivität führt zur Assemblierung von K48/K63 verzweigten Ub-Ketten. Basierend auf vorhandenen Strukturinformationen und meinen eigenen röntgenkristallographischen Untersuchungen habe ich eine Modellstruktur für den Übergangszustand dieser Reaktion erarbeitet. Homotypische Ubiquitinketten sind Gegenstand zahlreicher Studien, während über die Prävalenz und Funktion von gemischten oder verzweigten Ub-Ketten wenig bekannt ist. Für letztere bilden meine Ergebnisse eine wesentliche Untersuchungsgrundlage.

Ubc7 assembliert mit seinem Kofaktor Cue1 Ub-Ketten, die K48-verknüpft sind, für den Endoplasmatisches-Retikulum-assoziierten Proteinabbau (ERAD). Im Rahmen eines kollaborativen Projektes, konnten wir zeigen, dass die Ubiquitin-bindende CUE-Domäne in Cue1 eine Schlüsselrolle bei der Ausrichtung von Ubc7 spielt. Hierbei wird das E2-Enzym in der Nähe der distalen Spitze einer K48-verknüpften Ub-Kette positioniert, um eine schnelle Kettenverlängerung zu ermöglichen. Darüber hinaus konnten wir zeigen, wie die Bindung der CUE-Domäne an Ub besonders an den Kettenverlängungsprozess angepasst ist, und dass eine Beeinträchtigung dieser Bindung den Abbau des ERAD-Substrats Ubc6 inhibiert.

Contributions, publications and presentations

Results from my main project focussed on Ubc1 are presented in section 2.2 and are currently being prepared as a manuscript for publication.* For this investigation, I performed structural analysis (section 2.2.1) in the laboratory of Prof. Dr. Brenda Schulman at the Max Planck Institute for Biochemistry (MPIB) in Martinsried. Dr. David Krist (MPIB, Martinsried) assisted in conceptualising different protein purification and cross-linking strategies. Dr. Jérôme Basquin (MPIB, Martinsried) helped in optimisation of crystallisation conditions and recorded a diffraction dataset. Dr. Rajan Prabu (MPIB, Martinsried) performed initial phasing of this dataset. An NMR dataset (section 2.2.2.3) was recorded by Dr. Andreas Kniss from the group of Prof. Dr. Volker Dötsch (Goethe University, Frankfurt). Dr. Henrik Zauber from the group of Prof. Dr. Matthias Selbach (MDC, Berlin) as well as Dr. Oliver Popp from the laboratory of Dr. Philip Mertins (MDC, Berlin) performed mass spectrometric measurements (section 2.2.4 and 2.2.5.2). Dr. Janine Kirstein conducted genetic experiments in *C. elegans* (section 2.2.5.1).

* **L. Pluska** *et al.* "The UBA Domain of Ubc1 Facilitates Assembly of K48/K63 Branched Ubiquitin Chains."

I presented results from this study as a poster during the international "EMBO Conference on Ubiquitin and SUMO: From molecular mechanisms to system-wide responses" (15 – 19 Sept 2017 in Cavtat, Croatia) and as invited speaker at the SignGene Symposium "Ubiquitin: One Traveler, Two Roads" (1 – 3 Sept 2017 in Neuruppin, Germany).

Data presented in section 2.1.1 are parts of a collaborative project with Dr. Maximilian von Delbrück from the group of Prof. Dr. Thomas Sommer (MDC, Berlin) and Dr. Andreas Kniss and were published in the journal *Molecular Cell*.[1] For this study, I performed analysis of substrate degradation through cycloheximide chase assays, cloning of protein expression vectors, yeast cultivation, protein purification, preparative Ub chain assembly and assisted in the writing of the manuscript. Dr. Maximilian von Delbrück conducted all *in vitro* ubiquitination experiments presented in the section. Dr. Andreas Kniss carried out NMR titration experiments and their analyses.

[1] M. von Delbrück, A. Kniss, V. V. Rogov, **L. Pluska**, K. Bagola, F. Löhr, P. Güntert, T. Sommer and V. Dötsch, "The CUE Domain of Cue1 Aligns Growing Ubiquitin Chains with Ubc7 for Rapid Elongation.", *Mol Cell*, vol. 62, pp. 918-928, 2016.

The results presented in section 2.1.2 were published in the journal *Structure*.[2] I designed and performed *in vitro* ubiquitination experiments jointly with Dr. Andreas Kniss in the laboratory of Prof. Dr. Thomas Sommer. Dr. Andreas Kniss, Dr. Denise Schütz and Dr. Sina Kazemi performed pulsed electron-electron double resonance (PELDOR) spectroscopy in combination with molecular modelling. This was a collective effort between the laboratories of Prof. Dr. Volker Dötsch, Prof. Dr. Prisner and Prof. Dr. Güntert from the Goethe University (Frankfurt). Section 2.1.3 contains unpublished data on Ubc7 activity obtained from the joint *in vitro* ubiquitination experiments performed with Dr. Andreas Kniss. An analytical size exclusion experiment was performed by Dr. Andreas Kniss.

[2] A. Kniss, D. Schuetz, S. Kazemi, **L. Pluska**, P. E. Spindler, V. V. Rogov, K. Husnjak, I. Dikic, P. Güntert, T. Sommer, T. F. Prisner and V. Dötsch, "Chain Assembly and Disassembly Processes Differently Affect the Conformational Space of Ubiquitin Chains.", *Structure*, vol 26, pp. 249-258, 2018.

1. Introduction

1.1 The Ubiquitin Code

1.1.1 Ubiquitination

All living cells must react to changes in their environment to assure survival. This includes cells inside the protective surroundings of multicellular organisms. Among other external and internal factors they must rapidly adapt to changing chemical and electric stimuli, nutrient availability and temperature. The eukaryotic cell is capable of responding quickly to such changes by means of different molecular tools. Post-translational protein modifications (PTMs) like phosphorylation, acetylation and ubiquitination are pivotal to this ability. Ubiquitin-mediated protein degradation was a discovery in the early 1980s for which Aaron Ciechanover, Avram Hershko and Irwin Rose were jointly awarded the Nobel Prize in Chemistry in 2004.[3] Since its discovery, the highly stable 76-amino acid protein ubiquitin (Ub) was found to not only affect the half-life of its client proteins, but also their cellular localisation, their interactome and their activity.[4,5] Moreover, Ub itself is also a target of PTMs including ubiquitination. Thus, unlike many other modifications, Ub does not only encode a binary signal, which occurs in either of two states, but instead can harbour complex information. This so-called Ubiquitin Code was found to regulate widespread cellular functions in all kinds of eukaryotic tissue and organisms from yeast to human. The pleiotropic effects of ubiquitination are implicated in human development and disease in numerous ways.[6,7] Therefore, understanding how the Ubiquitin Code is generated and decoded by downstream acting factors is a fundamental and far-reaching question.

In the first part of this introduction, I describe general properties and structural features of Ub, which are the basis for the complexity of the Ubiquitin Code. In the second part, I introduce enzymes which are central in the generation of the Ubiquitin Code. The factors which guide the activity of these proteins remain largely elusive and are a major focus of this study. Ultimately, I formulate a simplified nomenclature to discuss complex Ub signals.

Ub is transferred to target proteins by the combined action of ubiquitin-activating enzymes (E1), ubiquitin-conjugating enzymes (E2) and ubiquitin ligases (E3).[4] As the result of this enzymatic cascade, a Ub monomer is covalently attached via its C-terminus to a target protein typically through the ε-amino group of a lysine residue (Figure 1). Eukaryotic cells employ a large number of proteins to ascertain assembly of Ub signals within particular cellular contexts on

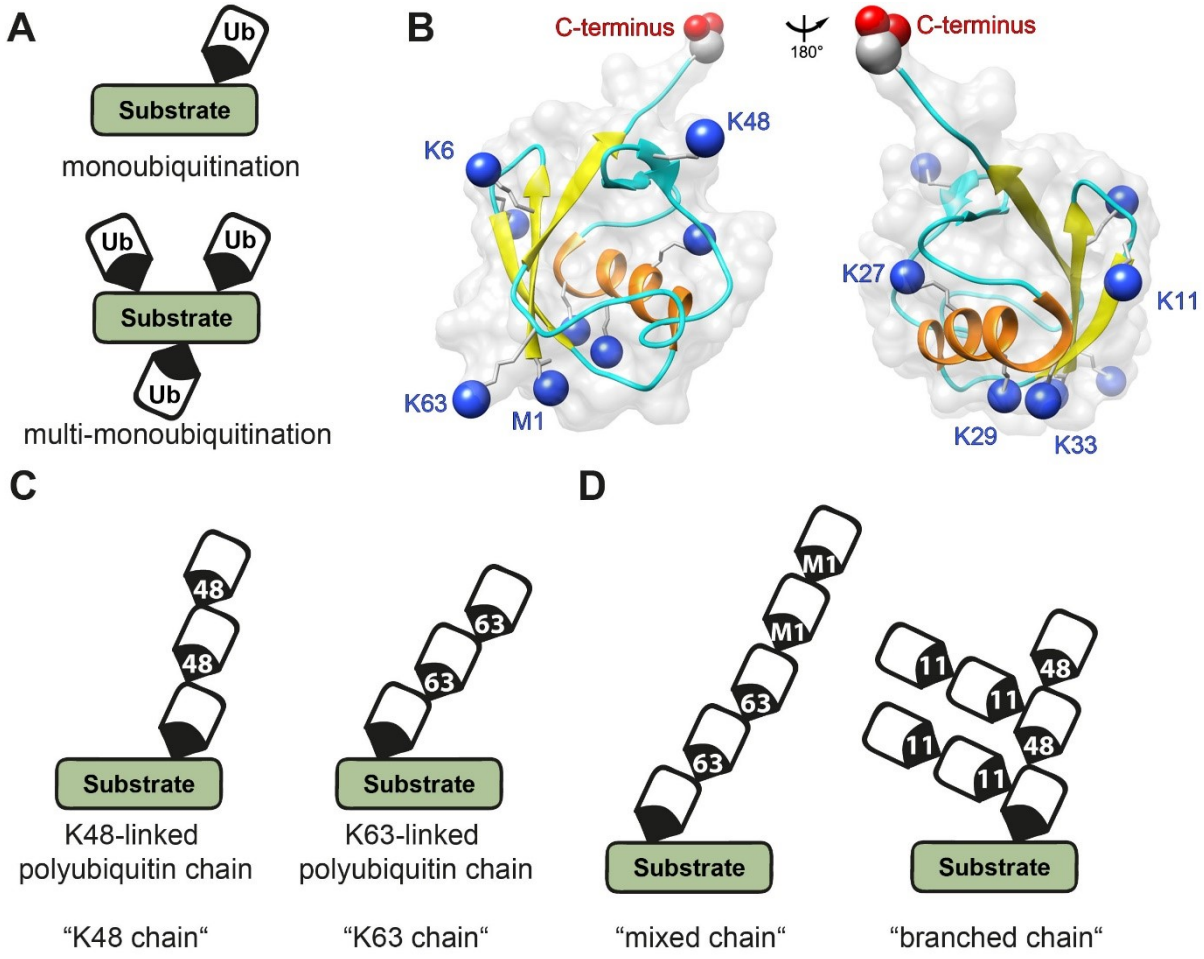

Figure 1: The Ubiquitin Code. (A) Ubiquitin is attached to a protein substrate through enzymatically catalysed formation of an isopeptide bond between the C-terminal carboxy group of ubiquitin (Ub) and an amino group of a target lysine. Ub may serve as a new binding site for effector proteins or block existing binding sites for interaction partners. (B) The three-dimensional structure of Ub (PDB: 2K39). Ub harbours seven lysine residues and the N-terminal M1 which can also be targeted by ubiquitination resulting in the assembly of polymeric chains. Amino groups are highlighted in blue and the C-terminal carboxy group in red. (C) Differently linked Ub chains lead to different biological outcomes. Ub chains linked through K48 (K48 chains) are typically associated with proteasomal degradation of a substrate. In contrast, K63 chains facilitate the recruitment of a range of non-proteasomal effector proteins. (D) Different linkage types can be combined into one signal yielding mixed and branched Ub chains.

defined substrates. The human genome encodes for an estimated total of 600-1000 E3 enzymes, approximately forty E2 enzymes and two E1 enzymes, which are involved in the transfer of Ub and ubiquitin-like proteins.[8] In some cases, enzymes have redundant functions and overlapping substrate pools which can complicate their study. This makes the yeast *S. Cerevisiae* an attractive model organism for the study of the Ubiquitin Code. Its genome encodes for approximately 60-100 E3 enzymes and 13 E2 enzymes.[9]

Signal termination plays an important role for ubiquitination as for any other signalling cascade. This is achieved by enzymes known as deubiquitinating enzymes (DUBs). These proteases catalyse a proteolytic reaction between the carboxy group of the C-terminus in Ub and its attachment site.[10] Different DUBs selectively cleave specific Ub signals depending on their topology. DUBs ensure maintenance of a steady pool of free Ub, but also mediate acute signalling events by removing binding sites for downstream effectors in a tightly controlled manner. In mammalian cells, approximately 100 DUBs have been identified which can be subdivided into six families.[11,12,13]

After the discovery of Ub more proteins emerged, which share its characteristic three-dimensional β-grasp fold (Figure 1B and section 1.1.4). These ubiquitin-like proteins (Ubls) were found to behave in many ways like Ub, but require distinct enzymes and typically affect specific cellular functions.[14] Among the best studied Ubls are SUMO – which governs transcriptional regulation and cell cycle progression among other functions, NEDD8 – which most prominently serves as activator of cullin-based E3 ligases, ISG15 – which was attributed anti-viral functions, and Atg12 – which is pivotal to formation of the autophagic pore.

1.1.2 Homotypic ubiquitin chains

Ubiquitin contains seven different lysine residues (K6, K11, K27, K29, K33, K48, and K63) as well as an N-terminus (M1), which can be targeted by ubiquitination (Figure 1B). This results in the assembly of polymeric Ub chains. Mass spectrometry studies revealed that all seven lysine residues and M1 serve as acceptor of Ub-conjugation *in vivo*.[15] Abundances of chain types vary dependent on cell type, stage of cell cycle progression[16] and exposure to stress conditions[17]. Historically, research on polyubiquitin has mostly focussed on homotypic Ub chains which are assembled exclusively through one linkage type. K48-linked polyubiquitin chains ("K48 chains") are overall the most abundant species and were the first to be discovered.[5] Canonically, substrates decorated with these chains are targeted to the 26S proteasome for degradation.[18] Assembly of K48 chains is an essential process and cells with K48 of Ub replaced with another amino acid are not viable.[19] This is crucial for the removal of misfolded and unfolded proteins, which can potentially be toxic for the cell. Moreover, K48 chains are also required for acute regulation of cellular processes. For instance, misfolded proteins can be recognised and removed from the lumen of the endoplasmic reticulum by the HRD-ligase complex in a process called endoplasmic reticulum associated protein degradation (ERAD).[20] Based on folding and glycosylation status, this process is able to target a large variety of proteins for modification with K48 chains to induce their proteasomal degradation.[21] In contrast, the

ordered transition through the cell cycle in eukaryotic cells requires timely controlled assembly of K48 chains for the degradation of specific cell-cycle proteins such as cyclins and securins.[22] Numerous enzymes assembling specifically K48 chains are known.[5]

Shortly after the discovery of K48 chains, K63 was also identified to be prominently involved in polyubiquitin chain formation.[23] Together, these two types of linkages account for the majority of polyubiquitin in cells.[24] In contrast to K48 chains, K63 chains were found to promote functions mostly unrelated to proteasomal degradation. They can facilitate complex assembly and thereby govern widespread processes such as DNA damage repair[23,25] transcriptional activation[26,27], innate immune responses[28], endocytosis[29,30,31] or protein trafficking[32,33]. Unanchored K63 chains were identified to promote cellular responses independently from any substrates.[34,35] Moreover, K63 chains play a central role in assembly of autophagosomal pores for macroautophagy – the degradation of protein aggregates and/or subcellular organelles in the lysosome. For example, this is required for the clearance of damaged mitochondria.[36,37] Among other proteins, the E2 enzyme Ubc13 has been shown to selectively assemble K63 chains by forming a hetero-dimer with the ubiquitin-conjugating enzyme variant Mms2 (or Uev1a), which lacks a canonical active site.[38,39] Its activity was shown to play a crucial role in DNA damage repair.[40]

Ub chains linked through other residues than K48 and K63 are often termed atypical Ub chains. Between these, M1 chains and K11 chains are the best studied. M1 chains were found to be quickly synthesised in the context of inflammatory signalling cascades[41,42], whereas K11 chains also mediate protein degradation through the proteasome, particularly in the context of cell-cycle progression[43,44]. Although data on the remaining Ub chain types is scarcer, proteins able to assemble and specifically recognise these exist. K6 chains have been identified in the process of removing damaged mitochondria.[36] K27 chains are implicated in regulating DNA damage repair and in autoimmunity.[45,46] K29 chains were associated with proteasomal degradation but also with formation of neuroprotective aggregates.[47,48] K33 chains are assumed to affect trafficking through the trans-Golgi network.[49] In contrast to enzymes responsible for assembly of K63, K48, K11 and M1 chains, enzymes associated with these atypical chains appear to exhibit less linkage specificity, *i.e.* they are capable of assembling Ub chains with multiple different linkages.[36,50,51]

The signalling output of a Ub chain is not only determined by its linkage but also by its length. A longer Ub chain contains more interaction sites for downstream effectors and thus may provide a more potent signal. For instance, multiple small substrates are degraded efficiently

by the proteasome upon modification with short Ub chains or even monoubiquitination.[52] However, larger substrates require longer K48 chains which putatively provide a stronger degradation signal.[53] In other cases, a hard threshold for length may exist for a specific interaction or process to occur. For example, the deubiquitinating enzyme MINDY has been found to only effectively cleave K48 chains which consist of at least four Ub molecules.[13] A first global assessment of Ub chain length distribution in yeast revealed that Ub chains predominantly exist in dimeric to heptameric form.[54]

1.1.3 Heterotypic ubiquitin chains

Although research has mostly focussed on the biological function of individual types of Ub chains, different linkages can also be combined into a single Ub polymer. This includes Ub chains with alternating linkage types – "mixed chains" – and Ub chains with a moiety that is targeted at multiple lysine residues within a single Ub moiety – "branched chains" (Figure 1D). Few biological processes dependent on mixed and branched chains are addressed in the literature. Chains with alternating linkages have been identified in the context of NF-κB signalling.[55] In this pathway K63 chains, which are attached to a substrate, are extended with M1 chains by the E3 LUBAC. A kinase complex can then associate with the M1 chains to phosphorylate components of another protein complex that is brought into proximity through interaction with the adjacent K63 chain. Moreover, subsequent studies suggested that this might protect the linear chains from disassembly by DUBs.[56] K11/K48 branched chains generated by the anaphase-promoting complex (APC/C) have been shown to accelerate proteasomal degradation of cell-cycle regulators as compared to homotypic K48 chains.[57] In recent years, Ohtake *et al.* demonstrated the existence of K48/K63 branched Ub chains in mammalian cell lines. They identified this signal to affect NF-kB signalling[58] and the balancing of autophagosomal and proteasomal degradation[59]. Further developments in mass spectrometric methods are required to systematically investigate branched Ub chains, which might help understand the significance of signals combining differently linked Ub chains. While some studies suggest that branched and mixed chains merely connect different signals to which interactors can bind independently[55,60], they might also confer unique binding interfaces for specific interactors. If and how branched and mixed Ub chains differ from the building blocks they are made of remains undetermined.

1.1.4 Structure of ubiquitin

The structure of monoubiquitin and Ub chains defines the signals of the Ubiquitin Code. Ub is highly conserved among species. Only three amino acids differ between the human and yeast orthologue in *S. cerevisiae* (P19S, D24E, S28A). This indicates high evolutionary pressure to maintain the structure of Ub reflecting its central position in a network of many interactors. This also implies most of its surface residues are involved in binding interaction partners. Binders most prominently associate with a cluster of amino acids located around I44-L8-V70, called the hydrophobic patch (Figure 2A, blue).[61] Another less prominently described hydrophobic surface clusters around I36-I71-I73 and also includes L8 (Figure 2A, green).[61] Ub shows a highly stable β-grasp fold, in which a hydrophobic core is formed between an alpha helix (Figure 1B, orange) and a beta sheet with three strands (Figure 1B, yellow).[62] Two regions of increased flexibility are known in the otherwise rigid fold of Ub. One is the β1/β2 loop spanning amino acids 6-10 (aa6-10, Figure 2A, orange), which notably harbours L8 – a constituent of the hydrophobic patch. The conformational equilibrium of this loop affects binding to interactors.[63] Secondly, the last six amino acids of Ub confer a flexible C-terminus (Figure 2B), which allows many different conformations between Ub and its attachment site.[64] The side chains of the seven lysine residues and the M1 terminus, which are required for chain formation, are solvent exposed. Only K27 is partially buried and not optimally accessible.[65]

To understand the distinct biological functions of differently linked Ub chains, structural differences between chain types have been extensively studied. X-ray crystallography experiments show that many diubiquitin molecules adopt compact conformations, in which the individual moieties tightly interact.[66,67,68,69] K48 chains prominently adopt a closed conformation, in which the hydrophobic patches around I44 of both moieties form an intramolecular interface (Figure 2C). In contrast, M1 chains and K63 chains predominantly adopt an extended open conformation, in which the isopeptide bond between the two moieties is the only contact site (Figure 2D). However, structures of diubiquitin molecules showing alternative conformations as well as experiments investigating the flexibility of Ub chains in solution indicate that each Ub chain can dynamically sample a wide landscape of conformations.[70,71] Computer simulations were used to shed some light into the frequency, with which the different chains adopt specific states in solution[72] (Figure 2E). Addressing the dynamics of the conformational space of Ub chains experimentally is a challenging endeavour, which might be necessary for a detailed understanding of linkage selective Ub binders and their ability to discriminate between differently linked chains. As part of a collaborative project,

partners from the Goethe University in Frankfurt devised a method to investigate this question. Together, we explored how Ub binders affect chain topology and in turn how this affects enzymes interacting with these Ub chains.

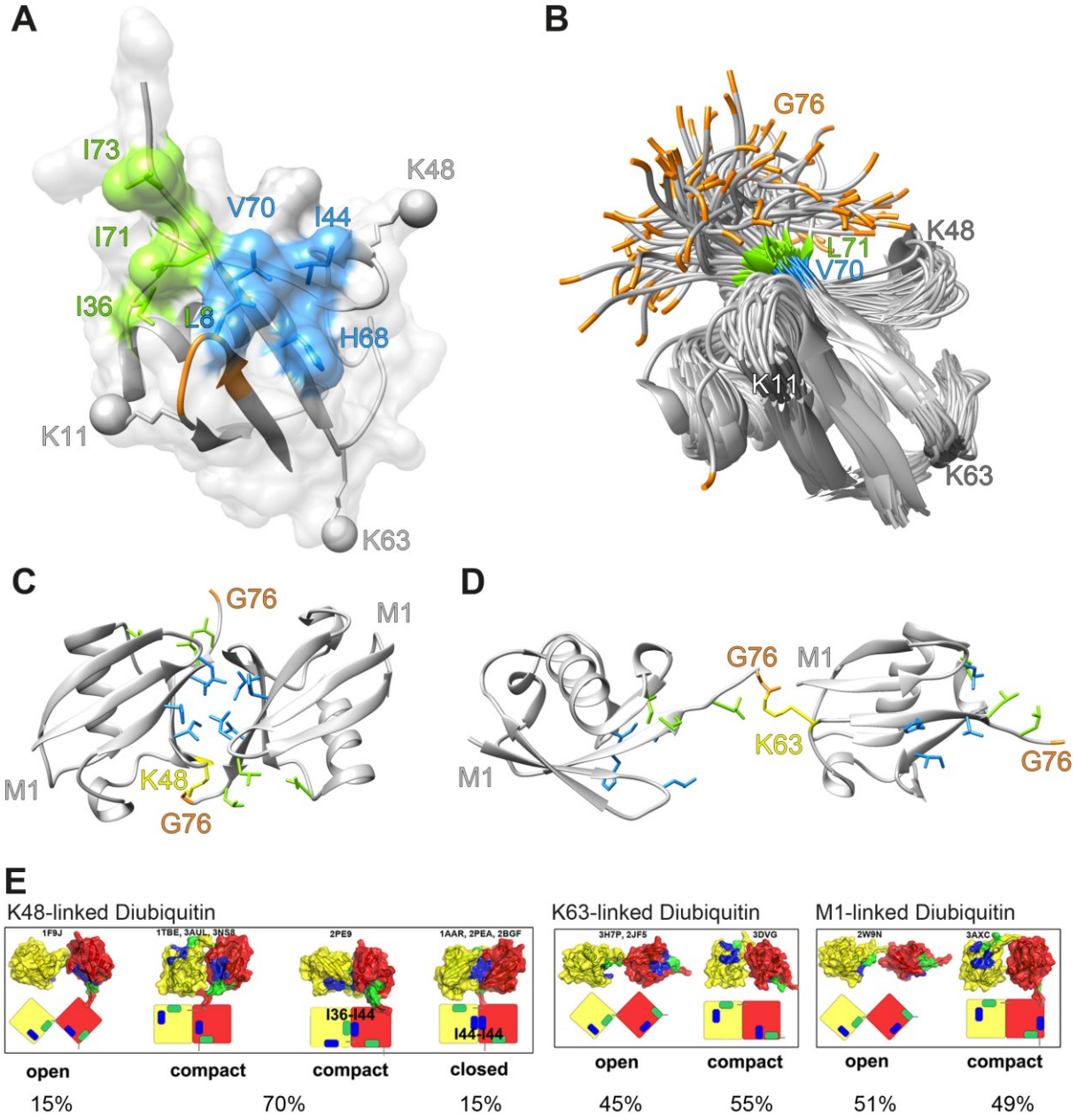

Figure 2: Structure of monoubiquitin and ubiquitin chains. (A) The hydrophobic patches around I44 (blue) and I36 (green) are highlighted in the three dimensional structure of Ub. (B) An NMR ensemble of Ub in solution highlights the flexibility of the C-terminal amino acids L71 through G76 (PDB: 2K39). (C) Crystal structure of K48-linked diubiquitin[66] (PDB: 1AAR). (D) Crystal structure of K63-linked diubiquitin (PDB: 3H7P). (E) Landscape of diubiquitin conformations was explored by computer simulations. (E adapted from Wang *et al.*[72])

1.1.5 Reading the Ubiquitin Code – ubiquitin binding domains (UBDs)

To translate the Ub signals into specific biological outcomes, substrates decorated with Ub interact with downstream acting proteins which often contain ubiquitin binding domains (UBDs).[73] More than twenty families of these domains with different binding specificities and diverse structures have been described.[74] While most UBDs bind to the hydrophobic patch around I44 in Ub, the footprint they leave on the surface of Ub differs.[75] Many UBDs show extremely low binding affinity for Ub with dissociation constants, which can reach into a high micromolar and even low millimolar range.[76] Binding events between low affinity UBDs and Ub have been described to be among the weakest protein-protein interactions in nature, which are still considered specific.[77] This might be due to the relatively high concentrations of Ub inside the cell[78] and the requirement for quick reversibility of binding as part of a signalling process.

Several mechanisms are known, through which Ub binding proteins can discriminate between different Ub chain types. For example, a single-domain UBD can simultaneously bind to two linked Ub molecules in a sandwich-like manner. This has been reported for the binding of Rad23A to $^{48}Ub_2$.[81] Alternatively, multivalent Ub binding interfaces can exploit the distance between Ub moieties within a chain. For instance, in the course of DNA double strand breaks Rap80 recognises K63 chains through two ubiquitin interacting motifs binding in tandem.[79] Similarly, the DUB OTUB1 features two distinct Ub binding sites in order to specifically recognise and cleave K48 chains.[80] We found catalytically inactive OTUB1 to be a particularly strong binder and exploited this in control experiments.

UBDs have been mostly studied as part of effector proteins which decode Ub signals into a cellular response. However, it is becoming increasingly clear that UBDs and other Ub binders fulfil pivotal roles in aiding the activity of chain building enzymes. For example, the E2 enzymes Ubc13[82] and Cdc34[83] rely on such Ub binding events for their activity. Moreover, the E2 enzyme Ubc7 requires the Ub binding cofactor Cue1 to efficiently assemble K48 chains.[84] Ub chain assembly requires coordination of a substrate, a growing chain and the associated enzymes. How exactly Ub binding facilitates this spatially dynamic process remains poorly understood. During my doctoral research, I studied molecular mechanisms of Ubc7 activation through Cue1 and activation of the E2 enzyme Ubc1 through its intrinsic UBA domain. The CUE domain in Cue1 and the UBA domain in Ubc1 belong to UBD families which show low sequence similarity. However, they share a common structure which is composed of a bundle of three alpha helices and associates with the hydrophobic patch in Ub.[85,86] In the following

section, I describe general properties of enzymes associated with Ub chain assembly, before outlining current knowledge on Ubc7 and Ubc1.

1.2 Writing the Ubiquitin Code

1.2.1 The ubiquitination cascade

Modification of substrates with Ub requires the coordinated and sequential activity of ubiquitin-activating enzymes (E1), ubiquitin-conjugating enzymes (E2) and ubiquitin ligases (E3). They cooperate in an energy consuming process termed ubiquitination cascade (Figure 3A).[4] In a first step which is driven by ATP-hydrolysis, a thioester bond between the sulfhydryl group of the active site cysteine in the E1 enzymes (UBA1) is formed with the free carboxyl group of the C-terminal G76 in Ub. The UBA1/Ub thioester (UBA1~Ub) then exposes a binding site, through which E2 enzymes can be recruited for a transthiolation reaction, in which Ub is transferred to the active site cysteine of the cognate E2 enzyme.[87] For the final step of ubiquitination, the E2 enzyme, which is charged with Ub (E2~Ub), typically cooperates with an E3 ligase, which are canonically categorised into three different families.[4] In a transthiolation reaction, E2~Ub can transfer Ub to HECT- or RBR-E3-ligases which harbour an active site cysteine themselves and consecutively engage with a substrate.[88,89] Alternatively, E2~Ub can associate with RING ligases. These account for the majority of E3 ligases.[90] The RING ligase mediates substrate recruitment and binds E2~Ub in a way which facilitates discharge. As a result, Ub is transferred onto a target lysine in the substrate. Recent studies suggest that specialised E2 and E3 enzymes are capable to transfer Ub to hydroxyl groups in serine or threonine residues.[91,92] Because E3 ligases typically confer substrate specificity, they have been a prominent object of research. However, it is becoming increasingly clear that E2 enzymes frequently are the deciding factor for linkage type and spatial organisation of the Ub signal.[93]

1.2.2 Structure of E2 ubiquitin-conjugating enzymes

The structure of E2 enzymes is defined by a catalytic core domain ("UBC domain") of about 150 amino acids and has been reviewed in detail[93] (Figure 3B). The UBC domain consists of a β-sheet of typically four antiparallel β-strands, which is flanked by four α-helices. The active site cysteine is located in a loop region which connects the C-terminus of the β-sheet (strand β4) with helix α2. Beta strand β4 is shortly followed by a conserved HPN triad, which is reported to be required for enzymatic activity. Helix α2 is also termed „crossover helix" as it is positioned across the β-sheet. A "gateway residue", which is located at the N-terminal end of helix α3, has been reported to regulate the activity of a number of E2 enzymes.[94,95,96] The

surface opposite to the catalytic site has been found to mediate "backside binding" of the E1 enzyme and regulatory factors such as RING domains or Ub itself (Figure 3B). Many E2 enzymes show variations of this pattern with C-terminal or N-terminal extensions or distinct insertions within the UBC domain. E2 enzymes charged with Ub (E2~Ub) can adopt a distinct closed conformation, in which the donor Ub (Ub_D) binds through its hydrophobic patch to the crossover helix in the UBC domain (Figure 3C,D).[97] This conformation was identified to be stabilised by the binding of RING domains and to be pivotal to enzymatic activity.[98]

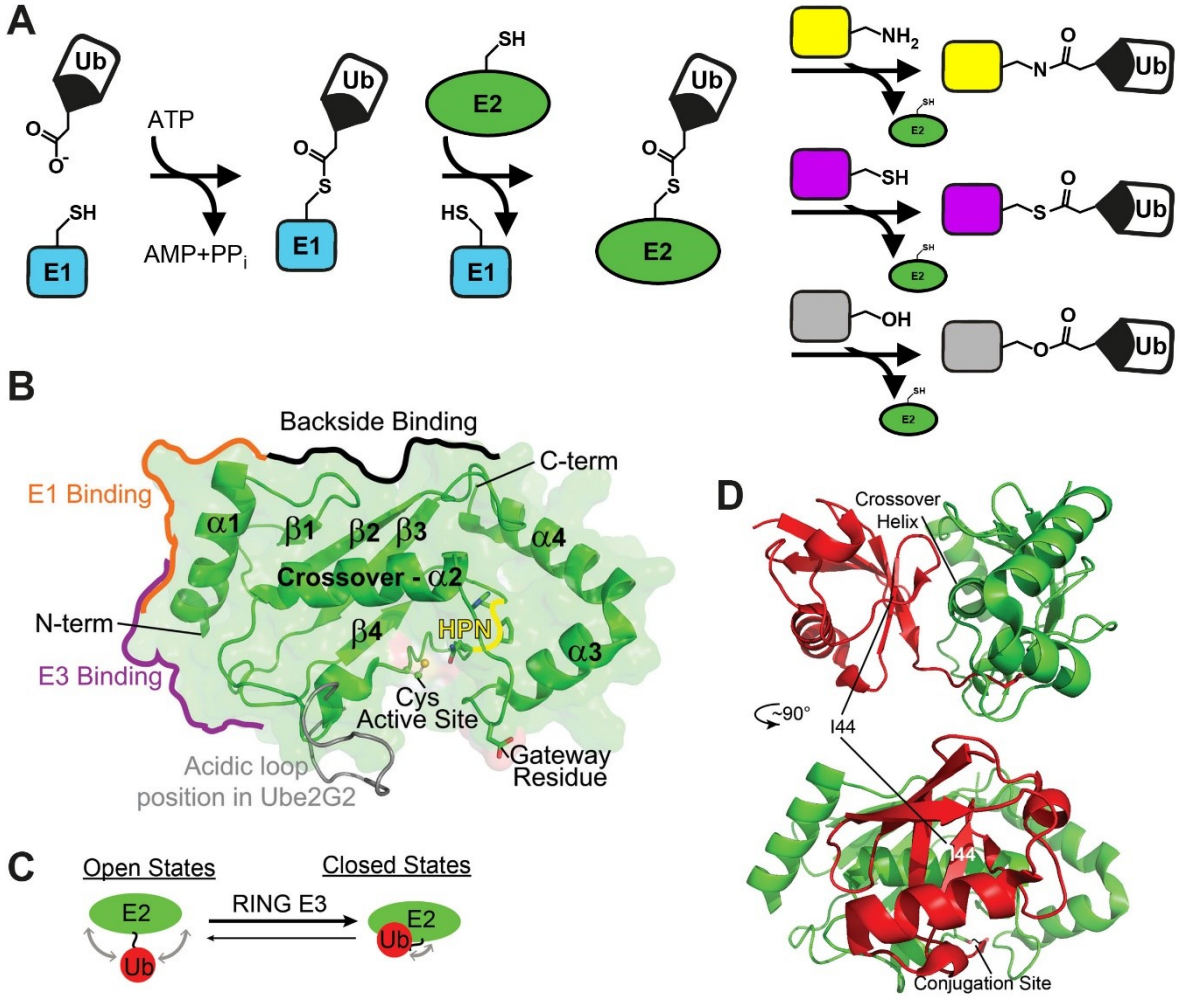

Figure 3: E2 ubiquitin-conjugating enzymes. (A) During the ubiquitination cascade, E2 enzymes are charged with Ub by E1 enzymes in an ATP consuming first step. Ub is transferred from the E2/Ub thioester to target proteins through aminolysis, transthiolation or esterification. (B) Structural features of E2 enzymes. (C) E2 enzymes charged with Ub adopt open and closed conformations. The latter are particularly important for enzymatic activity. (D) Structure of E2~Ub in closed conformation. (B-D adapted from Stewart *et al.*[93])

Some E2 enzymes target a wide substrate pool, while others target specific residues in particular proteins. For example, Ubc6 does not only mediate the degradation of a wide range of mostly misfolded proteins in the context of ERAD, it is also capable of targeting serine and threonine

residues highlighting its high promiscuity.[91] In contrast, E2 enzymes, which are involved in Ub chain assembly, typically target a specific lysine residue within Ub. Accordingly, the UBC domains of these E2 enzymes have been found to interact with the acceptor Ub (Ub_A) in specific ways. For example, a number of acidic residues in the UBC domain of Ube2S have been found to align Ub_A to mediate its specificity for K11.[99] However, chain assembling E2 enzymes have been found to interact with acceptor Ub (Ub_A) very weakly. For instance, the K_M value of the K63 specific Ubc13 or Mms2 to Ub_A has been quantified to 437 µM, which is indicative of its low binding affinity.[100]

1.2.3 E2 ubiquitin-conjugating enzyme Ubc7

The activity of the E2 enzyme Ubc7 is closely intertwined with its co-factor Cue1. Cue1 is a membrane anchored multi domain protein. It contains an N-terminal transmembrane helix, a Ub binding CUE domain and the Ubc7 activating binding region (U7BR) at its C-terminus. In absence of Cue1, Ubc7 is autoubiquitinated and degraded.[101] Cue1 and Ubc7 are essential components of the ERAD pathway.[102] Cue1 is required to recruit Ubc7 to the Hrd1-ligase complex – a central component of ERAD – and to activate Ubc7 via its U7BR-domain through backside binding.[103] Ubc7, like the homologous E2 enzyme Ube2g2, contains an acidic loop close to the C-terminus of the crossover helix, which endogenously adopts an alpha helical fold and thus obstructs the active site (Figure 3B). Co-factor binding leads to conformational changes in this region and thereby an activation of the enzyme.[104] Additionally, the CUE-domain of Cue1 binds to Ub and thereby facilitates assembly of K48-linked polyubiquitin by Ubc7.[84] Disrupting this interaction reduces degradation of Ubc7 substrates *in vivo*. Herein, I present how Ub binding by the CUE domain can stimulate Ub chain assembly on a molecular level.

1.2.4 Biological processes affected by the E2 enzyme Ubc1

Stimulated by the work on Ubc7, I aimed to look for other E2 enzymes, for which Ub binding could activate Ub chain assembly. A prominent candidate was Ubc1 which among yeast E2 enzymes uniquely harbours a UBD – specifically a ubiquitin associated domain (UBA domain).[105,106] When it was discovered, Ubc1 was found to be involved in protein turnover, to mediate resistance to proteotoxic stress induced by canavanine, to be vital for cell growth and to be essential for survival in yeast deleted for *ubc4*.[107] Later, it was found to selectively assemble K48 chains and prominently undergo autoubiquitination at K93 close to the active site (C88).[108] Ubc1 has been shown to be phosphorylated at S97 and S115 by mitogen-activated

protein (MAP) kinases.[109] This propensity appears to influence tolerance to thermal and reductive stress in *S. cerevisiae*. Ubc1 and Ubc4 were shown to act cooperatively in the degradation of substrates of the anaphase promoting complex (APC/C).[110] In this process, Ubc4 has been identified to promiscuously attach monoubiquitin to the targeted substrates, which can then be extended to K48 chains through the activity of Ubc1. Ubc1 can weakly replace Ubc4 activity in context of APC/C, but Ubc4 cannot replace Ubc1.[111]

Moreover, Ubc1 homologues have been implicated in the clearance of protein aggregates and in the development of neurological diseases. Accumulation and insufficient clearance of protein aggregates in neuronal cells is a shared mechanism for pathogenesis, observed in many neurodegenerative diseases as for instance in Alzheimer's disease (AD), Parkinson's disease (PD) and Huntington's disease (HD).[112] Accordingly, it has become increasingly clear that the cellular folding machinery as well as regulated protein degradation play pivotal roles in the development of these diseases.[113] For example, model systems for the study of mutant huntingtin protein (Htt) show that Htt can be degraded either through proteasomal degradation mediated by K48 chains or through the autophagosomal pathway induced by K63 chains.[114] The human Ubc1 homologue Ube2K has been implicated in PD[115] and HD[116,117]. In model systems used to study these diseases, Ube2K was found to increase cell death through its catalytic activity.[115]

A direct link between the activity of Ube2K in the context of protein quality control and neurodegenerative diseases could thus far not be established. However, growing evidence points to the importance of the cellular folding machinery, molecular chaperones and protein quality control pathways to keep these diseases in check.[113,118] For example, in AD, PD and HD, overactivation of the unfolded protein response (UPR) is commonly observed.[119,120] This stress response, which is conserved among all mammals as well as yeast and worm organisms, is activated upon accumulation of misfolded and unfolded proteins in the ER lumen. Its activation ultimately provokes the production of chaperones, the inhibition of protein translation and an increased degradation of misfolded proteins. Prolonged UPR activation may induce apoptosis.[121] To investigate the putative functions of Ubc1 in protein quality control, we collaborated with the group of Dr. Janine Kirstein from the Leibnitz-Institute for Molecular Pharmacology (FMP), Berlin. Dr. Kirstein uses elaborate *C. elegans* model systems to study proteostasis and more specifically, how molecular chaperones, the ubiquitin proteasome system as well as autophagy combat protein aggregation in aging and disease.

1.2.5 Structural features of Ubc1

Several key residues governing the activity and K48 selectivity of the UBC domain in Ubc1 and its human homologue Ube2K (E2-25K/HIP2) were identified. Where other E2 enzymes commonly contain a leucine or alanine residue as "gateway residue" as outlined in section 1.2.2 (Figure 3B), Ubc1 contains glutamine (Q122). Substitution of the corresponding glutamine residue in Ube2K (Q126) to leucine facilitates aminolysis of the E2~Ub thioester putatively by improving the accessibility of the active site. However, this amino acid substitution simultaneously interferes with the K48 specificity of the enzyme.[122] Y59 in Ub_A has been identified to be crucial for K48 specificity and enzymatic activity of Ubc1.[123] A study on Ube2K shows that Y59L in Ub could partially rescue impaired diubiquitin formation by Ube2K-Q126L, indicating a critical interaction between Q126 in Ube2K and Y59 in Ub.[124] Moreover, the authors show that K97E substitution in Ube2K, which also impairs diubiquitin formation, could in turn be rescued by E51R substitution in Ub. Based on their mutagenesis studies and structural modelling they propose that association of Ube2K with Ub_A is stabilised by an interaction interface between an area in Ube2K with several polar residues (S85, S86, T88, D127) and an acidic loop in Ub_A spanning from D58 to Q60. [124] In line with these findings, T84 and Q122 in Ubc1 are vitally important for K48 selectivity and Ubc1 activity in cell cycle progression.[123]

Despite thorough investigation of Ubc1 and its homologues, little is known about the function of the prominent C-terminal extension of helix α4, which harbours the Ub binding UBA domain. It adopts a compact fold of three short alpha helices typical for this family of UBDs. A solution NMR structure of full length Ubc1 suggests high flexibility in the linker region connecting the UBC domain and the UBA domain.[105] Moreover, mapping of the residues involved in Ub binding by NMR spectroscopy revealed that the interaction occurs in a conserved way between helices α1 and α3 in the UBA domain and the hydrophobic patch in Ub. The structure indicates that interaction between the UBA domain and Ub_D is unlikely, which was also suggested by other studies.[111,125] Based on qualitative activity assays, the UBA domain is thought to enhance processivity during assembly of K48 chains *in vitro*.[126] Although Ubc1 and its human homologue Ube2K (or HIP2/E2-25K) have been implicated in a number of biological processes, the functional significance of the UBA domain is poorly understood. The main goal of my work was to elucidate whether and how the UBA domain facilitates Ub chain synthesis by Ubc1.

1.3 Polyubiquitin nomenclature in this work

Few conventions on naming polyubiquitin chains have emerged. Most importantly, the Ub moiety attached to a substrate or with a free C-terminus in unanchored chains is referred to as the proximal Ub, while the moiety at the end of the chain, to which no more Ub is attached, is named distal Ub. However, no systematic nomenclature for polymers of Ub or ubiquitin-like proteins has been widely adopted. As increasingly complicated Ub structures become subject to study, an easy way to discuss complex polyubiquitin topology would be valuable. Ultimately, a unified machine-readable code would greatly benefit the study of Ub signals *in silico*. This section explains the abbreviations used for polyubiquitin in this thesis (Figure 4).

A system previously suggested by Nakasone *et al*. works similar to condensed structural formulas used in organic chemistry[60] (Figure 4A, "condensed"). All Ub molecules of a polymer are listed similar to the atoms of an organic molecule and linkage types are indicated between them. Branching points are described through brackets, which entails limited readability for complex chains. I suggest a simplification for nomenclature, which exploits the directional structure of polyubiquitin: Ub polymers are canonically linked through their C-terminus and thus form hierarchically ordered trees. This means each polymer contains a single root – the proximal Ub moiety. From this root, one or more paths of subsequently added Ub molecules emerge. The linkage types between the Ub monomers define each path. All paths end in a "leaf" – a moiety to which no further Ub is attached. Such a tree can be unambiguously described by specifying the paths to its leafs, *i.e.* by enumerating the sequence of linkages from the proximal Ub to every distal Ub.

In this work, Ub chains will be written as "$^{path(s)}Ub_{\#Ub}$" or "$^{path(s)}Ub\#P(mut)$", where "path(s)" lists the sequence of linkages from proximal to distal Ub separated by commas (Figure 4B,C). For branched chains, multiple paths exist, which are separated by a slash symbol. Identical linkages in sequence (*e.g.* "K48,K48,K48") can be abbreviated as multiplication indicated with "x" (*i.e.* "K48x3"). Optionally, "$_{\#Ub}$" in subscript is included to improve readability by indicating the number of Ub units in a chain (*i.e.* the length for unbranched chains). "#P" is a pointer that indicates specific moieties along a path in form of a number, a list of numbers separated by commas, a range defined by a minus symbol, or a list of ranges. The number indicates the position of the specified Ub moiety along the path, where 1 is the proximal moiety. The pointer is followed by a statement ("mut") in brackets, which contains residue specific information such as amino acid substitutions or labels. An advantage of this system is that topology and listing of substitutions or modifications can be separated and that different

statements can unambiguously describe the same Ub chain. This is especially useful for complex polymers and provides leeway to highlight specific features of a Ub chain.

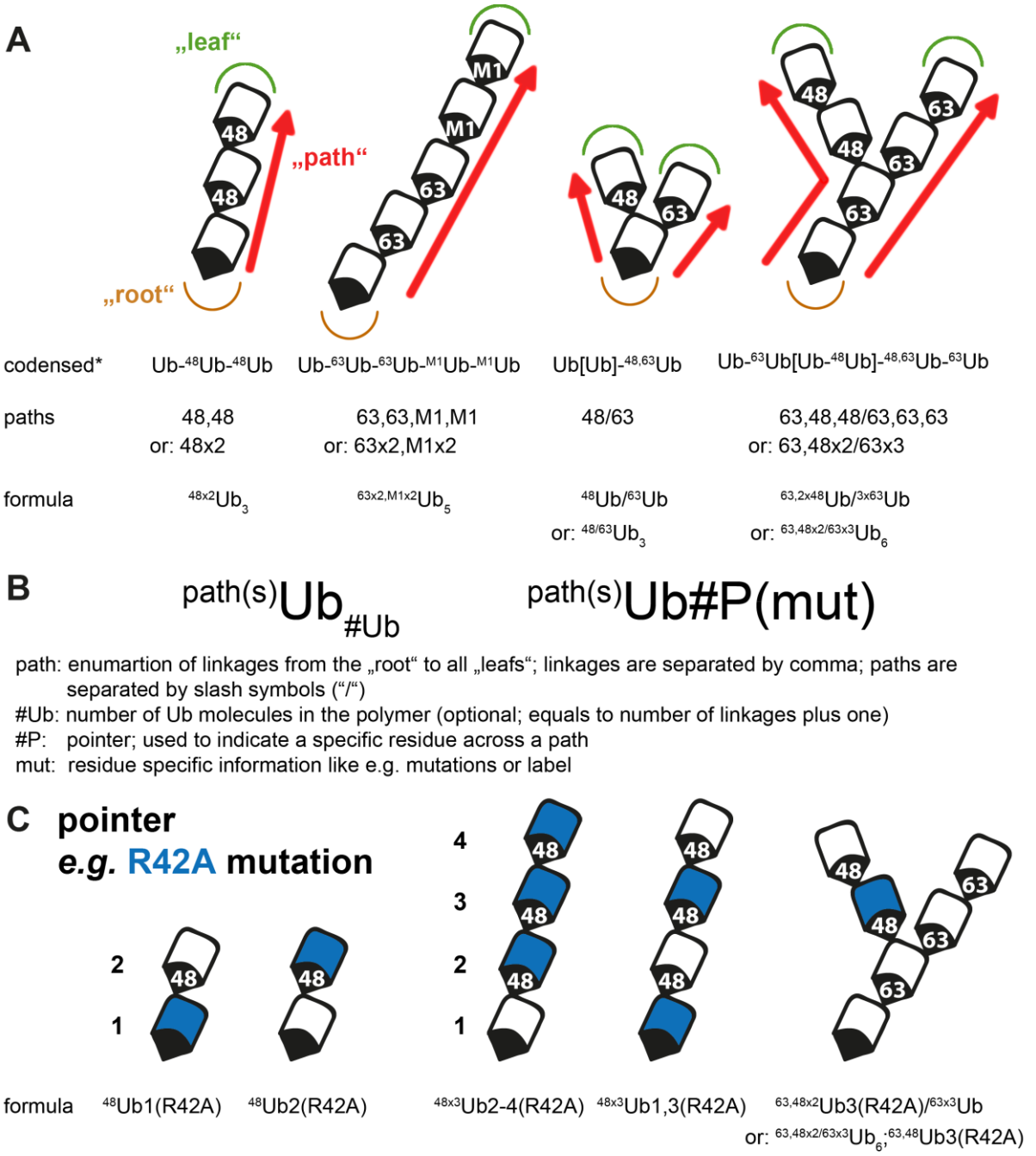

Figure 4: Notation of Ub chains in this work. (A) The topology of every Ub polymer can be fully described by enumerating all paths, *i.e.* the sequence of linkages from the proximal moiety (“root”) to each distal moiety (“leaf”). Condensed sum formula indicated with an asterisk describes the notations suggested by Nakasone *et al.*[60] (B) Formulas used in this work to name polyubiquitin molecules. (C) Pointers indicate residue specific information such as the location of the R42A substitution.

1.4 Aims of this study

The aim of this study is to explore how Ub binding interfaces can stimulate the assembly of polyubiquitin chains, specifically in the context of the activity of E2 ubiquitin-conjugating enzymes. To this end, the two E2 enzymes Ubc1 and Ubc7 should be studied. Both enzymes rely on associated Ub binding domains (UBDs) for stimulation. K48 chain assembly through Ubc7 relies on activation through the co-factor Cue1 which harbours a Ub binding CUE domain.[84] Similarly, the Ub binding UBA domain in Ubc1 is thought to promote K48 chain assembly by Ubc1[126], although this is still under debate due to conflicting results of several studies[123,127]. How exactly Ub binding facilitates the activation of these systems remained elusive.

The following objectives were set:

- Investigate CUE domain specific activation of Ubc7 by Cue1 in collaboration with Dr. Maximilian von Delbrück (MDC, Berlin) and Dr. Andreas Kniss (Goethe University, Frankfurt).
- Elucidate whether the UBA domain of Ubc1 facilitates Ub chain formation.
- Investigate mechanistic details of Ubc1 activity in the context of its UBA domain.
- Identify cellular processes affected by this activity and study their biological outcome.

2. Results

2.1 Binding of ubiquitin by Cue1 enables rapid elongation of K48 chains by Ubc7

2.1.1 The CUE domain of Cue1 facilitates assembly of K48-linked polyubiquitin chains by binding to the penultimate Ub moiety

Previous studies show that the E2 ubiquitin-conjugating enzyme Ubc7 relies on association with its Ub binding cofactor Cue1 for activation.[84] However, the exact mechanism of how Ub binding can stimulate Ub chain elongation remained largely unclear. To elucidate factors contributing to CUE domain mediated chain elongation through Ubc7, we performed *in vitro* ubiquitination experiments with Ubc7 and the cytosolic fragment of Cue1 (Ubc7/Cue1) in presence of fluorescent donor Ub and different acceptor Ub molecules, which were C-terminally hexahistidine-tagged (Figure 5). Ubc7 targets K48 in Ub exclusively and, thus, only the distal moiety in K48 chains. Therefore, K63 chains used in the experiment harboured Ub(K48R) in all moieties except the distal one. The substrate turnover was observed by fluorescence anisotropy and average initial reaction rates were calculated from three experiments. Reactions were faster for longer Ub chains than for shorter chains and faster for K48 chains than for K63 chains (Figure 5A).

To investigate whether binding to specific positions within a K48 chain is necessary for Ubc7/Cue1 activity, we performed *in vitro* ubiquitination experiments, before which the CUE domain was cross-linked to distinct Ub moieties within K48-linked diubiquitin ($^{48}Ub_2$) or triubiquitin ($^{48x2}Ub_3$) (Figure 5B). Cross-linking the CUE domain to the proximal position in $^{48}Ub_2$ led to the fastest Ub turnover, while cross-linking to the proximal position in $^{48x2}Ub_3$ led to slightly slower turnover. In contrast, cross-linking of the CUE domain to the distal position in $^{48}Ub_2$ reduced reaction rates as compared to non-cross-linked components (Figure 5B). In summary, this shows that Ubc7 is optimally activated through binding of the CUE domain to the penultimate moiety in a K48 chain.

To corroborate these findings, we aimed to perform single turnover ubiquitination experiments with acceptor Ub deficient in binding to the CUE domain. As R42 in Ub is pivotal for interaction with the CUE domain (see below), we introduced Ub(R42A) into different positions of K48-linked tetraubiquitin ($^{48x3}Ub_4$) and performed single turnover ubiquitination experiments as described above. Introduction of Ub(R42A) into the penultimate moiety of $^{48x3}Ub_4$ reduced

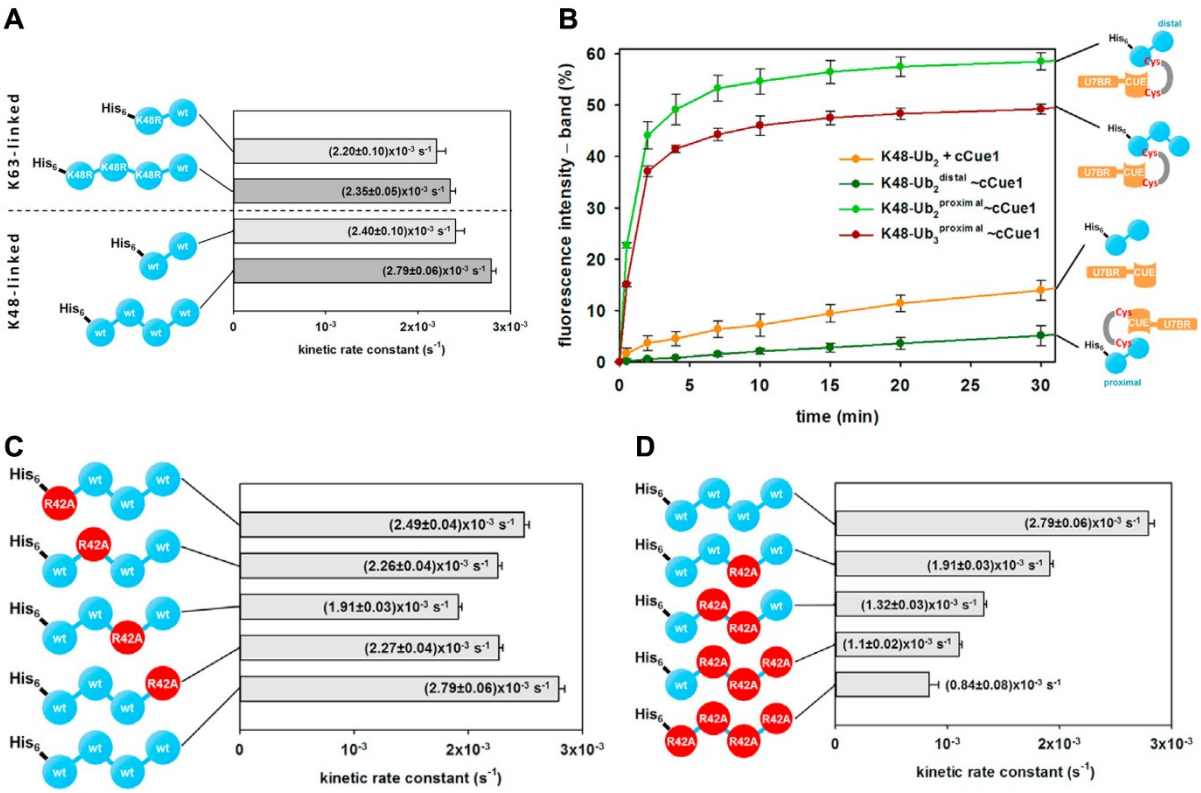

Figure 5: Binding of the CUE domain of Cue1 to the penultimate moiety in K48 chains stimulates chain assembly by Ubc7. (A) Initial reaction rates were determined for single turnover ubiquitination experiments with Ubc7/Cue1 in presence of different Ub chains as acceptors. (B) *In vitro* ubiquitination experiments were performed with Ubc7 and Cue1 T66C C147S, which was cross-linked to different Ub chains containing Ub(T9C). Cue1 was cross-linked to the proximal position in $^{48}Ub_2$ (light green), $^{48x2}Ub_3$ (red) or to the distal position in $^{48}Ub_2$ (dark green). A reaction with equimolar amounts of Cue1 and $^{48}Ub_2$ was performed as reference (orange). (C) Single turnover ubiquitination experiments as in A were performed in presence of $^{48x3}Ub_4$ as acceptor with Ub(R42A) in different positions. (D) The experiment in C was repeated with $^{48x3}Ub_4$ harbouring an increasing amount of Ub(R42A) moieties. Error bars show average and SEM of three experiments. Figure adapted from von Delbrück *et al.*[1] Experiments performed by Dr. Maximilian von Delbrück.

kinetic rates the most, while Ub(R42A) located at the proximal moiety had the smallest impact (Figure 5C). Additional Ub(R42A) moieties in a Ub chain with Ub(R42A) at the penultimate position cause a further reduction of kinetic rates (Figure 5D). Proposedly, Ub binding by Cue1 activates Ubc7 not only by arranging the involved proteins in an energetically favourable way, but also by increasing the local concentration of the enzyme near its substrate.

To investigate binding of the CUE domain towards K48 chains, we created K48- and K63-linked diubiquitin molecules, which were ^{15}N-labeled, either at the proximal or distal position. These probes were then applied to NMR titration experiments with the CUE domain. Chemical shift perturbations (CSPs) in Ub upon binding showed that the residues I44, L8, V70, R42, G47

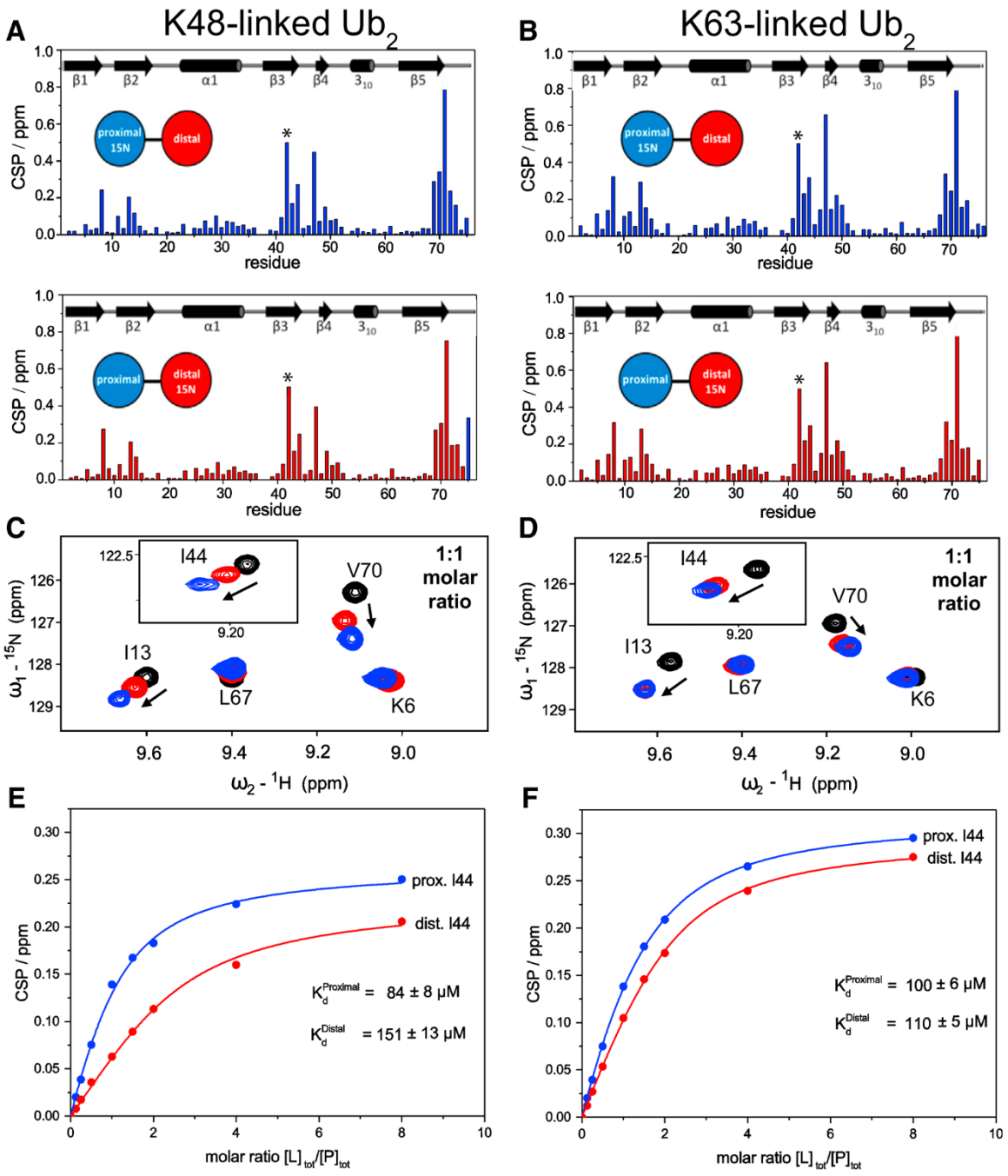

Figure 6: G75 in the proximal moiety of $^{48}Ub_2$ contributes to an enhanced binding interface with the CUE domain. Chemical shift perturbations (CSP) were quantified for the backbone amides in (A) $^{48}Ub_2$ and (B) $^{63}Ub_2$ respectively upon binding of the CUE domain to the proximal (blue) or the distal Ub moiety (red). The CSP for R42 is marked with an asterisk and arbitrarily set to 0.5. The signal for this residue disappeared during titration with the CUE domain and therefore its CSP could not be determined. ^{15}N-^{1}H-HSQC spectra were recorded at a 1:1 molar ratio of (C) CUE:$^{48}Ub_2$ and (D) CUE:$^{63}Ub_2$ for either proximally (blue) or distally (red) labelled Ub_2 as well as for Ub_2 (black) in absence of CUE domain. A representative section is shown. The CSP of I44 was plotted over the concentration ratio of CUE domain over (E) $^{48}Ub_2$ and (F) $^{63}Ub_2$ respectively. K_d values for binding of the CUE domain were determined assuming two independent but different binding sites. Figure as published in von Delbrück *et al.*[1] Sample preparation was performed jointly. NMR titration experiments and analyses were performed by Dr. Andreas Kniss.

and L71 were prominently involved in binding. They cluster around the hydrophobic patch in Ub. Interestingly, the CSP of G75 in the distal moiety in $^{48}Ub_2$ showed a significantly larger CSP than in the proximal moiety (Figure 6A), which could not be observed for $^{63}Ub_2$ (Figure 6B). This indicates that G75 in the distal Ub enlarges the binding interface between the CUE domain and the proximal moiety in $^{48}Ub_2$.

Accordingly, an overlay of the ^{15}N-^{1}H-HSQC spectra at a 1:1 molar ratio of CUE:$^{48}Ub_2$ revealed distinct CSPs between the individual moieties for residues involved in binding (Figure 6C). Residues in the proximal moiety of $^{48}Ub_2$ showed stronger CSPs than corresponding residues in the distal moiety as compared to unbound $^{48}Ub_2$. Such a difference could not be observed for $^{63}Ub_2$ (Figure 6D). We determined K_d values based on the CSP of I44 in Ub at different concentrations of diubiquitin and CUE domain (Figure 6E and F). The CUE domain showed a two-fold increase in binding affinity towards the proximal Ub in $^{48}Ub_2$ over other Ub moieties (Figure 6E and F). In other words, Cue1 preferentially associates with Ub moieties within a K48 chain over the distal one. This preference mirrors the binding sites for the CUE domain, which we showed to be optimal for Ubc7 activation.

Based on the NMR binding studies, we created a set of Cue1 variants with amino acid substitutions E96A, E100A and L103A, which showed increasingly lower binding affinities for Ub as measured by CSPs of V73, L76 and A77 (Figure 7A). We assessed the ability of these variants to promote Ub chain formation by Ubc7 in single turnover ubiquitination experiments (Figure 7B). To this end, elongation of $^{48x3}Ub_4$ with fluorescently labelled monoubiquitin by Ubc7/Cue1 was monitored by fluorescence anisotropy in the presence of Hrd1 RING-domain. Quantification of initial rates for the different variants correlates with CSPs observed in binding experiments (Figure 7A,B).

Next, we aimed to investigate the impact of the amino acids substitutions on Ubc7 activity in the living cell. Thus, constructs, which induce the expression of the Cue1 variants, were introduced into *S. cerevisiae* deleted for endogenous *cue1*. Subsequently, the degradation of Ubc6, which is dependent on Ubc7 activity[84], was analysed in cycloheximide chase assays (Figure 7C). We employed constructs encoding wild-type Cue1 or binding deficient Cue1 (Cue1-RGA) as references. Cue1-RGA, in which the LAP motif (aa76-78) was substituted for RGA, was previously shown to harbour an unfolded CUE domain.[84] Protein degradation was chased for three hours. Samples were analysed by SDS-PAGE and western blotting with the indicated antibodies. Sec61 served as input control. All Cue1 constructs showed equal expression levels and were not degraded during the chase (Figure 7C). Ubc6 degradation was

strongly impaired in yeast harbouring Cue1-RGA, while the Cue1 variants with moderately reduced binding affinity caused impaired Ubc6 degradation (Figure 7D). Evidently, gradual decrease of binding affinity of the CUE domain for Ub correlates with impeded chain elongation activity *in vitro* and substrate turnover *in vivo*.

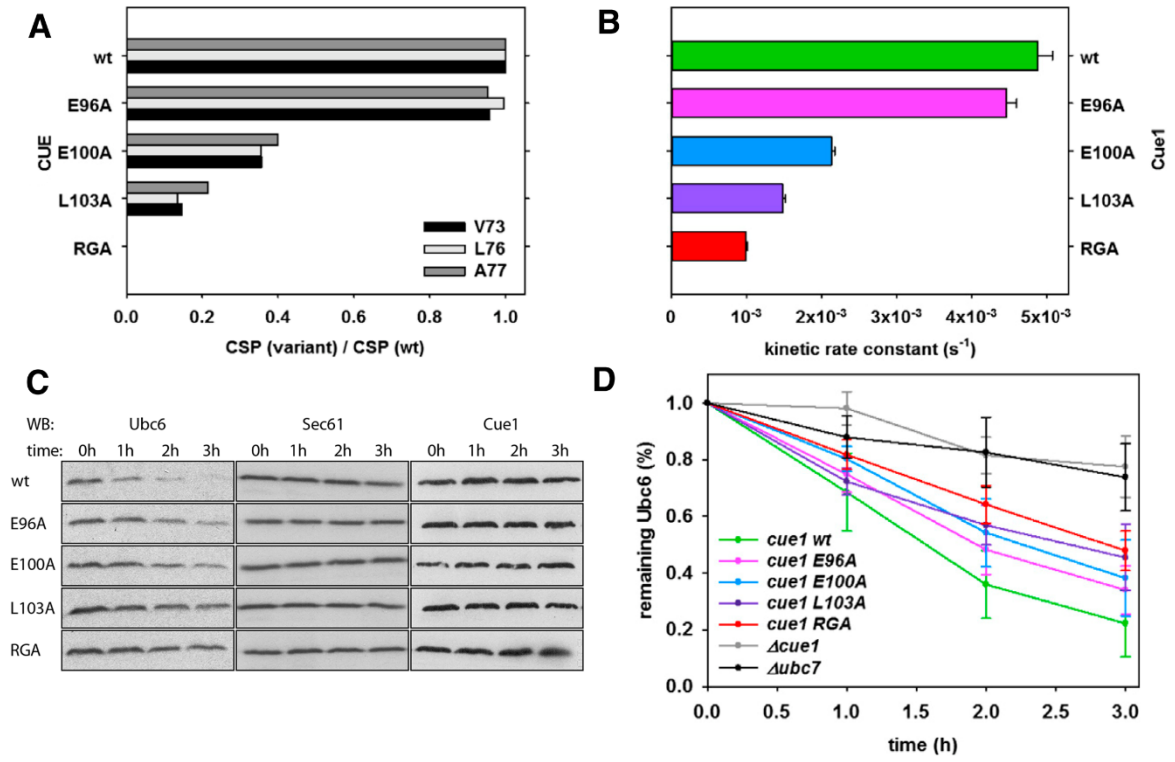

Figure 7: Reduced binding affinity of the CUE domain to Ub correlates with an impaired ability to stimulate Ubc7 activity *in vitro* and *in vivo*. (A) CSPs of V73, L76 and A77 in Ub were measured in NMR titration experiments at a 1:8 molar ratio of CUE domain to Ub. CSPs for different Cue1 variants were normalised to wild-type. Experiment performed by Dr. Andreas Kniss. (B) Initial reaction rates with $^{48x3}Ub_4$ were determined in single turnover ubiquitination experiments with Ubc7 and different Cue1 variants in presence of the Hrd1 RING-domain. Average of three experiments. Error bars are SEM. Experiment performed by Dr. Maximilian von Delbrück. (C) The degradation of the ERAD substrate Ubc6 was observed in *S. cerevisiae* expressing different Cue1 variants by cycloheximide chase assays. Samples were taken at the indicated time points and analysed by SDS-PAGE and western blotting with the indicated antibodies. (D) Band intensity for Ubc6 from C was quantified, normalised to the starting time point, averaged for each construct over a triplicate and plotted over time. Error bars indicate SEM. Data from a separate experiment was included, which shows degradation of Ubc6 in yeast deleted for *ubc7* (black) or *cue1* (gray). Figure modified from von Delbrück *et al.*[1]

2.1.2 Binding of the Cue1 CUE domain to K48 chains relies on conformational selection

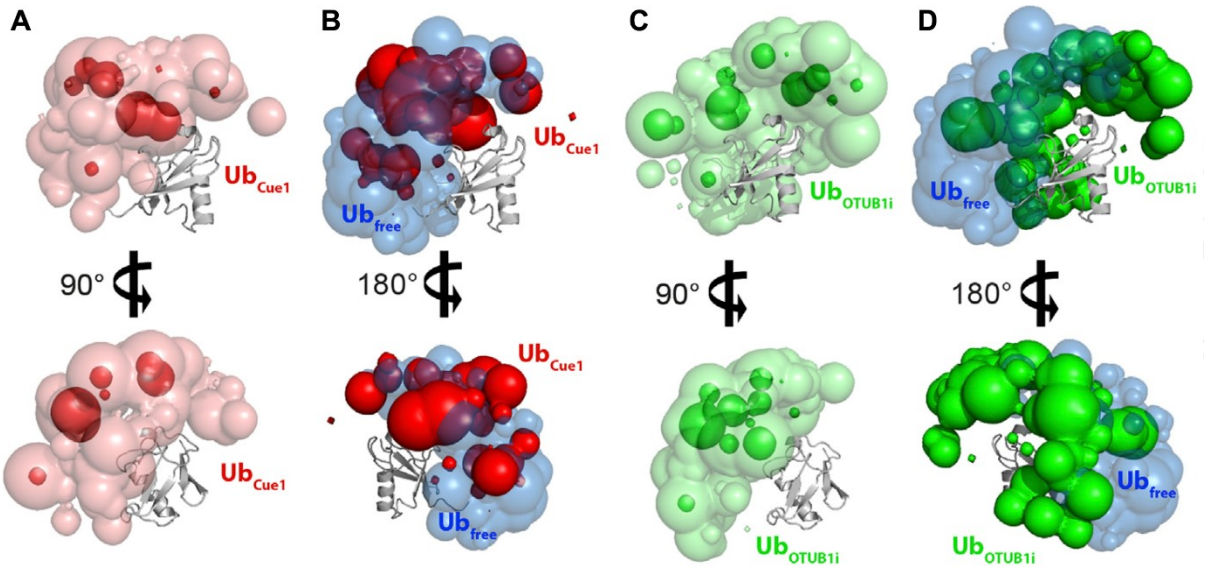

Figure 8: Ub binding proteins differently affect the conformational space of $^{48}Ub_2$. A conformational ensemble of $^{48}Ub_2$ was obtained through PELDOR spectroscopy and molecular modelling. The proximal Ub is shown in grey, while the position of the distal Ub is depicted as probability grid. (A) $^{48}Ub_2$ in presence of Cue1 CUE domain with probability cut-offs at 0.12 (pink) and at 0.4 (red). (B) $^{48}Ub_2$ in absence (blue) and presence (red) of Cue1 CUE domain with probability cut-offs at 0.2. (C) $^{48}Ub_2$ in presence of OTUB1-C91A with probability cut-offs at 0.12 (light green) and 0.4 (dark green). (D) $^{48}Ub_2$ in absence (blue) and presence (green) of OTUB1-C91A with probability cut-offs at 0.2. Figure adapted from Kniss *et al.*[2]

Ub chains are flexible and may adopt variable conformations, which affects how Ub binding proteins can interact with these chains. We hypothesised this layer of regulation might be particularly important for proteins mediating assembly or disassembly of chains. To investigate conformational space of $^{48}Ub_2$, PELDOR spectroscopy was combined with molecular modelling. In essence, PELDOR spectroscopy was used to record distance distributions between spin labelled amino acids introduced into the proximal and distal moiety of diubiquitin. Spectra were recorded for multiple spin label pairs located in different positions of $^{48}Ub_2$. The distance distributions were then used as restrains and probability factors for structural modelling by CYANA 3.9. The weighted structure ensemble was visualised as probability grid of the position of the geometric centre of the distal Ub (aa1-71). This novel approach revealed that K48 chains adopt a wide conformational space, which includes the closed conformation[66] reported by X-ray crystallography as one of many possible conformations. The CUE domain of Cue1 was found to stabilise conformations, which are inherently adopted by $^{48}Ub_2$ (Figure 8A,B), whereas other binders, for example OTUB1, were found to remodel the conformational distribution of these chains (Figure 8C,D).

2. Results

In order to examine how the binding mode of the CUE domain affects chain elongation by Ubc7, we performed single turnover ubiquitination experiments. A construct harbouring Ubc7 as well as the activating U7BR-domain from Cue1 (Ubc7-U7BR) was devised to separate the Ub binding activity of Cue1 from its activating activity through the U7BR domain (Figure 9A). We tested the ability of this enzyme to extend K48-linked diubiquitin and tetraubiquitin in the presence and absence of different Ub binding proteins (Figure 9B). Fluorescently labelled monoubiquitin and C-terminally blocked acceptor Ub were used in a 1:10 molar ratio. Acceptor Ub was either K48-linked diubiquitin or tetraubiquitin. Samples were taken over 15 min and analysed by SDS-PAGE and fluorescence scans. Ub binders were added in a 2:1 molar ratio to Ub in reactions with diubiquitin and 4:1 molar ratio in reactions with tetraubiquitin. Next to the Cue1 CUE domain, we employed the CUE domain of the human homologue gp78. A previous study shows that this domain has a higher binding affinity for Ub and apparently does not promote the position specific binding observed for Cue1.[128] The UBA2 domain of Rad23A preferentially associates with K48 diubiquitin by interacting with both moietites akin to Cue1 but also binds with higher affinity.[81] Ultimately, the K48 specific DUB OTUB1, which belongs to the Otubain protease family, was employed in the experiment by substituting the active site C91 with alanine. We found that all Ub binders impaired the elongation activity. This might occur due to obstruction of the acceptor K48 and/or through unfavourable conformational remodelling of the acceptor Ub chain. Quantification of initial reaction rates revealed a reduction of initial rates by ~30% in presence of the CUE domain whereas other binders diminish the initial rates by 70% or more (Figure 9C). Evidently, binding of Ub by the CUE domain minimally impairs chain elongation.

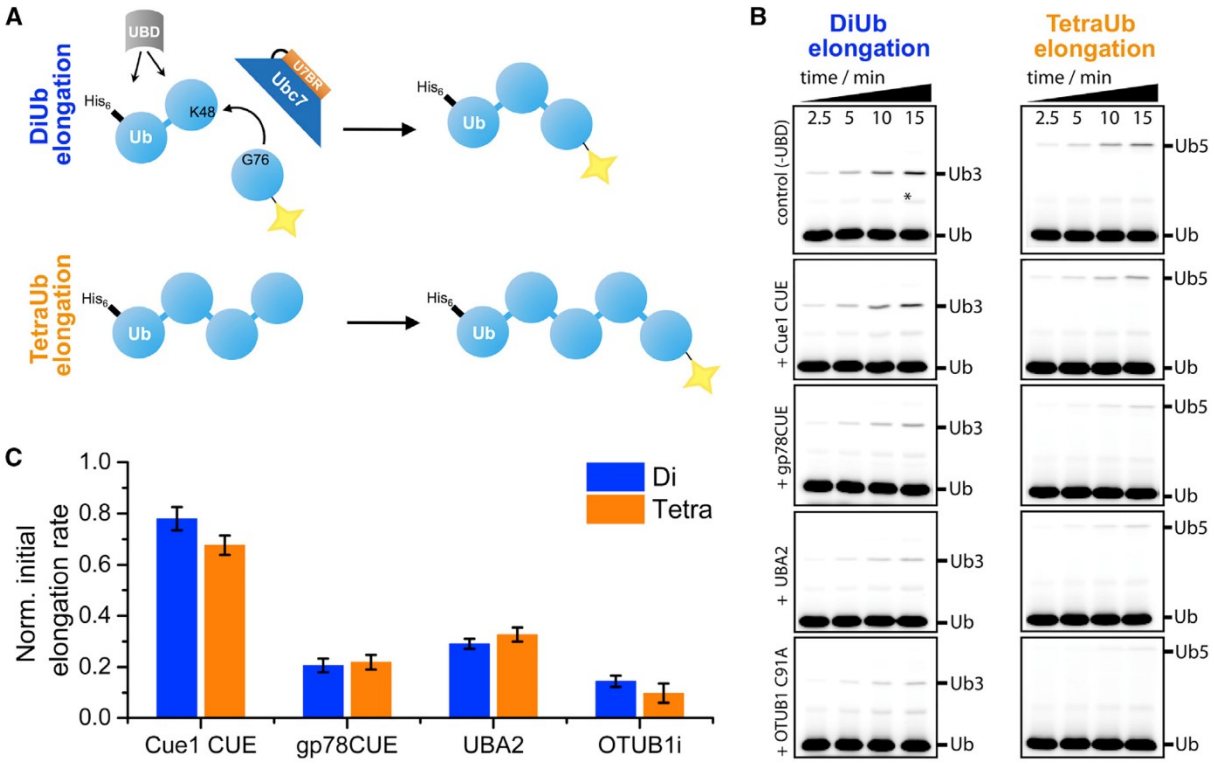

Figure 9: Ub binding proteins differently affect elongation of Ub chains by Ubc7-U7BR. (A) Overview of *in vitro* chain elongation reactions with Ubc7-U7BR. (B) *In vitro* chain elongation reactions with fluorescent donor Ub and $^{48}Ub_2$ or $^{48x3}Ub_4$ as acceptor were performed with Ubc7-U7BR in presence of different Ub binders. Samples were taken at the indicated time points and analysed by SDS-PAGE and fluorescence scan. Asterisk indicates diubiquitin, which is formed as product of a side reaction. (C) Fluorescence intensity of Ub_3 or Ub_5 over total fluorescence per lane was quantified from B and plotted over time. Initial reaction rates were determined as slope of a linear approximation and normalised to reaction rates without Ub binders. Error bars indicate average and SEM of three experiments. Figure adapted from Kniss *et al.*[2]

2.1.3 Putative Ubc7 dimerisation facilitates formation of diubiquitin

During our analysis of chain elongation reactions by Ubc7-U7BR we observed formation of diubiquitin as a side reaction (Figure 9B, asterisk). This occurred despite the relatively high ratio of acceptor Ub (10 µM Ub_A) to donor Ub (1 µM Ub_D). We repeated the experiment with titrations of various reaction components. While changing the concentration of E1 enzyme had no impact on the pattern of reactions products (data not shown), reducing the concentration of E2 enzyme yielded higher amounts of diubiquitin (Figure 10A). Reduced Ubc7-U7BR levels should increase the ratio of Ubc7-U7BR charged with Ub (Ubc7-U7BR~Ub) to uncharged enzyme (Ubc7-U7BR) in the reaction. We hypothesised that a high ratio of Ubc7-U7BR~Ub to Ubc7-U7BR might facilitate diubiquitin assembly through dimerisation of Ubc7-U7BR~Ub (Figure 10B). In contrast, a higher concentration of Ubc7-U7BR leads to increased formation of dimers between Ubc7-U7BR~Ub and Ubc7-U7BR, which are apparently incapable of diubiquitin formation. Increased salt concentrations in the experimental setup led to a reduced formation of diubiquitin, while assembly of triubiquitin was only slightly impaired (Figure 10C). This suggests that the dimer formation by Ubc7-U7BR charged with Ub, relies predominantly on electrostatic interactions. We aimed to validate our findings about the Ubc7-U7BR fusion protein using wild-type Ubc7. Thus, Ubc7 was investigated in *in vitro* ubiquitination reactions with the same conditions, in presence of either wild-type Cue1 or its binding deficient RGA variant[84] (Figure 10D). In both cases, formation of diubiquitin from Ub_D could be observed despite the ten-fold molar excess of Ub_A over Ub_D. However, in presence of wild-type Cue1 the assembly of triubiquitin was favoured, which can be attributed to acceleration of chain formation by the CUE domain. Analytical size exclusion experiments with Ubc7-U7BR(C89K) stably loaded with Ub showed salt concentration dependent elution profiles (Figure 10E). With lower ionic strength of the buffer the elution peak shifted toward fractions with higher apparent molecular weight, indicative of dimer formation.

A Ubc7 variant, which is capable of chain elongation, but does not readily form diubiquitin, would be desirable to investigate the significance of Ubc7 dimerisation *in vivo*. Thus, we created multiple Ubc7-U7BR constructs harbouring mutations in sequences coding for amino acids in the acidic loop (D98, D99, E104, E107, E108) and charged residues close to the active site (R109, D146, R145). *In vitro* chain elongation reactions showed that the Ubc7-U7BR variants were impaired in diubiquitin and triubiquitin formation (Figure 10F) with the exception of Ubc7-U7BR(D146R), which showed hyperactive formation of both products. Future attempts to create Ubc7 variants with the desired probabilities should be preceded by additional structural investigation of Ubc7 dimer formation. Further analyses are required to evaluate the role of Ubc7 dimerisation in the living cell.

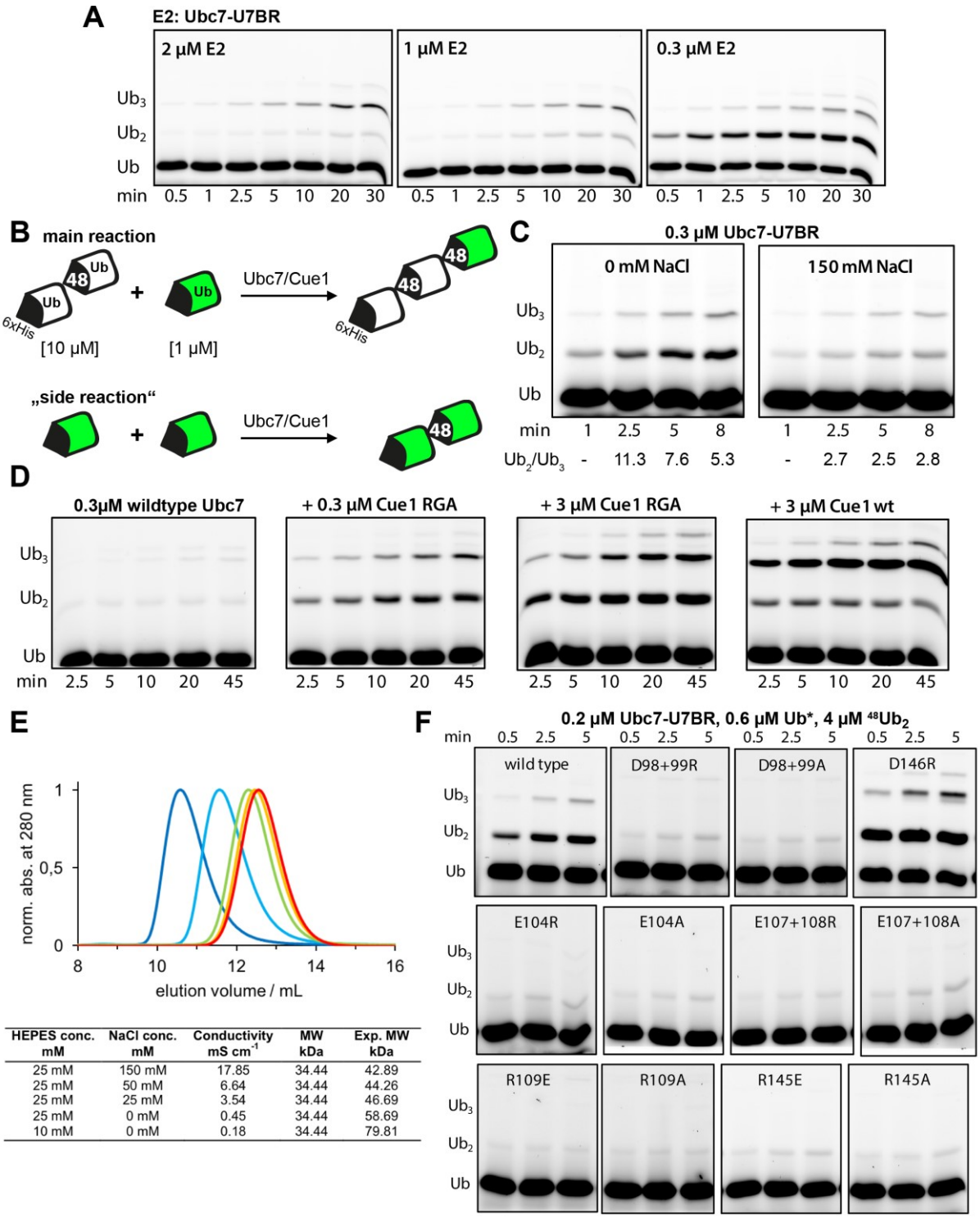

HEPES conc. mM	NaCl conc. mM	Conductivity mS cm^{-1}	MW kDa	Exp. MW kDa
25 mM	150 mM	17.85	34.44	42.89
25 mM	50 mM	6.64	34.44	44.26
25 mM	25 mM	3.54	34.44	46.69
25 mM	0 mM	0.45	34.44	58.69
10 mM	0 mM	0.18	34.44	79.81

Figure 10: Putative Ubc7 dimerisation facilitates formation of diubiquitin. (A) *In vitro* chain elongation experiments were performed in presence of different concentrations of Ubc7-U7BR. Samples were taken at indicated time points and analysed by SDS-PAGE and fluorescence scan. (B) Schematic representation of reaction pattern observed in A. (C) Chain elongation reaction from A (right panel) was repeated in absence and presence of 150 mM NaCl. Fluoresnce intensity of reaction products was quantified and the ratio of Ub_2 to Ub_3 was calculated. Signal intensity for t=1 min was too low for quantification. (D) Chain elongation reaction from A (right panel) was repeated with wild-type Ubc7 and Cue1 or Cue1-RGA instead of Ubc7-U7BR. (E) Analytical size exclusion experiments with Ubc7-U7BR (C89K) stably loaded with Ub were performed by Dr. Andreas Kniss at different salt concentrations. Apparent molecular weights were calculated based on a calibrated Superdex 75 10/300 GL and are listed below the elution profiles. (F) *In vitro* chain elongation experiments with Ubc7-U7BR variants with different amino acid substitutions.

2.2 The UBA domain of Ubc1 facilitates the assembly of K48/K63 branched chains

2.2.1 Structural analysis of Ubc1

2.2.1.1 Analysis of existing structural information on Ubc1 and its homologue Ube2K

Previous studies suggest that the UBA domain of Ubc1 assists in assembly of K48 chains through binding of Ub,[112] while other reports challenge this observation.[123,127] I aimed to analyse existing structural information on Ubc1[105] and its human homologue Ube2K[124,129,130,131] in order to assess whether these enzymes might exploit a similar reaction mechanism to Ubc7 and Cue1. Based on X-ray crystallographic data for Ube2K and HADDOCK modelling, an interaction interface between acceptor Ub (Ub_A) and the UBC domain has been proposed[124] (Figure 11A). This Ube2k/Ub_A complex was validated through mutagenesis studies and *in vitro* ubiquitination experiments.[124] Interestingly, G76 in the modelled Ub_A is located on the opposite side relative to the position of the UBA domain (Figure 11B). This positioning is incompatible with the UBA domain binding to a proximal Ub moiety relative to the immediate Ub_A. Thus, this geometry presents a stark contrast to Ubc7/Cue1, which requires binding of the penultimate moiety in a Ub chain for activation. Several X-ray crystallographic structures of Ube2k are available from the protein databank (PDB: 5DFL, 6IF1, 3E46, 3F92, 3K9P). In all of these structures the UBA domain closely coordinates with the UBC domain through a hydrophobic interface.[130] In contrast to this, an NMR solution structure of Ubc1 reveals high flexibility in the linker region of Ubc1 (aa151-167) located between the UBA domain and the UBC domain (Figure 11C). Despite this high flexibility, no conformation was observed that allows for the association of the UBA domain with a proximal Ub highlighting the contrast to Ubc7/Cue1.

Lee et al.[131] report a structure of Ube2K (PDB: 6IF1) in complex with $^{48}Ub_2$, in which two Ube2K molecules are coordinated through their UBA domain with either the proximal or the distal moiety of the diubiquitin molecule respectively. Structural comparison of the Ube2K molecules reveals an identical conformation of the UBC domain, UBA domain and the Ub moiety coordinated by the UBA domain. Ko *et al.*[130] report structures of Ube2K in complex with monoubiquitin or a mutant Ub (UBB+1), which has been implicated in the regulation of amyloid-β neurotoxicity, and also display the same general topology of UBC domain, UBA domain and Ub_{dist} (PDB: 3K9P and 3K9O). Across multiple studies equivalent binding interfaces between Ub and UBA domain of Ube2K were reported[130,131,124] (PDB:

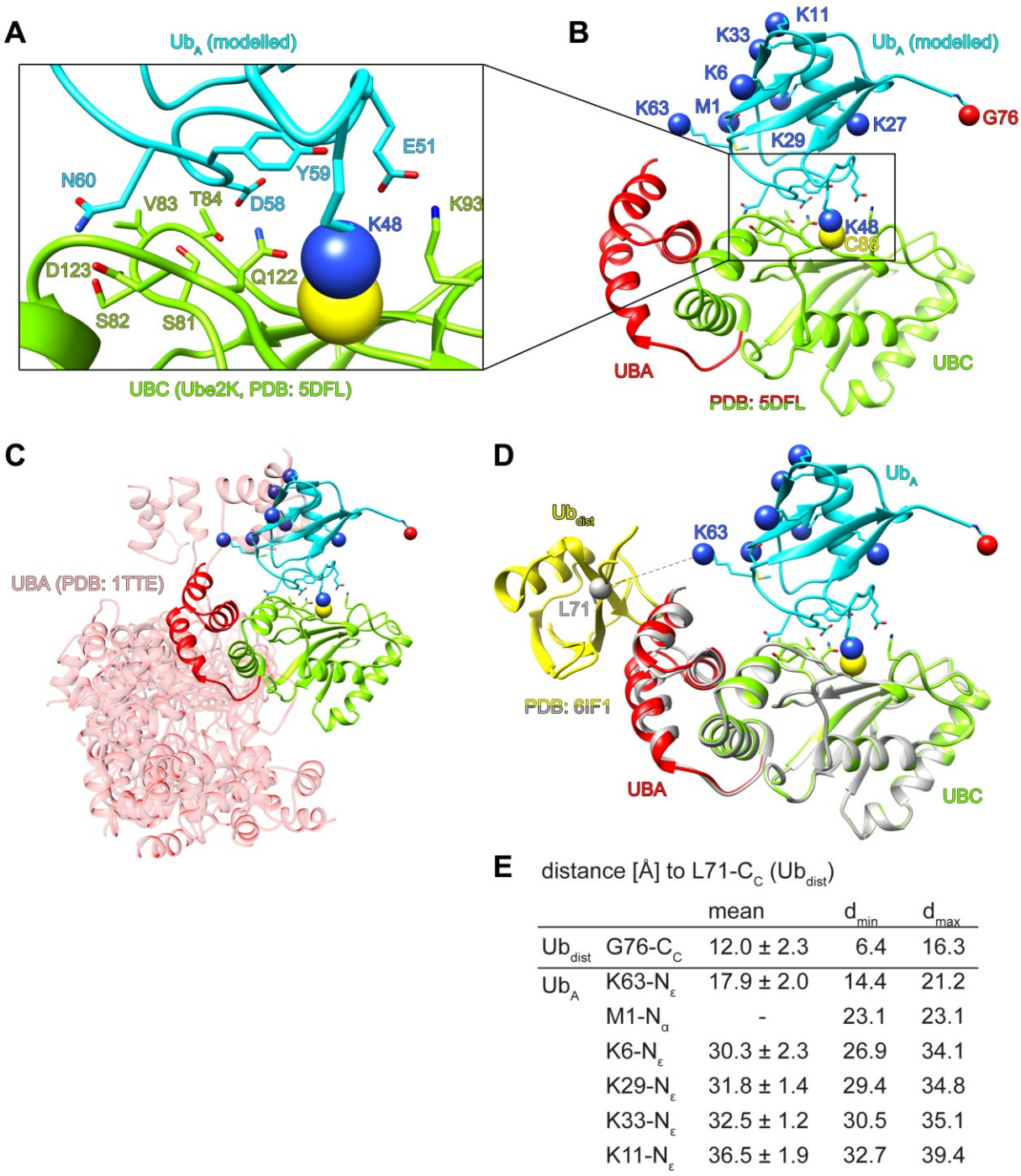

E distance [Å] to L71-C_C (Ub_{dist})

		mean	d_{min}	d_{max}
Ub_{dist}	G76-C_C	12.0 ± 2.3	6.4	16.3
Ub_A	K63-N_ε	17.9 ± 2.0	14.4	21.2
	M1-N_α	-	23.1	23.1
	K6-N_ε	30.3 ± 2.3	26.9	34.1
	K29-N_ε	31.8 ± 1.4	29.4	34.8
	K33-N_ε	32.5 ± 1.2	30.5	35.1
	K11-N_ε	36.5 ± 1.9	32.7	39.4

Figure 11: Compilation of existing structural information on Ubc1 and Ube2K. (A) The interaction interface between Ub_A (teal) and the UBC domain (green) of Ube2K (PDB: 5DFL) was replicated according to HADDOCK modelling by Middleton and Day.[124] (B) Selected atoms in the complex of Ub_A and Ube2K are highlighted as spheres: C in carboxy group of Ub_A G76 (red), S in Ube2K active site Cys (yellow), N in Ub_A ε –amino groups of Lys-residues and in the backbone of M1 (blue). (C) An NMR ensemble of Ubc1 (PDB: 1TTE) was superimposed through alignment of the UBC domain on the model from A. The linker region connecting the UBA domain (red, transparent) and the UBC domain shows high flexibility.[105] (D) The structure of Ube2K with Ub bound to the UBA domain (PDB: 6IF1) was superimposed on the model from A. L71 in the C-terminus of Ub_{dist} is represented as white sphere. (E) Distances were measured in the model complex for different known conformations.

6IF1, 3K9P, 5DFL), which are consistent with structures of other UBA domains in complex with Ub as shown for UBR5 (PDB: 2QHO)[132] and Dsk2 (PDB: 4UN2)[133]. Superimposition of Ube2K, which binds Ub (Ub_{dist}) through the UBA domain (PDB:6IF1), with the Ube2K/Ub_A complex reveals that Ub_{dist} resides in close proximity to Ub_A (Figure 11D). This data supports a model in which the UBA domain associates with a distal Ub moiety relative to the immediate acceptor Ub.

To evaluate whether Ub_{dist} and Ub_A are sufficiently close to be covalently linked, I assessed distances between Ub_{dist} and Ub_A in different known protein conformations using Chimera 1.13 (Figure 11E). For a covalent bond to be possible in the model complex the carboxy C-atom in G76 of Ub_{dist} needs to be located within 1.32 Å of an N-atom in a lysine side chain or the backbone amino group of M1 in Ub_A. Because Ub has a highly flexible C-terminus between L71 and G76 (Figure 2B), I measured the distance between the carboxy C-atoms (C_C) of L71 and G76 in an NMR ensemble of 116 structures (PDB: 2K39). The average distance was 12.0 ± 2.3 Å with a maximal distance of 16.3 Å. Thus, a putative attachment site in Ub_A should be no further than 17.6 Å away from L71-C_C. The distance between L71-C_C and N_ε-atoms in Ub_A was measured for the 25 most frequent Lys-rotamers.[134] The ε-amino group in K63 (K63-N_ε) was found to be the closest attachment site in Ub_A with a minimal distance of 14.4 Å, which is compatible with a covalent link between Ub_{dist} and Ub_A. The next closest attachment was found to be M1-N_α, which was at a distance of 23.1 Å from L71-C_C. All other possible attachment sites were at least 26.9 Å away. In conclusion, I propose based on previously reported structural information that the UBA domain associates with a Ub moiety in a distal position relative to the immediate acceptor Ub. Moreover, the presented structural model implies that association of the UBA domain with the UBC domain creates a binding interface suitable for interaction with two adjacent Ub moieties in a K63 chain.

2.2.1.2 Purification of Ubc1 cross-linked to K63-linked diubiquitin for crystallisation

To explore the putative association of Ubc1 with K63 chains, which I also confirmed in *in vitro* binding experiments and activity assays (sections 2.2.2 and 2.2.3), I aimed to investigate a complex of Ubc1 and $^{63}Ub_2$ by X-ray crystallography. To this end, a purification strategy was devised, in which the active site of Ubc1 should be cross-linked through ethane-dithiol (EDT) to acceptor Ub with a K48C substitution. This should be achieved through sequential transthiolation reactions (Figure 12A), which exploit activation of sulfhydryl groups with 2,2-dithiodipyridine (AT2). By using EDT to connect the two molecules, a product (Figure 12B)

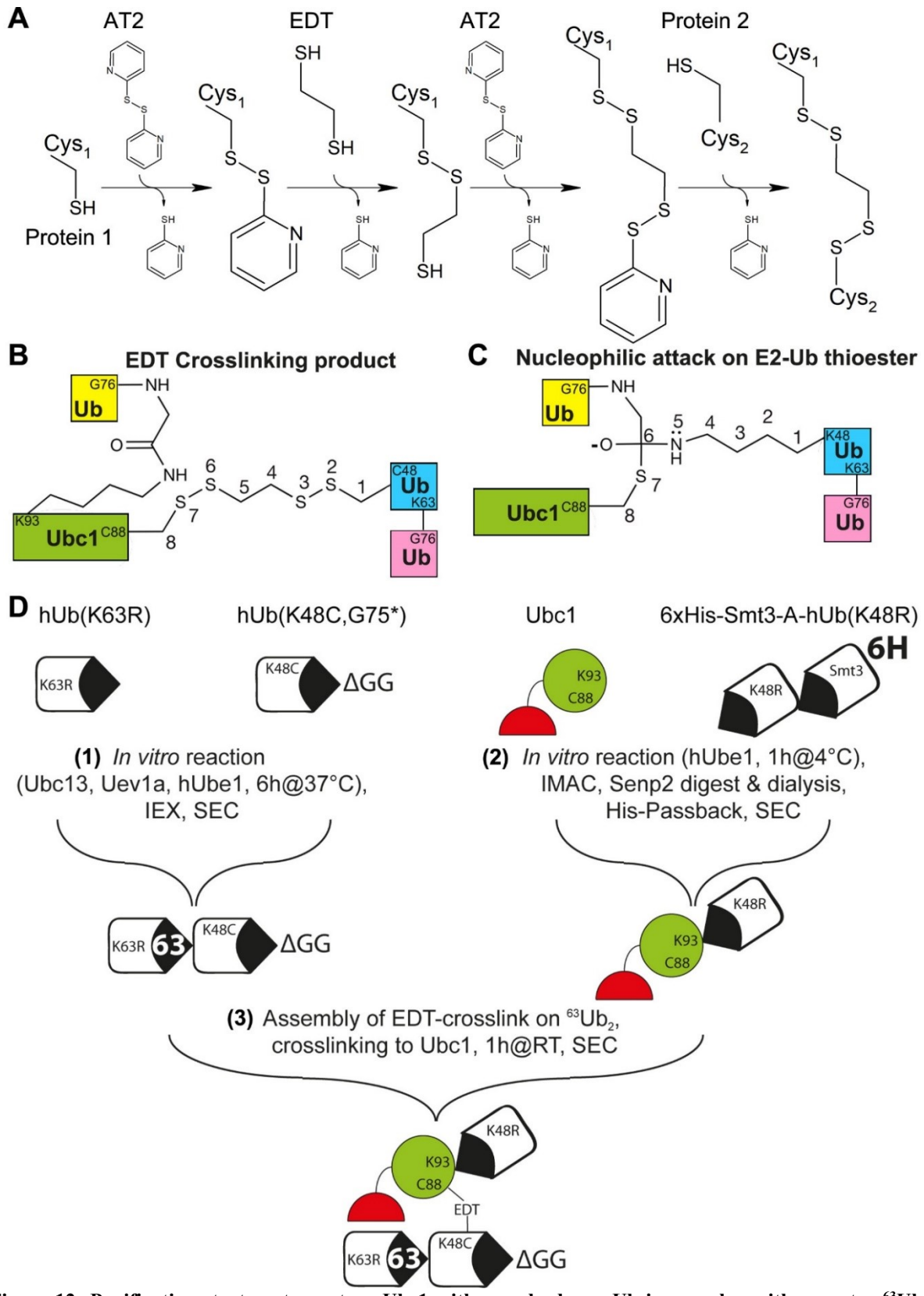

Figure 12: Purification strategy to capture Ubc1 with pseudo donor Ub in complex with acceptor $^{63}Ub_2$. (A) Cross-linking of two proteins through sequential use of 2,2-dithiodipyridine (AT2) and ethane-dithiol (EDT). (B) Cross-linking product of Ubc1-Ub and $^{63}Ub_2$ with Ub(K48C) at the proximal position. (C) Transition state of a nucleophilic attack by the **ε**-amino group of K48 in Ub on the Ubc1~Ub thioester. Concept adapted from Streich Jr and Lima.[135] (D) Purification strategy for a tag-free complex of autoubiquitinated Ubc1 cross-linked through EDT to $^{63}Ub_2$ (Ubc1-Ub-X-$^{63}Ub_2$).

should be formed, which contains the exact same number of atoms between C_α of C88 in Ubc1 and C_α of Ub C48 (originally K48) as the native transition state (Figure 12C). The difference in distance should be no more than 1-2 Å.[135] This approach emulates a strategy, which has previously been reported for the investigation of the ubiquitin like protein SUMO in the context of its cognate E2 enzyme Ubc9.[135] Moreover, Ubc1 should be autoubiquitinated at K93 (Ubc1-Ub) to mimic an active Ubc1~Ub thioester.

The final purification strategy, which aimed to produce a complex completely free of affinity-tags, consisted of three main steps (Figure 12D). (1) $^{63}Ub_2$ was enzymatically assembled from Ub(K48C, G75*) and Ub(K63R) in a reaction with Ubc13 and Uev1a. Ub(K48C, G75*) could serve only as acceptor in the reaction because it lacks C-terminal glycine residues, which are required for activation by E1 and E2 enzymes. Ub(K63R) blocks extension of K63 chains beyond diubiquitin, enhancing the yield. $^{63}Ub_2$ was purified from the reaction mix using ion exchange chromatography (IEX) and size exclusion chromatography (SEC) as described elsewhere.[136] (2) Ubc1 was autoubiquitinated with a fusion of hUb(K48R) and n-terminally 6xHis tagged Smt3. Autoubiquitinated Ubc1 was isolated from the reaction mix by metal affinity chromatography (Figure 13A). Senp2 protease was used to separate Smt3 from autoubiquitinated Ubc1. The protease and cleavage products were removed by a second IMAC step ("His-Passback"). Ubc1-Ub was further purified from the flow-through by SEC (Figure 13B). (3) $^{63}Ub_2$ and Ubc1-Ub were cross-linked by sequentially adding $^{63}Ub_2$ to AT2, EDT and then again AT2, before mixing it with Ubc1-Ub (Figure 13C). Between each step excess cross-linking reagents were removed with desalting columns. The final complex (Ubc1-Ub-X-$^{63}Ub_2$) was purified from the reaction mix through SEC. Ubc1-Ub-X-$^{63}Ub_2$ was analysed by SDS-PAGE (Figure 13D) and mass-spectrometry to confirm integration of EDT (data not shown). The stability of the complex was tested by incubation at 4°C or at RT for 16 days respectively. Untreated sample and sample incubated with 50 mM DTT for 5 min on ice were analysed by SDS-PAGE and coomassie staining (Figure 13E). No degradation over time was observed. Therefore, Ubc1-Ub-X-$^{63}Ub_2$ was subsequently employed in crystal trials as outlined in section 4.2.5.1.

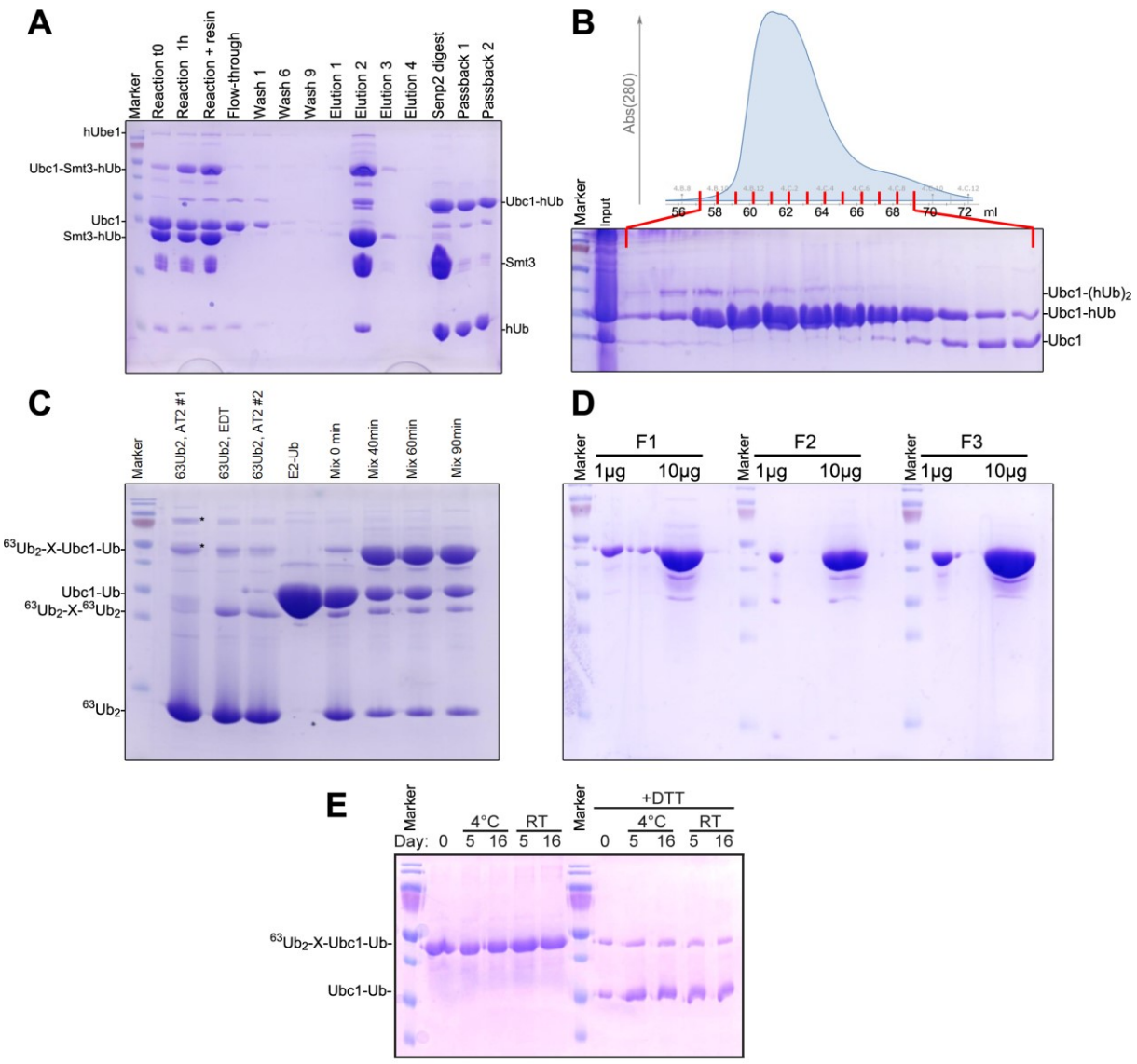

Figure 13: Purification of Ubc1-Ub-X-$^{63}Ub_2$. Samples taken during purification were analysed by SDS-PAGE and Coomassie staining. (A) Metal affinity purification of Ubc1 autoubiquitinated with 6xHis-Smt3-hUb. Ubc1-Ub was obtained after Senp2 digest and His-passback. (B) Elution profile and corresponding samples of size exclusion chromatography for purification of Ubc1-Ub using Superdex HiLoad 16/60 75 pg. (C) Chemical cross-linking of $^{63}Ub_2$ to Ubc1-Ub. (D) Reaction product from C after purification by SEC. Side fractions with impurities were subjected to a second (F2) and third (F3) SEC run. For crystallisation experiments protein from F1 was used. (E) The stability of the complex was tested by incubation at 4°C or at RT for 16 days respectively. Samples were taken at indicated time points and flash frozen. Untreated samples and samples incubated with 50 mM DTT for 5 min on ice were analysed.

2.2.1.3 Crystal structure of Ubc1-Ub cross-linked to K63-linked diubiquitin

Crystallisation and data collection was performed according to section 4.2.5. In brief, crystals were grown for two weeks at 10°C in 6.5% PEG 6000, 100 mM $MgCl_2$ and 100 mM HEPES pH 7.0 and diffracted to 3.2 Å at Swiss Light Source. Together with Dr. Jérôme Basquin (MPIB, Martinsried) and Dr. Rajan Prabu (MPIB, Martinsried), I was able to solve the structure by molecular replacement. The final model had an R_{work} of 20.2% and R_{free} of 23.2%. Data collection and refinement statistics (Table 1), as well as exemplary images of the electron density map (Figure 30), are shown in the supplementary data (pp. 91-92)

The complex arrangement observed in the asymmetric unit is displayed in Figure 14A. The distal Ub moiety in the acceptor diubiquitin (Figure 14B, pink) is missing from the structure (Figure 14C). Despite indications of another Ub monomer in the electron density map and sufficient space to accommodate this protein, any attempts to model Ub at the respective position failed. High flexibility of the distal moiety in $^{63}Ub_2$ and a lack of coordination to other domains within the complex might be reasons for this. Ub_D and Ubc1 adopted an open conformation within the complex (Figure 14A, right panel). Examination of crystal packing revealed that the UBA domain made extensive contacts with Ub_D from a symmetry related complex (Figure 14D). Accordingly, superimposition of the Ube2K/Ub_A model, outlined in section 2.2.1.1, on the obtained structure (Figure 14A, grey) showed that the UBA domain was differently positioned relative to the UBC domain (Figure 14B*). The symmetry related Ub_D formed a binding interface with the UBA domain (Figure 14E) which closely resembles previously reported data for this family of UBDs (Figure 15A). While UBA domains share little sequence similarity across the family, they share a common fold, in which three α-helices with approximately ten amino acids form a bundle. The helices are labelled α1, α2 and α3 from N- to C-terminus. Helix α1 and α3 comprise a hydrophobic binding interface, which associates with the hydrophobic patch in Ub clustering around I44. Strinkingly, the side chain of R42 in Ub may form hydrogen bonds with polar side chains of helix α3 in each respective UBA domain (E211 in Ubc1). Other components of the Ubc1-Ub-X-$^{63}Ub_2$ complex do not contribute to the association of the UBA domain with Ub_D. Thus, binding of Ub_D by the UBA domain does not appear to have unique properties as compared to binding monoubiquitin in solution. This inter-complex contact or Ubc1 oligomerisation have no obvious implication for Ubc1 activity and might occur as a result of crystal packing.

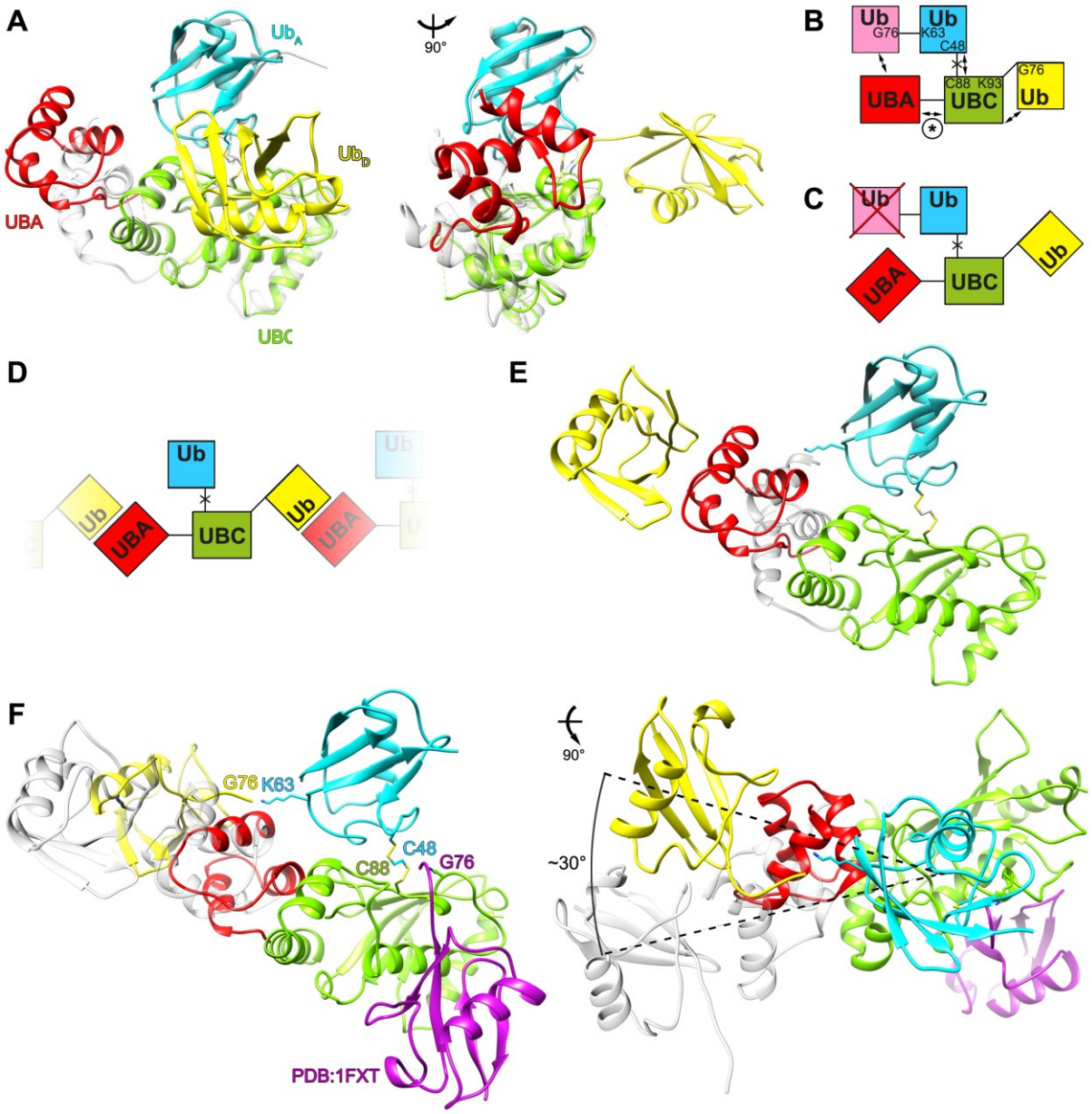

Figure 14: Structure of Ubc1-Ub in complex with $^{63}Ub_2$ was determined by X-ray crystallography. (A) Structure of Ubc1-Ub-X-$^{63}Ub_2$. The model for Ube2k/Ub_A complex (Figure 11B) was superimposed on the structure and is shown in grey. (B) Cartoon of structural model for Ubc1 based on *in silico* modelling (Figure 11D). Asterisk (*) indicates UBC/UBA interface. (C) Cartoon of the observed Ubc1-Ub-X-$^{63}Ub_2$ structure in A. (D) Cartoon of crystal contacts, which were formed between the UBA domain and Ub_D from a symmetry related complex. (E) Structure of Ubc1-Ub-X-$^{63}Ub_2$ with Ub_D from symmetry related complex. (F) Hypothetical model of Ubc1-Ub interacting with $^{63}Ub_2$. A structure of Ubc1 with donor Ub (magenta) in closed conformation (PDB: 1FXT) was superimposed on the UBC domain. The experimentally observed UBA/Ub complex is shown in grey. Additionally, the interface between UBA domain (red) and Ub (yellow) was aligned with the position of the UBA domain in crystal structures of Ube2K (section 2.2.1.1). An alternative conformation of the C-terminus in Ub_{dist} (yellow) was integrated from an NMR ensemble of Ub (PDB: 2K39 , Figure 2B)

The binding interface between the immediate acceptor Ub and the UBC domain (Figure 15B) closely resembled the proposed model for Ube2K (Figure 11A,B), which was originally obtained through HADDOCK modelling. Consistent with the model, residues around the active site in Ubc1 associated with a loop in Ub_A, which includes D58, N60 and the catalytically important Y59[124]. Ub_A D58 was sufficiently close for hydrogen bonds to S81 and T84 in Ubc1 corresponding to S85 and T88 in Ube2K respectively. Moreover, Ub_A N60 could adopt hydrogen bonds to S82 and D123 in Ubc1 corresponding to S86 and D127 in Ube2K respectively. The amino acids involved in this binding interface are conserved between Ubc1 and Ube2K and superimposition of the model with the structure showed analogous topology (Figure 15C).

Further analysis of symmetry molecules showed that Ub_D was restricted from adopting a closed conformation by crystal packing (Figure 15D-F). Symmetry related Ub_D (Figure 15F, grey) was located in proximity to the crossover helix α2 of Ubc1 (Figure 15F, green). Superimposition of the thioester Ubc1~Ub in closed conformation (PDB: 1FXT) on the complex, showed that the symmetry related Ub_D occupies the same space as Ub_D from 1FXT (Figure 15F, magenta). C-terminal residues of Ub_D from 1FXT align with Ub attached to K93 in Ubc1. Thus, in principle Ub attached to K93 in Ubc1 should be able to associate with the crossover helix α2. The position of Ub_A in the complex is compatible with open and closed conformations of Ubc1 with Ub_D (Figure 15F).

The overall complex architecture observed for Ubc1-Ub-X-$^{63}Ub_2$ does not provide an obvious implication for Ubc1 activity or the function of the UBA domain. The value of the structural data lies in the confirmation of the binding interfaces between Ub_A and the UBC domain as well as between the UBA domain and the associated Ub molecule. These interfaces were the basis for the structural model presented in section 2.2.1.1. However, the postulated position of the UBA domain relative to the UBC domain could not be observed. The distance between L71-C_C in Ub associated with the UBA domain and Ub_A K63-Nε is 23.8 Å. To accommodate the model of Ube2K/$^{63}Ub_2$ complex for Ubc1, intramolecular motions between the UBA domain and the UBC domain in Ubc1 would have to reduce this distance by 7.5 Å (Figure 14F). This could be achieved by a rigid body rotation of approximately 30° of the UBA domain with associated Ub around the UBC domain (Figure 14F). Both positions of the UBA/Ub complex are compatible with Ub_D in closed conformation with the UBC domain (Figure 14F).

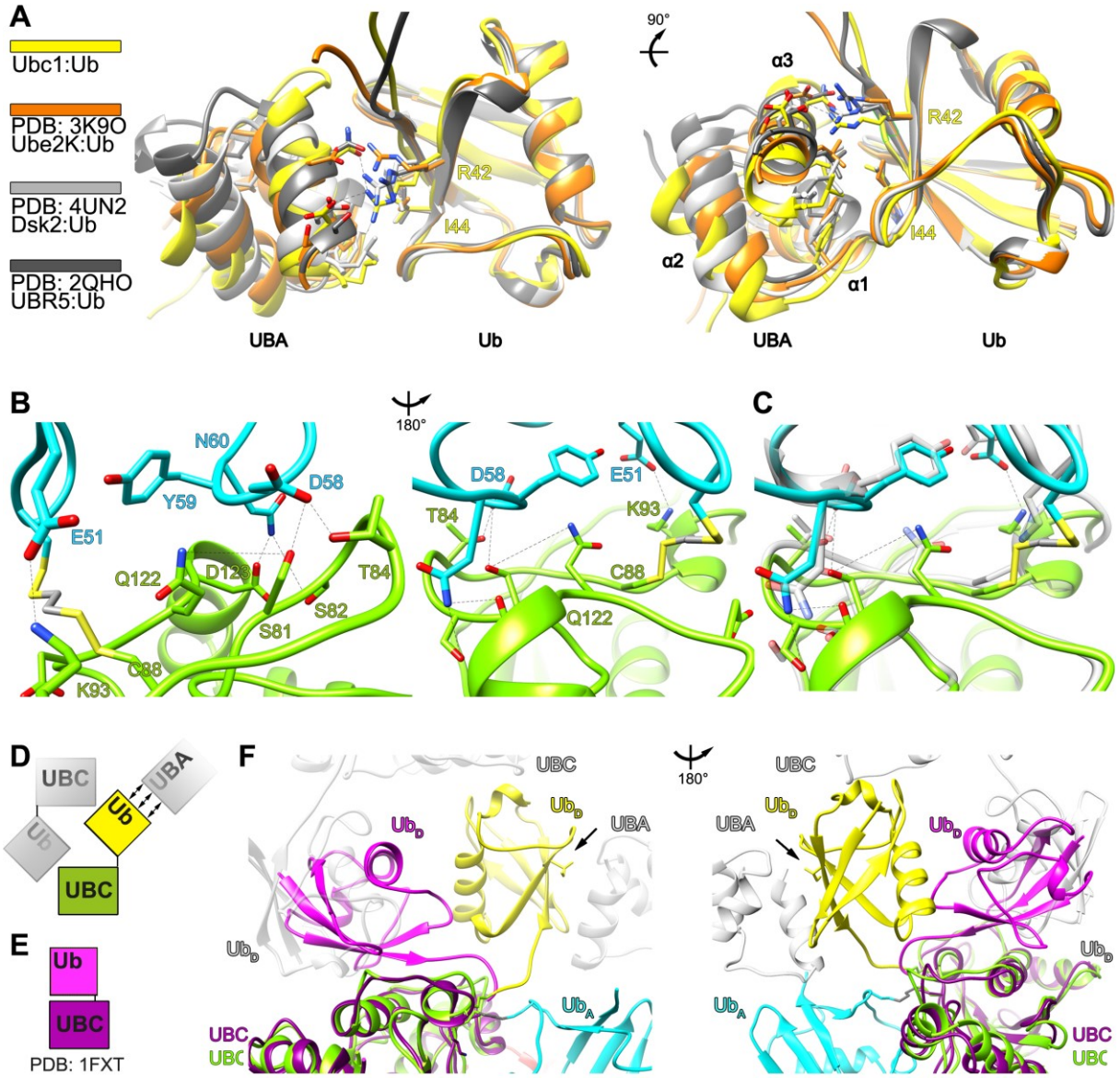

Figure 15: Interaction interfaces in the crystal structure of Ubc1-Ub in complex with $^{63}Ub_2$. (A) Superimposition of the interface between UBA domain and Ub_D from Ubc1-Ub-X-$^{63}Ub_2$ on UBA/Ub interfaces of Ube2K, Dsk2 and UBR5. Selected side chains are shown in stick representation. (B) The interaction interface between the UBC domain and Ub_A from Ubc1-Ub-X-$^{63}Ub_2$. (C) The interface of Ube2K/UbA (grey) inferred from HADDOCK modelling (Figure 11A) was superimposed on B. (D) Cartoon of crystal contacts to Ub_D in Ubc1-Ub-X-$^{63}Ub_2$. Ub_D associates with the UBA domain from one symmetry related complex and with the UBC domain of another symmetry related complex. (E) Cartoon of a structure of the Ubc1 UBC domain with Ub in closed conformation[137] (PDB: 1FXT). (F) The structure depicted in E (magenta) was superimposed on Ubc1-Ub-X-$^{63}Ub_2$ through alignment of the UBC domain. Symmetry related molecules are shown in transparent grey. I44 in Ub_D is highlighted by an arrow to indicate the binding interface with the UBA domain. Symmetry related Ub_D from the adjacent Ubc1 complex clashes with Ub_D from 1FXT.

2.2.2 Characterisation of Ub binding by Ubc1

2.2.2.1 Ubc1 preferentially binds to K63 chains over K48 chains via its UBA domain in *in vitro* binding experiments

To investigate the putative preference for K63 chains over K48 chains inferred from structural modelling, I aimed to assess binding preference of Ubc1 towards differently linked Ub chains. To this end, I performed qualitative *in vitro* binding experiments. Preliminary experiments suffered from a limited dynamic range in Ub detection based on western blotting and antibody binding (not shown). Therefore, I devised a fluorescence based *in vitro* binding assay. K63 chains or K48 chains were assembled from wild type Ub and Ub(S20C,G76-6xHis), which was the target for fluorescent labelling. A mix of Ub chains with different lengths was generated, in which each Ub chain contains a single fluorophore facilitating quantitative detection. Binding of these chains to different GST-fusion proteins immobilised on glutathione sepharose was analysed (Figure 16A). The UBA domain of Dsk2 (aa241-374) served as a positive control, as it was previously reported to bind different Ub chains relatively unspecifically.[81] GST expressed from an empty pGex6p1-vector was used as negative control. Ubc1 expression vectors harboured either the full length enzyme (GST-Ubc1), only the catalytic core domain (GST-UBC, aa1-150), the UBA domain (GST-UBA, aa151-215) or a Ubc1 variant with amino acid substitutions, which were previously reported to disrupt Ub binding[129] (GST-LRV, aa179-181QGF to LRV). Protein amounts were adjusted based on SDS-PAGE and Coomassie staining (Figure 16C). After the immobilised fusion proteins were incubated with the respective mix of fluorescently labelled Ub chains, supernatant and resin were separated. Fluorescent Ub chains associated with resin ("bead bound") or remaining in the supernatant were analysed by SDS-PAGE and fluorescence scan (Figure 16A). Total fluorescence in each sample was quantified and fluorescence signal from bead bound Ub chains over total fluorescence in both fractions was normalised to GST-Dsk2 for each construct (Figure 16B). Full length Ubc1 and the Ubc1 UBA domain interacted with K63 chains more tightly than with K48 chains. Weak or unspecific binding of Ub chains was observed for the GST-tag alone as well as for the UBC domain and Ubc1-LRV. The UBC domain and Ubc1-LRV were found to be poorly expressed in *S. cerevisiae* (data not shown). Therefore, I created and tested different Ubc1 variants, among which only Ubc1 E211A, E212A (Ubc1-EEAA) was stably expressed in *S. cerevisiae* (not shown) and impaired in binding to Ub (Figure 16D). These findings corroborate the proposed structural model as they show that Ubc1, via its UBA domain, interacts preferentially with K63 chains over K48 chains, which are its enzymatic product.

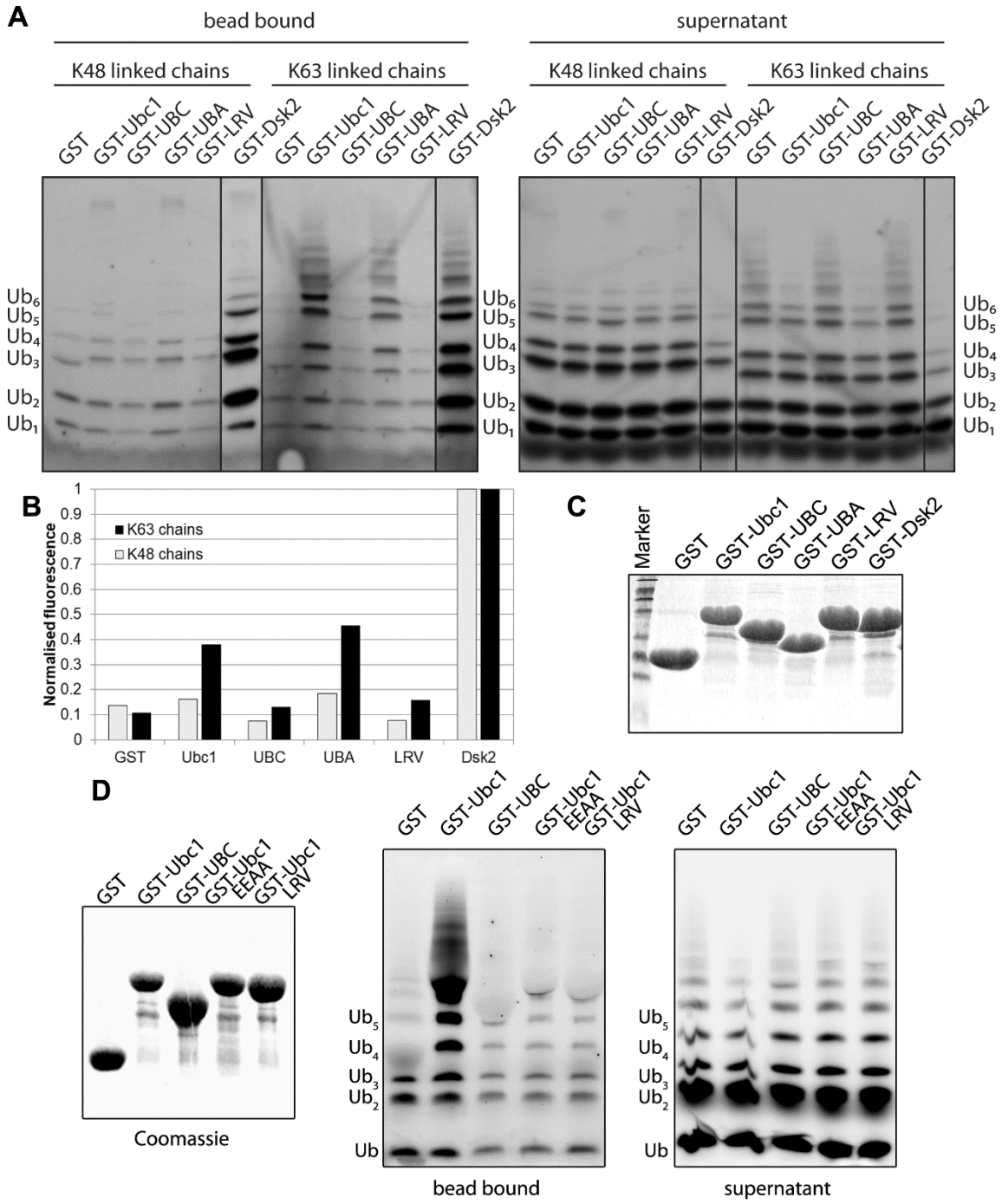

Figure 16: The UBA domain of Ubc1 mediates preferential binding to K63 chains over K48 chains. (A) Fluorescence scan of *in vitro* binding experiment with fluorescently labelled K48 chains and K63 chains. (B) Total fluorescence per lane in A was quantified. Fluorescence in bead bound fraction over total fluorescence in both fractions was normalised to Dsk2-UBA. (C) Input controls of immobilised GST fusion proteins for binding experiments were analysed by SDS-PAGE and Coomassie staining. (D) The binding experiment from A was repeated to assess the binding of K63 chains by Ubc1 with amino acid substitutions E211A and E212A (GST-Ubc1 EEAA). First panel shows input controls as described in C.

2.2.2.2 Assessment of binding affinity between Ubc1 and differently linked diubiquitin probes by microscale thermophoresis (MST)

I carried out microscale thermophoresis experiments in the biophysical core facility of the Max Planck Institute for Biochemistry (Martinsried) with Dr. Stefan Übel, who supervised method development.

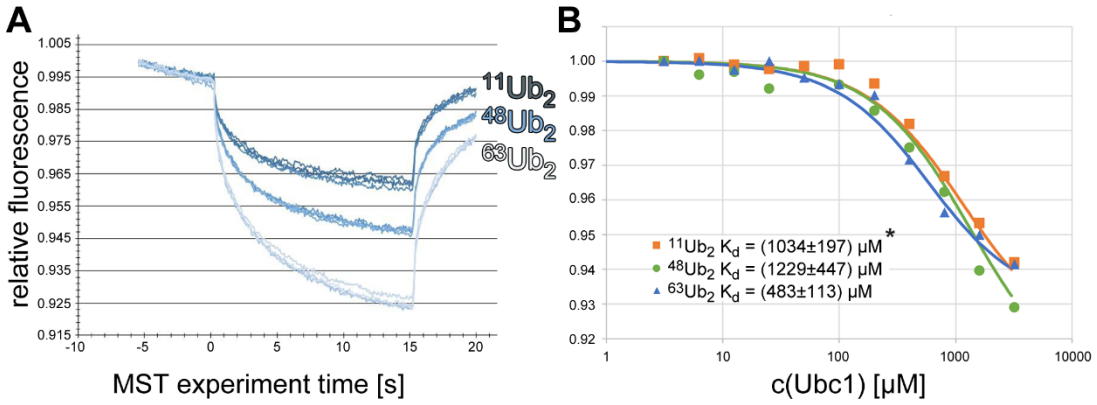

Figure 17: Microscale Thermophoresis experiments with Ubc1 and $^{11}Ub_2$, $^{48}Ub_2$ and $^{63}Ub_2$ respectively. (A) Relative fluorescence is traced over time. Upon excitation (t0) Ub chains diffuse out of the induced temperature gradient and fluorescence intensity decreases until heating is stopped (15s). Subsequently fluorescence is recovered through back diffusion. (B) The different Ub chains in (A) were titrated with Ubc1 and relative fluorescence was integrated from t(-1s) to t(0s) and from t(14s) to t(15s). The difference between these time points (ΔFluo.) decreases with increasing concentration of Ubc1. ΔFluo. was normalised to buffer controls, plotted for different concentrations of Ubc1and approximated with a sigmoidal function to obtain estimated(*) dissociation constants.

To validate the findings from qualitative binding experiments, I aimed to measure binding affinities between full-length Ubc1 and differently linked diubiquitin probes by microscale thermophoresis (MST). MST relies on observation of a fluorescently labelled ligand and its directed movement in a microscopic temperature gradient (thermophoresis), which can be altered by inter-molecular binding events. Therefore, I created fluorescently labelled $^{48}Ub_2$ and $^{63}Ub_2$ with a proximal Ub harbouring a C-terminal cysteine residue and a 6xHis-tag. Dr. Edmund Watson (MPIB, Martinsried) kindly provided $^{11}Ub_2$ created from the same Ub monomers. I tested thermophoretic mobility of diubiquitin probes (Ub_2*) in different buffers and conditions. Ultimately, thermophoresis of 200 nM Ub_2* was measured in 200 mM NaCl and 50 mM MES (pH 6.2) in polymer coated capillaries (Figure 17A). A response rate was defined as change in fluorescence between the time frames t0 (-1s to 0s) and t1 (14s to 15s). Upon addition of Ubc1 into the samples the response rate of Ub_2* decreased indicating reduced thermophoretic mobility due to complex formation. The change in response rate was quantified

for different concentrations of Ubc1 (Figure 17B). At the maximal concentration of 2.3 mM (56 mg/ml) Ubc1 the change of response was still increasing. Extrapolation of the data suggests that the inflection point for $^{63}Ub_2$ was reached. Exact determination of K_d values requires signal saturation as the K_d value is extracted from the inflection point of a sigmoidal curve approximation. Previous attempts to quantify binding affinities between UBA domains and Ub through comparable biophysical methods (*e.g.* surface plasmon resonance) have encountered similar problems.[132] Based on extrapolation of the recorded data set, K_d values were estimated to several hundred micromolar for $^{63}Ub_2$ and to up to 1 mM for binding to $^{11}Ub_2$ and $^{48}Ub_2$. Ubc1 showed generally low binding affinity for Ub with a weak preference for $^{63}Ub_2$.

2.2.2.3 Binding of individual moieties in K48 and K63 diubiquitin by the UBA domain was assessed by NMR titration experiments

NMR titration experiments shown in this section were performed by Dr. Andreas Kniss from the laboratory of Prof. Dr. Volker Dötsch (Goethe University, Frankfurt).

We showed that the CUE domain preferentially binds to K48 chains through coordination with additional amino acids in the C-terminus of the distal moiety in $^{48}Ub_2$. The Rad23A UBA domain employs a similar mechanism, which relies on binding two adjacent moieties in K48 chains simultaneously. We hypothesised that Ubc1 might preferentially associate with K63 chains in a similar way. Thus, we performed NMR titration experiments of the Ubc1 UBA domain with ^{15}N labelled diubiquitin probes (Figure 18), as described in section 2.1.1. The strongest chemical shift perturbations (CSPs) were observed for amino acids within the hydrophobic patch (I44, L8, G47, V70, R42, H68). Interestingly, several residues in the C-terminus of Ub were also implicated in binding (L71, R72). A prominent difference to binding of Ub by the CUE domain is a strong CSP of K48 in Ub, which appears to contribute to binding by the UBA domain. No striking difference in CSPs could be observed between individual moieties of $^{63}Ub_2$ (Figure 18A,B). In contrast, CSPs in the proximal moiety of $^{48}Ub_2$ were generally lower than in the distal moiety, which was most prominent for K48 (Figure 18C,D). Previous studies report a K_d value of 228 ± 68 µM for binding of monoubiquitin by the Ubc1 UBA domain as assessed by NMR experiments.[105] To determine dissociation constants between individual Ub moieties within the diubiquitin probes and the UBA domain, the CSP of I44 was measured for increasing concentrations of UBA domain (Figure 18E). Based on this titration experiment dissociation constants were calculated (Figure 18F). K_d values of 193 ± 13 µM and 188 ± 20 µM were determined for the distal and proximal moiety in $^{63}Ub_2$ respectively, whereas

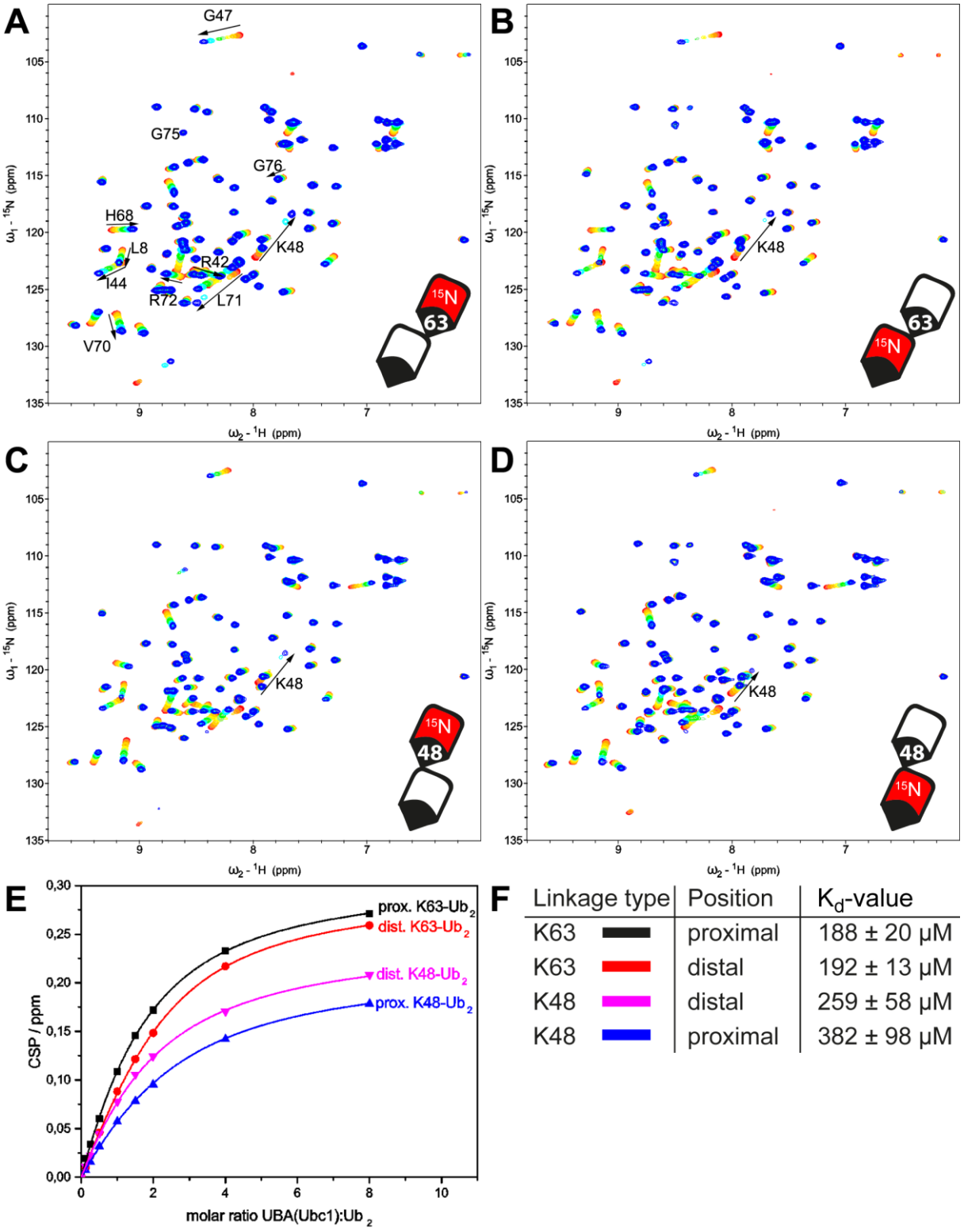

Figure 18: Interaction of individual ubiquitin moieties in $^{48}Ub_2$ and $^{63}Ub_2$ with the UBA domain of Ubc1. ^{15}N labelled diubiquitin probes as introduced in section 2.1.1 were titrated with the UBA domain up to molar ratio of 8:1 (UBA : Ub_2). The spectra were recorded for ^{15}N labelling of (A) distal moiety in $^{63}Ub_2$, (B) proximal moiety in $^{63}Ub_2$, (C) distal moiety in $^{48}Ub_2$ and (D) proximal moiety in $^{48}Ub_2$. (E) CSP of I44 for individual moieties was plotted over UBA domain concentration to calculate binding affinities as in Figure 6E and F. (F) K_d values obtained from E.

K_d values of 259 ± 58 µM and 382 ± 98 µM were determined for the distal and proximal moiety in $^{48}Ub_2$, respectively. It appears ubiquitinated K48 in Ub interferes with the association of the Ubc1 UBA domain. In summary, no site specific interaction with K63 chains could be observed for the UBA domain of Ubc1. However, impaired binding of Ubc1 to its enzymatic product (K48 chains) is in agreement with the proposed structural model.

2.2.3 *In vitro* ubiquitination activity of Ubc1

2.2.3.1 Ubc1 acts cooperatively with Ubc4 and assembles K48-linked polyubiquitin

As a starting point for the investigation of Ubc1 activity through *in vitro* ubiquitination experiments, I aimed to test the ability of Ubc1 to assemble K48 chains processively under conditions previously used to study Ubc7.[84] In the presence of Hrd1 RING domain and its activating co-factor Cue1, Ubc7 forms a distinct ladder of short Ub chains with increasing length as well as high molecular weight polyubiquitin (Figure 19A). Previous studies showed that Ubc1 is also activated by the E3 ligase Hrd1 in the context of ER associated protein degradation (ERAD).[21] However, unlike for Ubc7, formation of a distinct Ub ladder indicative of sequential *de novo* chain synthesis could not be observed in reactions with Ubc1 (Figure 19B). Instead, slow formation of high molecular weight Ub species and a prominent signal below the 30 kDa marker band indicative of autoubiquitination were observed. (Figure 19B). The binding deficient Ubc1 variant Ubc1-LRV (section 2.2.2.1) showed a similar product pattern as wild type Ubc1 (Figure 19A, right panel). Ubc1 was previously reported to be cooperatively active with the E2 enzyme Ubc4.[110] Thus, I included Ubc4 into the *in vitro* ubiquitination assays. The pattern of polyubiquitin bands generated by Ubc7/Cue1 was not affected by the presence of Ubc4 in the reaction (Figure 19A). Employing Ubc1 together with Ubc4 yielded more rapid formation of high molecular weight products than for Ubc1 or Ubc4 alone suggesting cooperative activity (Figure 19B). To assess consecutiveness in the cooperative activity of Ubc1 and Ubc4, I performed sequential *in vitro* ubiquitination reactions (Figure 19C). GST-tagged Hrd1-RING was employed in an *in vitro* ubiquitination reaction with either Ubc1 or Ubc4, subsequently removed from the reaction using glutathione sepharose and employed in a second reaction with the other E2 enzyme. Incubation with Ubc4 first and with Ubc1 second resulted in a distinct pattern of reaction products compared to reactions with only the individual E2 enzymes (Figure 19B). This sequence of reactions resulted in a shift towards higher molecular weight Ub species. It appears Ubc1 extends Ub modifications generated by Ubc4 in presence of the Hrd1-RING domain. To investigate what kind of Ub chains were

formed in the *in vitro* ubiquitination reactions, samples from reactions with Ubc1 and Ubc4 were submitted for analysis by targeted proteomics as described elsewhere[138] (Figure 19E). In short, the reaction mix was subjected to tryptic digest and isotope labelled marker peptides for different linkage types were added. Subsequent analyses by single reaction monitoring showed the abundance of differently linked Ub chains. In line with previous reports, Ubc1 exclusively assembled K48 chains. Ubc4 generated small amounts of K11, K48 and K63 chains. In summary, I found Ubc1 to exclusively assemble K48 chains, albeit with lower processivity than Ubc7/Cue1, and to extend ubiquitin modifications generated by Ubc4.

The performed experiments did not allow for distinction between the formation of free ubiquitin chains and the modification of E2 or E3 enzyme with multiple monoubiquitins or ubiquitin chains. To assess the ability of Ubc1 to extend preformed Ub chains in the absence of Hrd1 RING domain and Ubc4, I aimed to devise single turnover ubiquitination experiments, in which a single product should be formed allowing determination of kinetic rates. To this end, I performed *in vitro* ubiquitination reactions with a 10:1 molar ratio of K48-linked tetraubiquitin ($^{48x3}Ub_4$), which was C-terminally capped with a 6xHis-tag, and fluorescent Ub as donor (Figure 19D). To discriminate between modification of the designated acceptor Ub and other reaction products, I used Talon metal affinity resin to remove His-tagged proteins from the reaction mix. Samples were analysed by SDS-PAGE and subsequent fluorescence scan, as well as Coomassie staining. Coomassie staining revealed the efficient removal of the 6xHis-tagged Ub chains (Figure 19D, bottom panel). Reactions with wild type Ubc1 and the Ubc1 UBC domain yielded multiple fluorescence signals in the supernatant corresponding to autoubiquitination. These signals were not observed for Ubc1 and the UBC domain with K93R amino acid substitution. The formation of pentaubiquitin as product of the elongation reaction was not affected by the introduction of K93R. However, less product was formed in presence of the UBC domain as compared to full length Ubc1. By employing Ubc1(K93R), I was able to identify reaction conditions suitable to investigate the elongation of different acceptor Ub molecules by Ubc1.

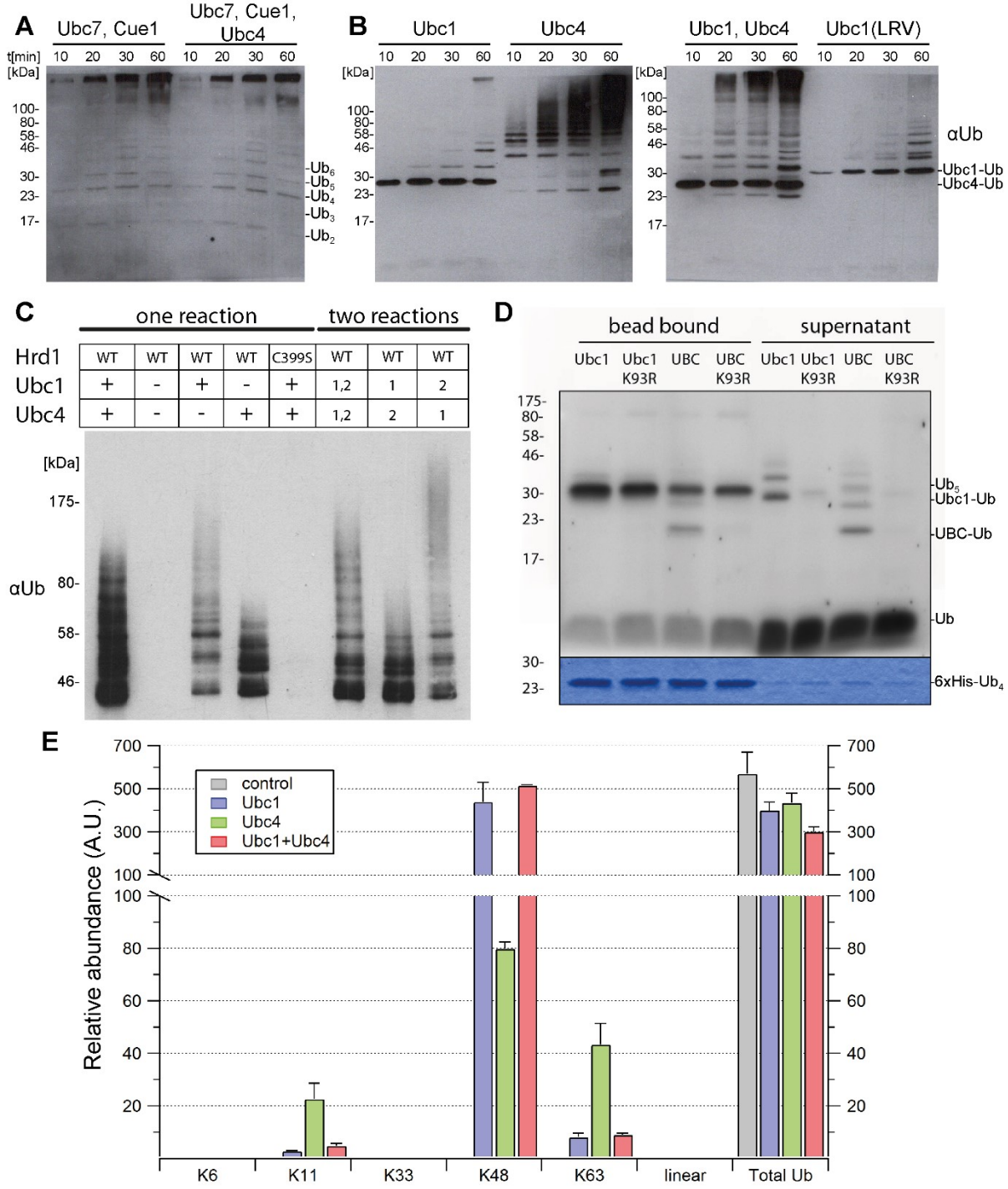

Figure 19: Ubc1 displays cooperative activity with Ubc4, assembles K48 linked chains and autoubiquitinates through K93. (A) *In vitro* ubiquitination experiments were performed with Ubc7/Cue1 and Ubc4 in the presence of Hrd1 RING-domain. Samples were taken at indicated time points and analysed by SDS-PAGE and western blotting using a primary antibody against Ub. (B) Reactions as in A with Ubc1 and Ubc4 (without Cue1). (C) *In vitro* ubiquitination reactions as in B were performed sequentially. Numbers in the table indicate presence of the respective component during the first or second reaction. C399S amino acid substitution in Hrd1 renders RING domain dysfunctional. (D) Single turnover ubiquitination reactions were performed with fluorescent monoubiquitin and K48-linked tetraubiquitin with a C-terminal 6xHis tag as acceptor over night. Acceptor Ub was separated from the reaction mix through metal affinity chromatography. Subsequent coomassie staining (E) Mass spectrometric quantification of polyubiquitin linkage types formed in *in vitro* ubiquitination reactions as in B with Ubc1 and Ubc4. The analysis was performed by Dr. Patrick Beaudette from the MS core facility at MDC (Berlin) under the lead of Dr. Gunnar Dittmar.

2.2.3.2 Ubc1 selectively assembles K48/K63 branched chains

To test the model of Ubc1 interaction with K63 chains, I aimed to quantitatively assess the ability of Ubc1(K93R) to extend different preformed Ub chains. Therefore, I performed kinetic analyses of single turnover ubiquitination experiments, which were introduced in section 2.2.3.1. Different C-terminally capped Ub probes as acceptors and fluorescently labelled monoubiquitin as donor were employed at a 10:1 molar ratio in reactions with Ubc1(K93R). Under these conditions only a single product was formed, which was analysed by SDS-PAGE and fluorescence scans (Figure 20A). I quantified product fluorescence over total fluorescence per lane and plotted this ratio over time. The resulting curves revealed a linear increase of fluorescence over the first 20 min for all probes (Figure 20B). Initial reaction rates were determined as the slope of the linear increase in fluorescence intensity over this time period. Exemplary fluorescence scans for all probes are shown in the supplementary data (Figure 31, pp. 93). Initial rates in presence of full-length Ubc1 were approximately 16 times faster for $^{63}Ub_2$ than for $^{48}Ub_2$ or monoubiquitin (Figure 20C). Reactions with only the UBC domain – *i.e.* Ubc1 lacking its UBA domain – showed ~20% reduced reaction rates for $^{48}Ub_2$ and monoubiquitin as acceptors, whereas this reduction was 85% for $^{63}Ub_2$ (Figure 20C). In summary, Ubc1 preferentially targets $^{63}Ub_2$ in a UBA domain dependent manner.

To investigate this preferential turnover of $^{63}Ub_2$, I performed mutational analysis. I introduced Ub(K48R), which blocks the acceptor site for Ubc1, or Ub(R42A), which interferes with binding of the UBA domain, into different positions of $^{63}Ub_2$ and performed single turnover ubiquitination experiments with Ubc1(K93R) (Figure 20D). Blocking the proximal acceptor site impaired Ubc1 activity strongly, while blocking the distal acceptor site had only a minor impact. Conversely, introducing R42A into the proximal Ub moiety had no effect on Ubc1 activity, whereas R42A in the distal moiety disrupted the rapid turnover of ^{63}Ub2(K48R). The position specific effects of the amino acids substitutions support a mechanism, in which the Ubc1 UBA domain binds to the distal moiety of $^{63}Ub_2$ to align the UBC domain with the proximal moiety in line with the structural model proposed in section 2.2.1.1. This leads to the formation of a K48/K63 branched Ub chain. Accordingly, the binding deficient Ubc1(K93R,E211A,E212A) showed reduced activity towards ^{63}Ub2(K48R) as compared to Ubc1(K93R) (Figure 20F).

To assess preference of Ubc1 towards K63 chains over other substrates, I aimed to compare Ubc1 activity in presence of $^{63}Ub_2$ and the structurally related $^{M1}Ub_2$. M1 chains have been shown to mostly adopt open conformations similar to K63 chains.[72] Moreover, M1 in Ub is

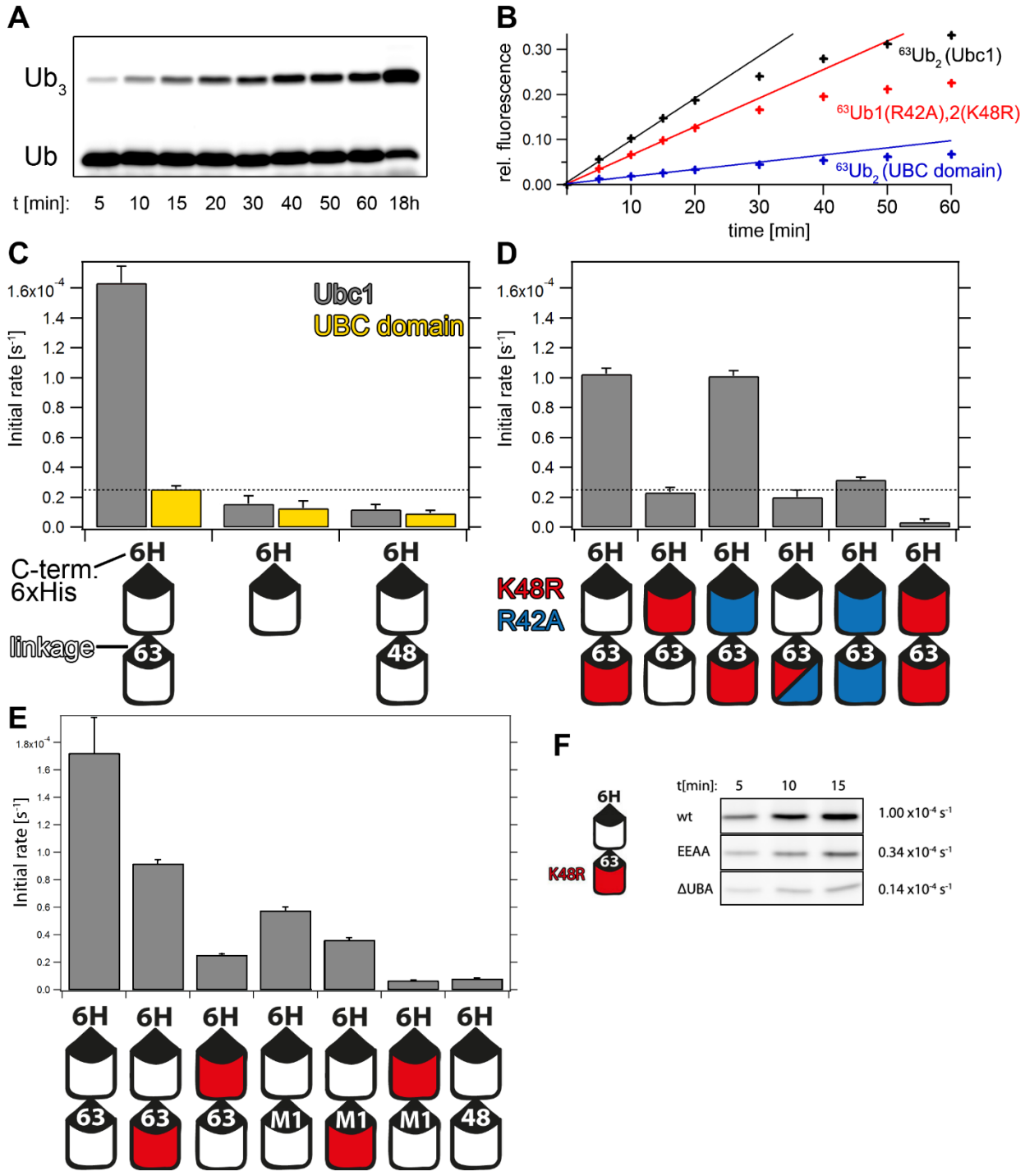

Figure 20: The UBA domain of Ubc1 facilitates the assembly of K48/K63 branched chains. (A) Single turnover ubiquitination experiments with Ubc1(K93R) were performed in presence of fluorescently labelled monoubiquitin and different acceptor Ub molecules at a 1:10 molar ratio. Samples were taken at indicated time points and analysed by SDS-PAGE and fluorescence scan. (B) Fluorescence of reaction product over total fluorescence per lane was plotted over time for reactions with different acceptor Ub. Data points over the first 20 min were approximated by a linear fit to determine initial reaction rate (slope). Representative traces for reactions containing indicated components. (C) Experiments from B were performed in triplicate for the indicated acceptor Ub with either full-length Ubc1-K93R (grey) or Ubc1 UBC-K93R domain (aa1-150, yellow). Error bars show mean and SEM. (D) In the same set of experiments as in C, the activity of full-length Ubc1-K93R towards $^{63}Ub_2$ with the indicated amino acid substitution(s) was analysed. (E) The experiment from D was repeated with K63 chains and M1 chains with Ub(K48R) at the indicated positions. (F) Experiment from A was performed with ^{63}Ub2(K48R) in presence of Ubc1 (wt), Ubc1-E211A,E211A (EEAA) or only the UBC domain (ΔUBA).

located in close proximity to K63 (Figure 2D). Thus, I created different M1-linked Ub probes harbouring Ub(K48R) at different positions and repeated the single turnover ubiquitination experiments outlined in the preceding paragraphs (Figure 20E). Higher initial rates were observed in reactions with ^{M1}Ub2(K48R) than with ^{M1}Ub1(K48R). Evidently, the region-selectivity of Ubc1 observed in K63 chains translates to turnover of M1 chains. However, initial rates for the M1-linked probes were approximately three times lower than for K63 chains. At this point no factor has been identified that assembles M1 chains in *S. cerevisiae*. Accordingly, I propose K63 chains as the preferential substrate of Ubc1.

I aimed to verify my results from the single turnover ubiquitination experiments through *in vitro* ubiquitination reactions, in which formation of branched chains by Ubc1 competes with *de novo* chain synthesis (Figure 21A). I hypothesised that under conditions favourable for chain assembly by Ubc1 ("*de novo*"), K63 chains could provide a scaffold for Ubc1, which induces processive assembly of K48 chains ("processive"). Alternatively, adjacent moieties in a K63 chain could enable Ubc1 to rapidly form multiple branching points. First, I identified conditions for *in vitro* ubiquitination reactions with fluorescently labelled monoubiquitin favourable for *de novo* chain synthesis by Ubc1 (lane 2) and the UBC domain (lane 4, Figure 21B). Subsequently, C-terminally blocked ^{63x3}Ub$_4$ was introduced in a 4-fold lower concentration than fluorescent monoubiquitin into the reaction mix (Figure 21B, right panel). At these concentrations, ^{63x3}Ub$_4$ provides an equimolar concentration of acceptor sites relative to monoubiquitin. I tested the product pattern which resulted from modification of ^{63x3}Ub$_4$ by using methylated fluorescent monoubiquitin as a donor, which cannot be assembled into chains ("met"). In the presence of full length Ubc1 three prominent signals could be observed (lane 6) corresponding to one, two and three times modified ^{63x3}Ub$_4$, while the UBC domain only efficiently produced one modification of ^{63x3}Ub$_4$ (lane 8). Accordingly, Ubc1 showed a prominent shift in reaction products towards modified ^{63x3}Ub$_4$ (lane 5) over *de novo* chain synthesis (lane2), which was less pronounced for the UBC domain (lane 7 versus lane 4). The same results could be observed for a binding deficient Ubc1(K93R,E211A,E212A) variant (Figure 21C). These findings imply that Ubc1 is proficient in rapidly introducing multiple K48/K63 branching points.

To investigate the conservation of this reaction mechanism among species, I performed single turnover ubiquitination experiments with the Ubc1 orthologues from *C. elegans* (ubc-20) and *homo sapiens* (Ube2K). Ubc-20 and Ube2K showed preference towards the proximal moiety in ^{63}Ub$_2$ akin to Ubc1 (Figure 21D).

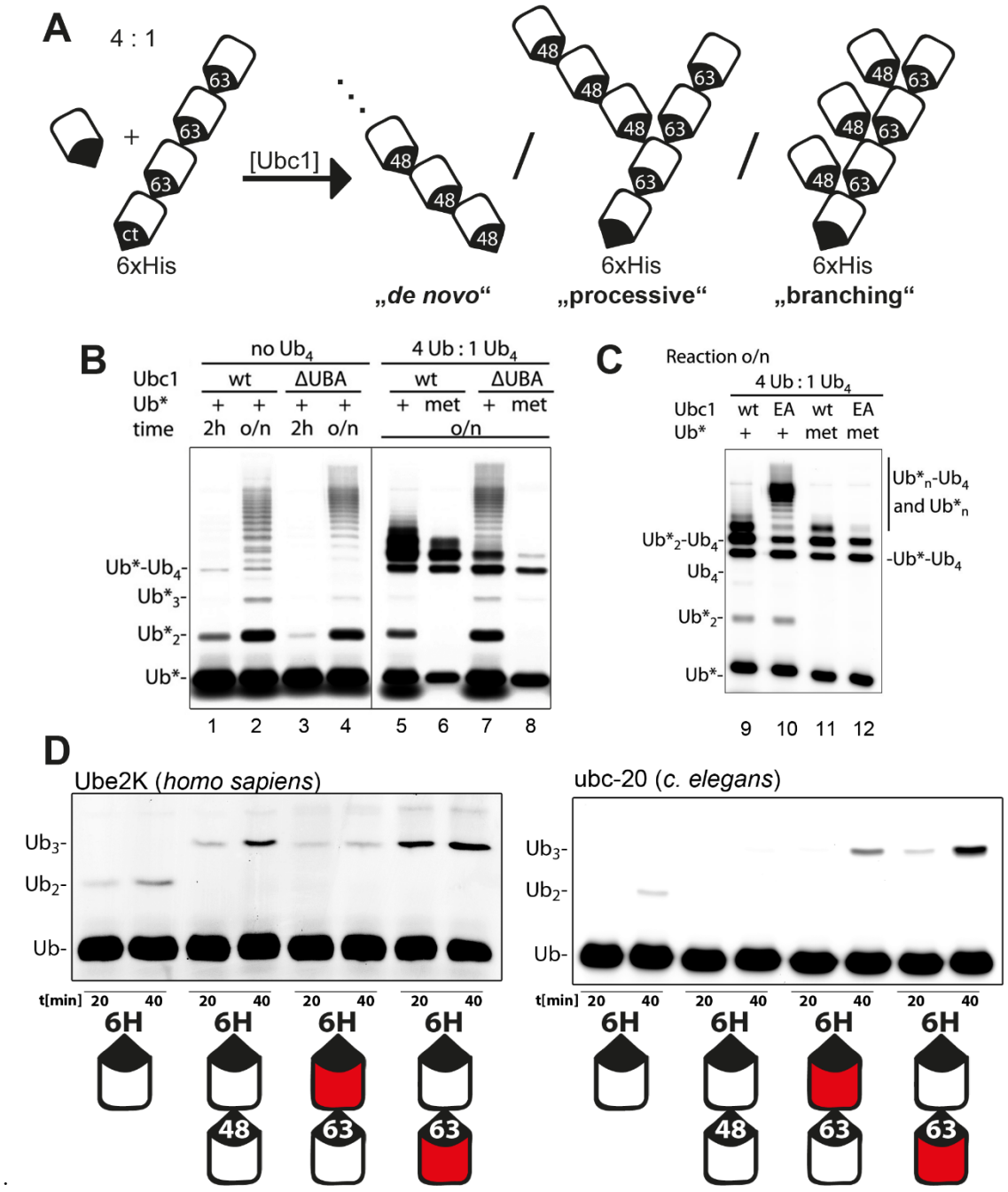

Figure 21: Formation of K48/K63 branched chains by Ubc1 outpaces *de novo* chain synthesis and is conserved among species. (A) Schematic representation of ubiquitination reactions in B and C and their putative products. (B) *In vitro* ubiquitination reactions with Ubc1(K93R) were performed under conditions favorable for free chain synthesis through fluorescently labelled monoubiquitin (left panel) in absence or presence (right panel) of C-terminally capped $^{63x3}Ub_4$ in a 4:1 molar ratio. Fluorescence scan of PAGE-gels. (C) Experiment from B, right panel, was repeated with Ubc1-wt (K93R) and Ubc1-EA (K93R,E211A,E212A). (D) The Ubc1 orthologues ubc-20 from *C. elegans* and the human Ube2K were expressed in E. Coli, purified and used for single turnover reactions with the indicated Ub probes as in Figure 20.

2.2.3.3 Ubc1 mutants containing exogenous Ub binding domains are impaired in assembling K48/K63 branched chains

My results show that Ubc1 is dependent on its UBA domain for efficient assembly of K48/K63 branched chains. I aimed to test whether this activity could be restored to the catalytic core domain of Ubc1 by linking it to other Ub binding domains which also interact with the hydrophobic patch in Ub. To this end, I devised expression plasmids for the Ubc1 UBC domain (aa1-150) linked through different linkers harbouring multiple GS repeats of either 2, 6 or 12 amino acids length to either the CUE domain of Cue1 or the UBA domain of Dsk2 (Figure 22A). The activity of the chimeric enzymes towards different Ub probes was tested in single turnover ubiquitination assays as described previously (Figure 22B). Although the variants slightly differed in activity towards different acceptor probes, the activity of wild type Ubc1 towards the proximal moiety in $^{63}Ub_2$, eclipsed the efficiency of all other reactions. These results suggest that activation of Ubc1 by its UBA domain is dependent on unique features within this domain.

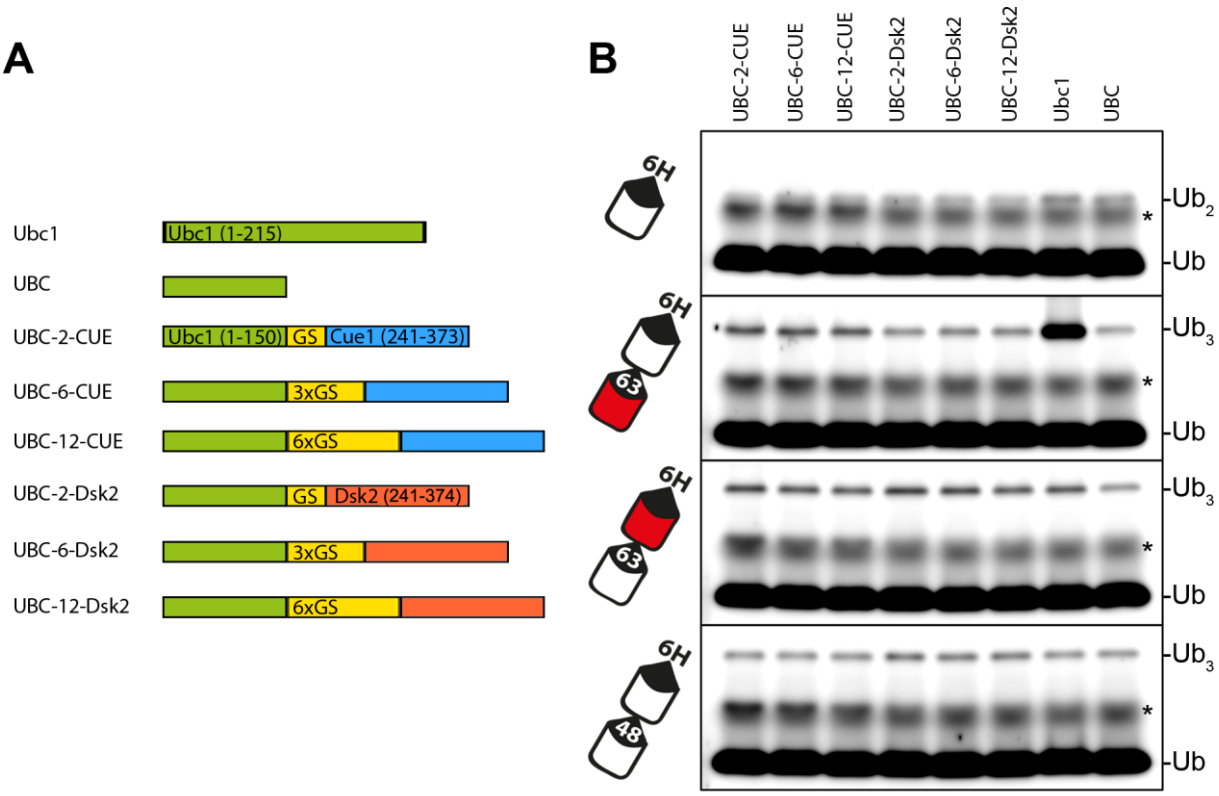

Figure 22: Single turnover ubiquitination reactions with Ubc1 variants containing Ub binding domains from either Cue1 or Dsk2. (A) Fusion proteins with the catalytic core domain of Ubc1 (aa1-150), a linker region with one to six repeats of GS and either the CUE domain of Cue1 (aa241-373) or the UBA domain of Dsk2 (aa24-203) were created. (B) Single turnover ubiquitination reactions were performed as in Figure 20. Reaction endpoints were analysed by SDS-PAGE and fluorescence scan. Asterisk indicates free dye contaminant from fluorescently labelled Ub.

2. Results

2.2.4 The enzymatic product of Ubc1 – K48/K63 branched ubiquitin chains

2.2.4.1 Detection of branched chains *in vitro* and *in vivo*

Having discovered the preference of Ubc1 to assemble K48/K63 branched chains, I aimed to interrogate the existence of this little studied chain architecture in *S. cerevisiae*. At this point Ohtake *et al.* succeeded in detecting K48/K63 branched chains in a mammalian cell line by a novel mass spectrometric method.[58] In collaboration with Dr. Henrik Zauber from the group of Prof. Dr. Matthias Selbach (MDC, Berlin), we emulated this approach. The detection method relies on introducing an R54A amino acid substitution into Ub and thereby removing a cleavage site for trypsin. Lysine residues targeted by ubiquitination are protected from the tryptic digest, thus resulting in lysine with two glycine residues attached (K-GG). Consequently, if K48 and K63 in a single Ub molecule were subjected to ubiquitination, a marker peptide for K48/K63 branched chains ranging from L43 to R72 in Ub can be obtained after tryptic digest (Figure 23A). To establish this detection method at our institute, I assembled a ubiquitin trimer in a one step *in vitro* reaction from C-terminally 6x-His-tagged R54A-Ub as acceptor and Ub(K48R,K63R) as donor by using Ubc1 and the K63-specific enzyme pair Ubc13/Uev1A (Figure 23B). The desired reaction product $^{48/63}Ub_3$ (Figure 23C, right lane) was purified by metal affinity chromatography and subsequent size exclusion chromatography. The fragmentation properties of K48/K63 branched chains were analysed by shotgun proteomics to obtain a spectral library. The results reflected data from Ohtake *et al*.[58] (data not shown).

Having measured the fragmentation properties of this relatively large marker peptide (3.6 kDa), we aimed to detect its occurrence in total cell lysate of *S. cerevisiae*. To this end, I created two yeast strains which exclusively harbour N-terminally 10xHis-tagged Ub(R54A) or Ub(R54A,K63R). The amino acid substitution K63R should block any formation of homotypic or branched Ub chains though K63 and thereby serve as negative control. Total cell lysate was prepared from yeast grown in YPD medium and 10xHis-tagged Ub was enriched using metal-affinity chromatography. On-bead digest with trypsin was performed with the enriched fraction and the eluate was analysed by Parallel Reaction Monitoring (PRM) by Dr. Henrik Zauber (section 4.2.4.8).[139] The marker peptide for K48/K63 branches and the corresponding fragment-ions, were detected in samples of yeast expressing Ub(R54A), but not Ub(R54A,K63R) (Figure 23D). A dotp value[140] of 0.79 revealed good correlation of the fragmentation pattern between the spectral library obtained from the synthesised Ub-trimer and the sample from yeast lysate (Figure 23E). The presence of K48/K63 branched Ub in *S. cerevisiae* implies that mechanisms to specifically assemble these Ub chains are conserved among eukaryotic organisms.

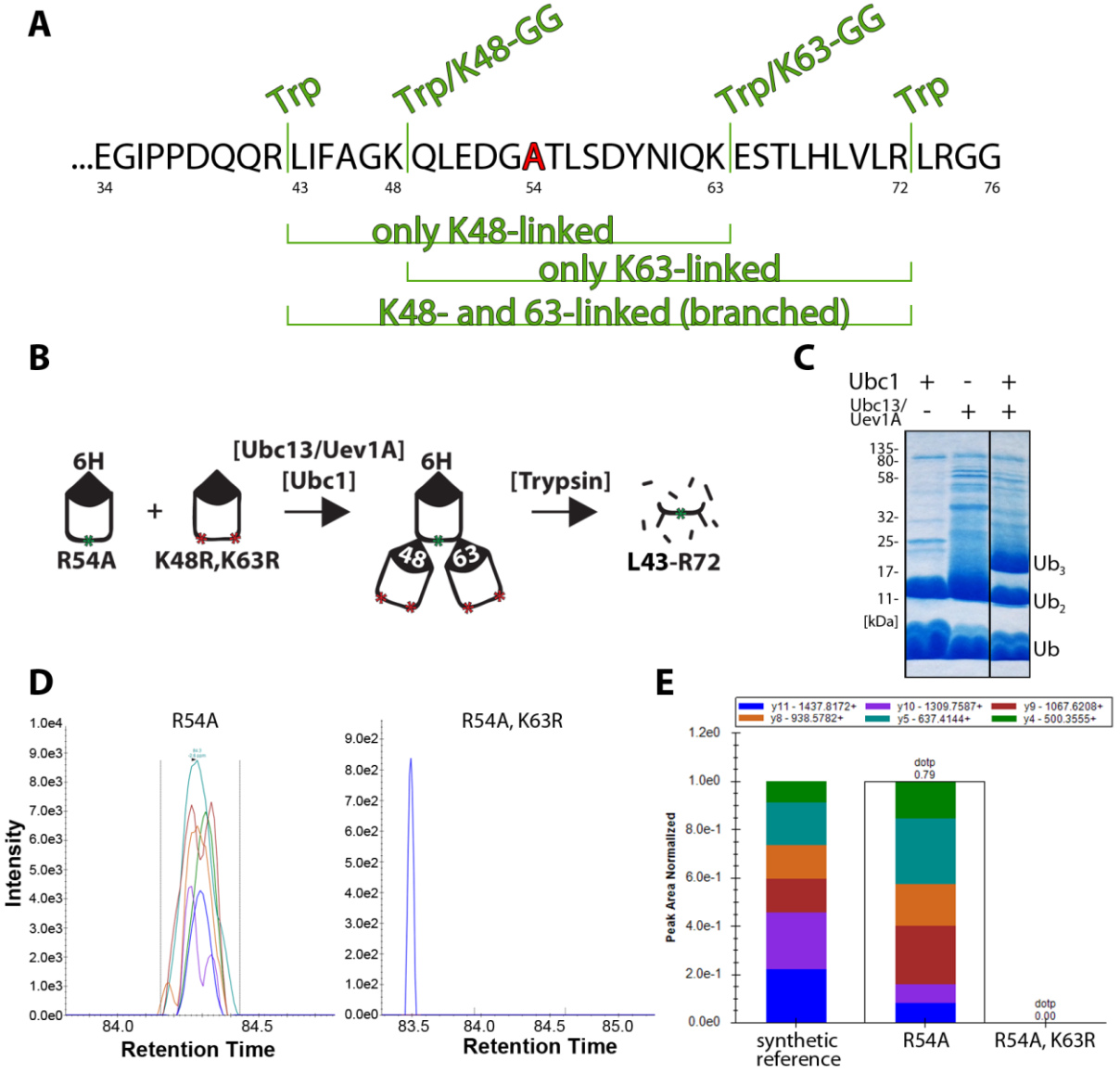

Figure 23: *In vitro* assembly of K48/K63 branched chains and their mass spectrometric detection by parallel reaction monitoring. (A) Amino acid sequence of Ub(R54A). "Trp" indicates trypsin cleavage sites. Modification of lysine residues protects them from tryptic digest (K48-GG/K63-GG). Marker peptides for homotypic chains and K48/K63 branched chains are indicated below the amino acid sequence. (B) Reaction scheme for preparative assembly of $^{48/63}Ub_3$ for method development. (C) Reaction products of Ubc1 and/or Ubc13/Uev1a respectively were analysed by SDS-PAGE and Coomassie staining. Branched triubiquitin was used to create a spectral library ("synthetic reference"). (D) Identification of K48/K63 branched Ub chains by PRM from lysate of *S. Cerevisiae* expressing either Ub(R54A) or Ub(R54A,K63R). Graphs display excerpts of the chromatogram at peak retention time from the six most abundant fragment ions observed for Ub(R54A) and Ub(R54A,K63R) respectively. (E) The different coloured bars show the contribution of each fragment to the total integrated fragment ion signal of the marker peptide (colours as in D). The dotp value of 0.79 confirms good matching of the spectrum obtained from yeast lysate with Ub(R54A) with the reference spectrum. PRM measurements performed by Dr. Henrik Zauber.

2.2.4.2 Levels of K48/K63 branched chains in *S. cerevisiae* deleted for *ubc1*

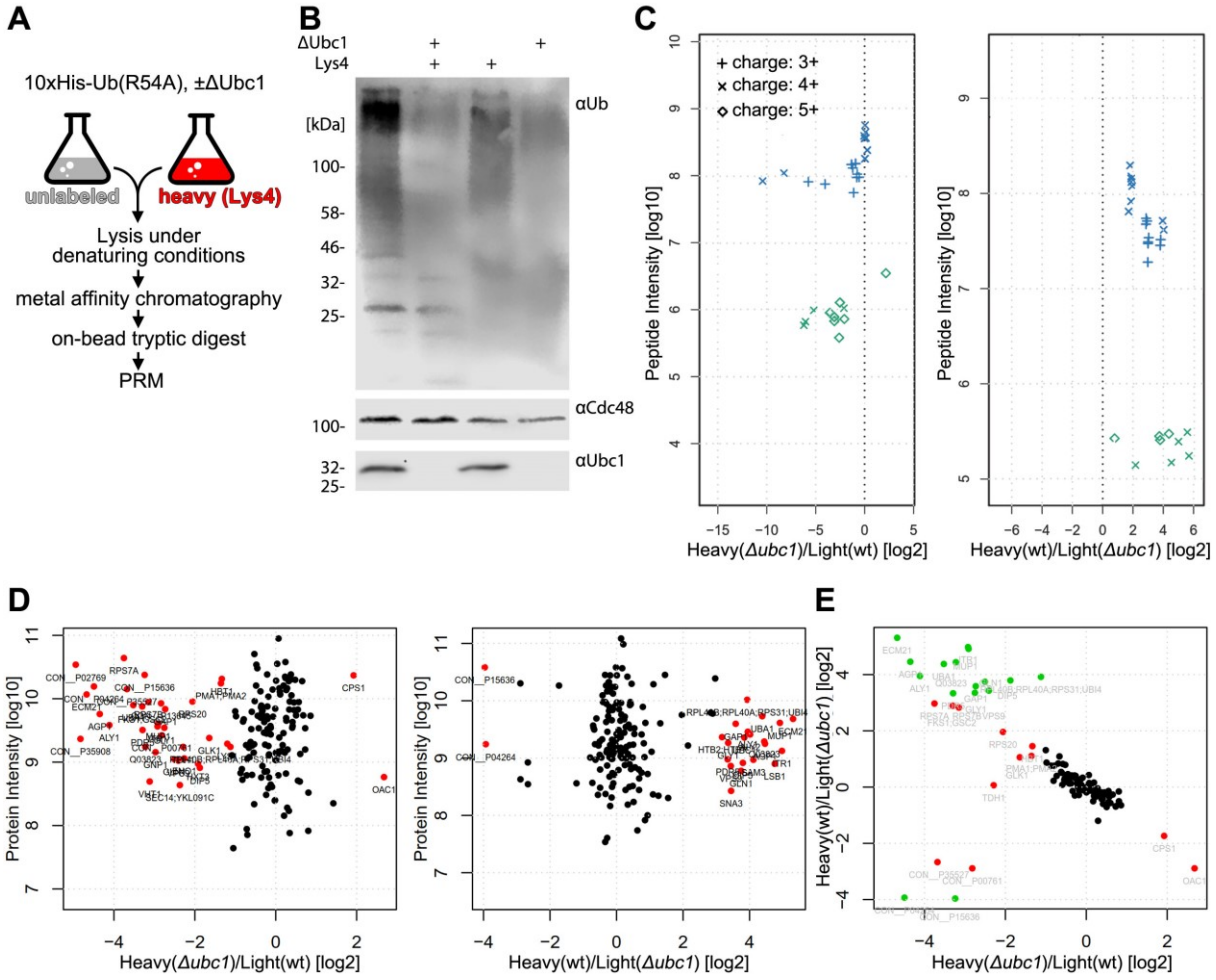

Figure 24: Quantification of K48/K63 branched chains from yeast lysate in presence and absence of Ubc1. (A) Schematic of workflow. (B) Input controls. First lane is wildtype. Analysis by SDS-PAGE and western blotting using the indicated primary antibodies. (C) SILAC ratios and intensities for individual marker peptide fragments for homotypic K63 chains (blue) and K48/K63 branched Ub (green). Different symbols indicate charges of fragment ions. (D) Christmas tree projections from the shotgun proteomics analysis of the SILAC experiment. log2-fold changes were plotted against protein intensity. Significant outliers from the log2 FC-distribution were detected in an abundance binned manner and are coloured in red. (E) Pairwise comparison of protein ratios from experiments in D. Green colour indicates proteins with a significant fold-change observed in both experiments, while red colour indicates proteins observed in only one experiment.

We aimed to investigate the impact of Ubc1 on the abundance of K48/K63 branched chains. To do so, we combined stable isotope labelling in cell culture (SILAC) in *S. cerevisiae* with the PRM detection method outlined in the previous section (Figure 24A). First, I introduced a *ubc1*-deletion into the strain expressing Ub(R54A) with N-terminal 10xHis-tag. Wild type and *ubc1*-deleted yeast cells were grown in label-free SD medium or in SD medium containing ^{2}H4-lysine (Lys4). Input controls revealed reduced levels of high molecular weight polyubiquitin in *ubc1* deleted cells (Figure 24B). Equal amounts of cells expressing endogenous Ubc1 grown in

label-free medium were mixed with cells deleted for *ubc1* grown in Lys4-medium or vice versa to control for label dependent effects. Cell lysis was performed under denaturing conditions. Enrichment of 10xHis-Ub and on-bead digest for the detection of K48/K63 branched chains were performed as outlined in the previous section. Samples were analysed by PRM to detect relative differences of homotypic K63 chains and K48/K63 branched chains (Figure 24C). The observed peptide ratios showed reduced levels of K48/K63 branched chains in cells deleted for *ubc1*. However, conflicting results were obtained for the fold-changes of K63 chains. No difference was observed for cells expressing Ubc1 grown in unlabelled media as compared to *ubc1*-deleted cells grown in Lys4-labelled medium. In contrast, Lys4-labelled cells expressing Ubc1 contained more K63 chains than *ubc1*-deleted cells grown in unlabelled medium. MS1 spectra revealed that there was no overall shift in protein ratio distribution for the individual samples (Figure 24D) and that samples correlated well between label swaps (Figure 24E). Reduced expression of multiple ribosomal proteins could be observed for *ubc1*-deleted strains. Although, this preliminary data suggests reduced levels of K48/K63 branched chains in *ubc1*-deleted cells, this observation requires further validation.

2.2.5 Huntingtin (Htt) as model substrate of Ubc1 and its homologues

2.2.5.1 Htt in C. elegans

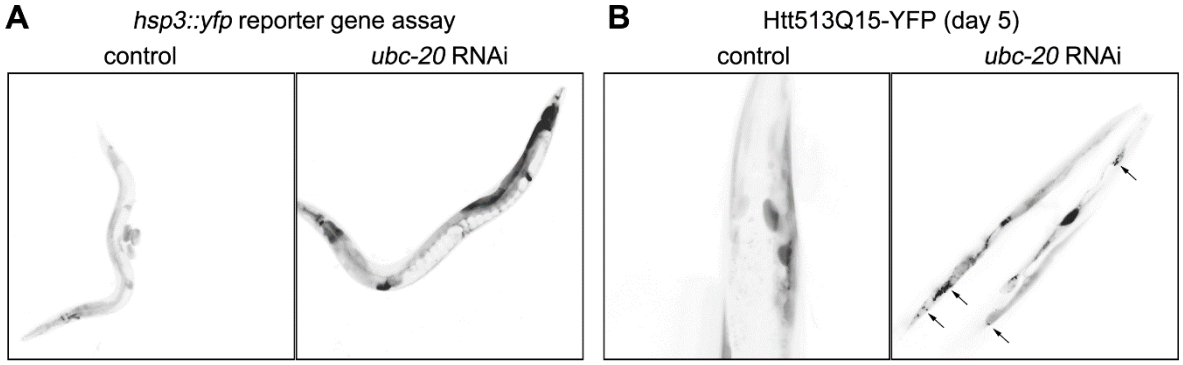

Figure 25: Depletion of the Ubc1 orthologue ubc-20 in *C. elegans* induces the unfolded protein response and leads to aggregation of a Huntingtin derivate. (A) Fluorescence microscopy of *C. elegans* harbouring a reporter gene construct, in which YFP expression is governed by the hsp-3 (ER Hsp70) promoter. Nematodes were grown on *E. coli* expressing dsRNA against *ubc-20* or the empty vector L4440 (control). Higher fluorescence signals indicate induction of the unfolded protein response upon depletion of ubc-20. (B) Fluorescence microscopy of *C. elegans* expressing a fusion protein of Huntingtin (aa1-513) and YFP. Depletion of ubc-20 via RNAi induces formation of distinct punctae (arrows) indicative of protein aggregation.

We hypothesised that K48/K63 branched chain assembly by Ubc1 might be involved in fine-tuning degradation of proteins, which can be subject to autophagosomal degradation mediated by K63 chains as well as to proteasomal degradation mediated by K48 chains.

Therefore, we collaborated with Dr. Janine Kirstein (FMP, Berlin), who developed model systems suitable for studying disruption of proteostasis and its organismal effects in *C. elegans*. We induced RNAi mediated knockdown of the Ubc1 homologue ubc-20 in different *C. elegans* reporters. Depletion of ubc-20 had no striking effect on development or fecundity and did not noticeably activate heat shock response (data not shown), but caused the induction of the unfolded protein response as assessed by a *hsp-3* reporter assay (Figure 25A). Moreover, we observed that ubc-20 depletion induced the aggregation of the model substrate Htt513Q15-YFP (Figure 25B). The propensity of Htt to form aggregates strongly correlates with increased length of the polyQ stretch with a critical threshold at approximately 35 amino acids.[141] Thus, it was surprising that ubc-20 depletion led to an aggregation of a Htt construct harbouring a relatively short polyQ stretch of 15 amino acids. Typically, this is only caused by severe disruption of the cellular protein folding machinery upon, for example, knockdown of Hsp70.

2.2.5.2 Htt in S. cerevisiae

Because it was not feasible to create a *C. elegans* variant suitable for the detection of K48/K63 branched chains, I aimed to test whether the findings from *C. elegans* could be transferred to *S. cerevisiae*. Htt has been previously used as a model substrate to study protein aggregation in *S. cerevisiae*.[142] I obtained plasmids used by Duennwald *et al.* from Addgene (15576, 15577) and genomically integrated them into our strain background (Figure 26). These constructs are governed by an inducible GAL-promoter and encode for Htt Exon-1 with either Q25 or Q103 fused to GFP and a Flag-tag. Wild type and *ubc1*-deleted yeast cells expressing either Htt construct were shifted to galactose containing media for 2h and analysed by fluorescence microscopy (Figure 26A). Distinct staining patterns could be observed for the different constructs. Htt(ExonI)25Q-GFP-Flag showed even distribution across the cytosol indicating good solubility (Figure 26A, left panels). In contrast, expression of Htt(ExonI)103Q-GFP-Flag induced the formation of distinct punctae indicating aggregate formation (Figure 26A, right panels). These staining patterns did not differ between wild type and *ubc1*-deleted cells. To asses protein half-life of the different Htt constructs, I performed cycloheximid chase assays (Figure 26B). Over the course of three hours no degradation of Htt(ExonI)25Q-GFP-Flag could be observed (bottom panel). Signal for Htt(ExonI)103Q-GFP-Flag decreased over time (top panel). However, a high molecular weight band increased in intensity over time indicating aggregate formation. No difference could be observed between wild type and *ubc1*-deleted cells.

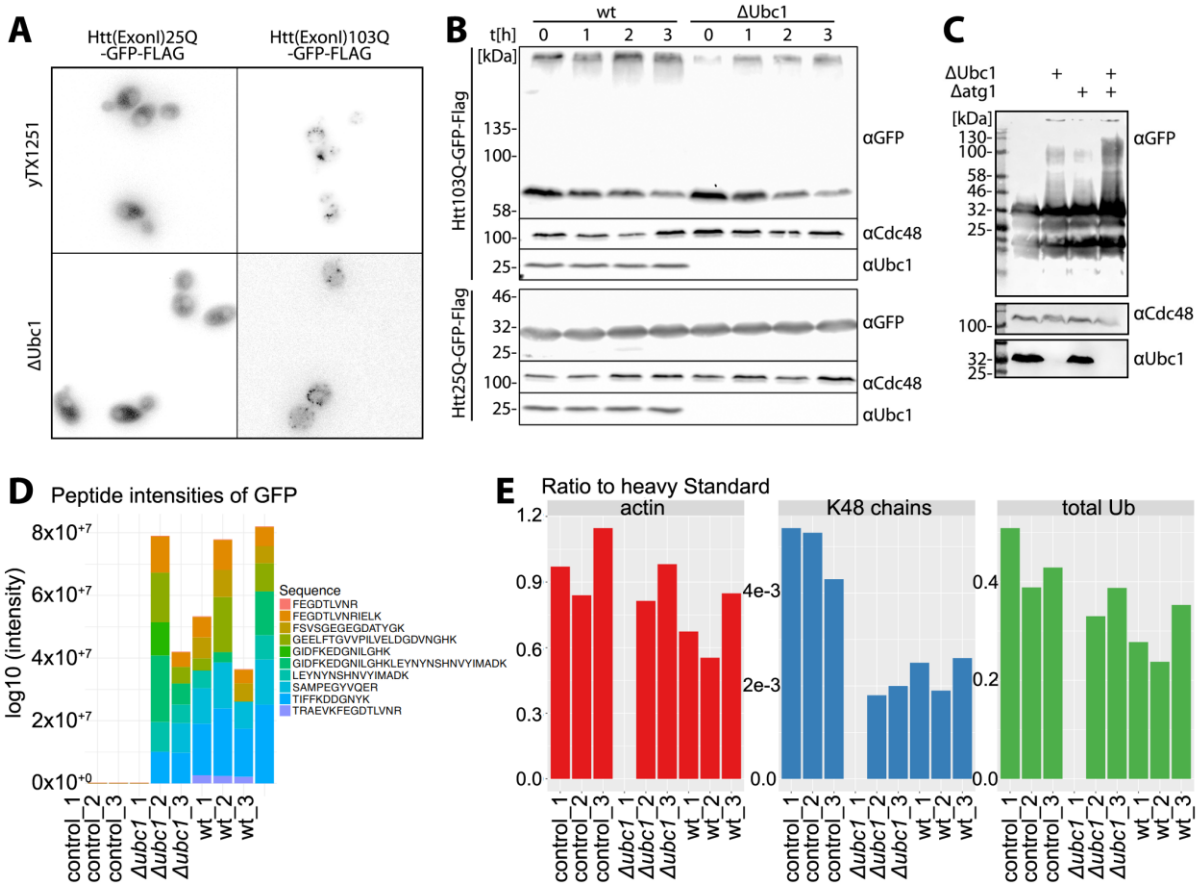

Figure 26: Htt as model substrate in *S. cerevisiae*. (A) Wildtype (yTX1251) and *ubc1*-deleted yeast cells expressing different Htt constructs were analysed by fluorescence microscopy. (B) Degradation of Htt(ExonI)25Q-GFP-Flag or Htt(ExonI)103Q-GFP-Flag was assessed by cycloheximide chase assays. Samples were analysed by SDS-PAGE and western blotting with the indicated antibodies. Cdc48 was used as a loading control. (C) Different yeast strains expressing Htt(ExonI)25Q-GFP-Flag were grown in galactose containing medium over night. Total cell lysate was prepared and analysed as in B. (D) In a pilot experiment, intensities of different GFP marker peptides were measured by shotgun proteomics in samples obtained by Flag affinity purification from yeast lysate. Wild type (wt) or *ubc1*-deleted yeast cells (*Δubc1*) expressing Htt(ExonI)25Q-GFP-Flag or untransformed cells (control) were compared. (E) Samples obtained in D were also analysed by targeted proteomics (PRM) for actin (red), K48 chains (blue), total Ub (green) and K63 chains (undetectable). No signal was detected for the replicate *Δubc1*_1 most likely due to technical issues with the electrospray.

Extended growth of yeast expressing Htt(ExonI)25Q-GFP-Flag in galactose containing medium revealed an increase in total fluorescence per cell (~30%) in the *ubc1*-deletion background as compared to wildtype (data not shown). Accordingly, yeast expressing Htt(ExonI)25Q-GFP-Flag was grown in galactose containing medium over night and total cell lysate was analysed by SDS-PAGE and immunoblotting (Figure 26C). *ubc1*-deleted and *atg1*-deleted cells, which are deficient in lysosomal degradation, showed increased levels of Htt(ExonI)25Q-GFP-Flag and additional higher molecular weight bands indicating possible

aggregation. A yeast strain deleted for both genes showed cumulative increase in Htt(ExonI)25Q-GFP-Flag and the higher molecular weight smear. I aimed to assess the ubiquitination status of Htt(ExonI)25Q-GFP-Flag in yeast. To this end, I performed a pilot experiment in collaboration with Dr. Oliver Popp from the MS core facility (MDC, Berlin) with supervision from Dr. Philipp Mertins. Htt(ExonI)25Q-GFP-Flag was immuno-precipitated from lysate of either wild type or *ubc1*-deleted cells expressing the Htt fusion-protein. Cells not harbouring the construct were used as a background control. Samples were prepared in triplicate and enrichment of the fusion-protein was assessed by identification of multiple GFP derived peptides using shotgun proteomics (Figure 26D). Samples were also subjected to PRM measurements, which showed no enrichment of K48 chains (blue), total Ub (green) or Actin (red), while K63 chains could not be detected (Figure 26E). In summary, it appears *S. cerevisiae* is not a suitable model system for the study of Ubc1-dependent Htt aggregation.

2.3 The E2 ubiquitin-conjugating enzyme Ubc3 contains C-terminal Ub binding motifs and shows distinctive activity towards differently linked Ub probes

Ubc3 (Cdc34) is an E2 ubiquitin-conjugating enzyme, which generates polyubiquitin linked through lysine 48. It encompasses two C-terminal motifs (UBS1 and UBS2), which have been reported to bind Ub.[83] As part of a collaboration with Dr. Mohit Misra, who studied the activation of Ubc3 by the E1 enzyme UBA1 in the group of Prof. Dr. Herrmann Schindelin (Julius-Maximillians-Universität, Würzburg), I evaluated the ability of Ubc3 to extend preformed Ub chains. Full length Ubc3 (Ubc3-FL), a variant lacking both Ub binding motifs (Ubc3ΔC, aa1-178) and a variant additionally lacking a loop region close to the active site (Ubc3ΔCΔloop, aa1-178Δ100-113) were purified by Dr. Misra. I tested their activity against a panel of Ub probes in single turnover ubiquitination assays (Figure 27A) as introduced in section 2.2.3.2. While Ubc3-FL and Ubc3ΔC were both able to efficiently extend different kinds of preformed Ub chains, Ubc3ΔCΔloop rapidly formed a covalent bond between E2 and donor Ub instead. To test, if this occurs as a result of intramolecular auto-ubiquitination, I performed *in vitro* ubiquitination experiments with untagged and his-tagged Ubc3ΔCΔloop (Figure 27B). Both Ubc3ΔCΔloop variants efficiently formed E2-Ub conjugates (lane 1 and 2). His-tagged Ubc3ΔCΔloop, which was treated with iodoacetamide (IAA) lost its activity (lane 3). When His-tagged and Ubc3ΔCΔloop were both employed in the same reaction, both were ubiquitinated (lane 4). If the His-tagged Ubc3 was previously treated with IAA only one band corresponding to untagged E2-Ub could be observed, which indicates intramolecular auto-

ubiquitination (lane 5). Interestingly, turnover of the distal moiety of $^{63}Ub_2$ in presence of Ubc3-FL appeared to occur faster than for other probes and also faster than in presence of Ubc3ΔC. This suggests Ubc3 might – similar to Ubc1 –preferentially modify K63 chains, but selectively target the distal moiety instead of the proximal one. Unlike for Ubc1 this did not coincide with an increased turnover of $^{M1}Ub_2$. However, further experiments are required to understand the significance of these observations.

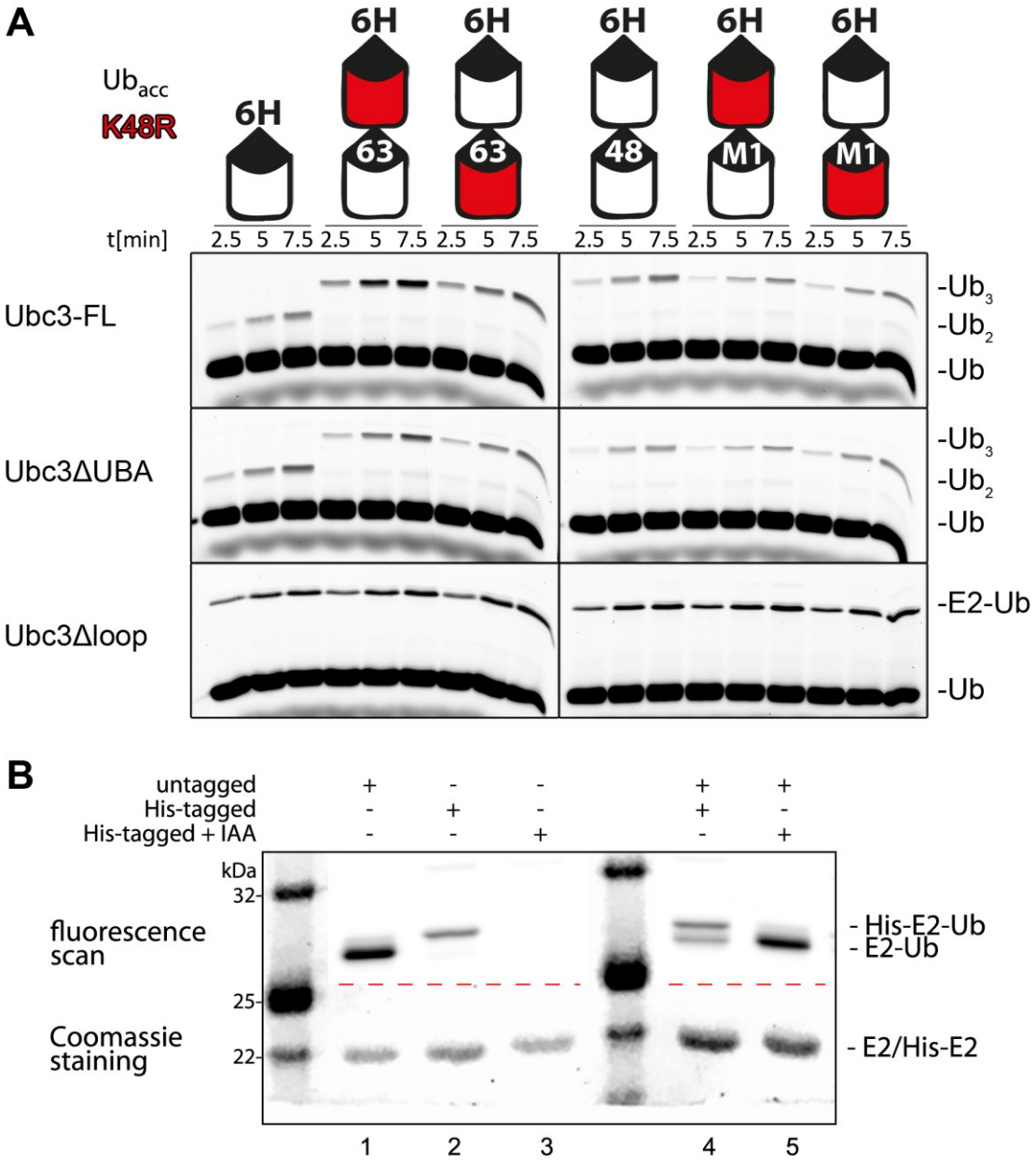

Figure 27: *In vitro* ubiquitination experiments with Ubc3. (A) Different Ubc3-constructs were employed in single turnover ubiquitination experiments as introduced in section 2.2.3.2. Samples were taken at indicated time points and analysed by SDS-PAGE and fluorescence scan. (B) Tagged and untagged Ubc3ΔCΔloop, which was previously treated with IAA or buffer control, was employed in a ubiquitination reaction for 5 min. Samples were analysed by SDS-PAGE, fluorescence scan and Coomassie staining.

3. Discussion

3.1 Stimulation of ubiquitin chain assembly by ubiquitin binding domains

3.1.1 Polyubiquitin chain assembly requires coordinated orientation of acceptor ubiquitin

Ubiquitination plays a key role in virtually all cellular processes in the eukaryotic cell. Ubiquitin (Ub) is assembled into differently linked polymeric chains, which not only enables versatile signalling but also raises unique challenges for the involved molecular machinery. Iterative addition of the 8.6 kDa Ub molecule causes significant topological changes after each successive step. A process capable of Ub chain assembly needs to coordinate a substrate and the respective set of enzymes with a growing Ub chain between them. Moreover, specificity needs to be established on multiple levels. First, selective targeting of a substrate and in some cases of the correct attachment site within the substrate is required. Second, a defined linkage type between Ub molecules must be generated to guarantee the corresponding biological outcome. In other words, a specific lysine residue in Ub must be aligned with the active site of an enzyme. Third, the appropriate Ub moiety within a Ub chain must be targeted to produce the correct chain topology. In most cases, this means that a distal Ub must be aligned with an enzyme to enable chain elongation. Conceptually, this could be viewed as particularly challenging because a specific unit within identical building blocks must be recruited. Consequently, chain elongation should be a self-attenuating process because the chance to randomly target the distal Ub moiety decreases with length. However, because chain length can determine signal potency, transfer of sufficient Ub moieties must be ensured while the substrate is retained at its cognate E3 ligase. Additionally, Ub chain assembly is an energy consuming process and is constantly counteracted by the activity of DUBs. Thus, the multiple demands for specificity need to be integrated into an efficient process. Which molecular mechanisms do chain building enzymes employ to overcome these challenges?

This question was addressed in this study through detailed characterisation of the two E2 enzymes Ubc7 and Ubc1. Key experiments which I performed to achieve this goal included cell-based assays with *S. cerevisiae*, protein structure determination and *in vitro* ubiquitination assays. The results show that both E2 enzymes rely on associated ubiquitin binding domains (UBDs) to position acceptor Ub (Ub_A) for an optimal discharge of the donor Ub (Ub_D). In both cases, the respective UBD interacts with a Ub moiety adjacent to the immediate Ub_A. The

necessity for chain building E2 enzymes to act in concert with Ub binding factors emerged as an overarching principle over the recent years. Branigan *et al.*[143] revealed through structural investigation of the K63 specific enzyme Ubc13 how its co-factor Mms2 (Uev1a in *S. cerevisiae*) aligns Ub_A with the active site of Ubc13. Moreover, Brown *et al.*[144] showed that the activity of the K11 specific E2 enzyme Ube2S is enhanced by binding of Ub_A by APC11 – a subunit of its cognate E3 ligase.

In the following sections, I discuss the biochemical investigation of Ubc7 and Ubc1, and I present reaction mechanisms for Ub chain assembly by both enzymes. In the second part of this discussion, I address how the activity of these enzymes may affect the eukaryotic cell.

3.1.2 Efficient assembly of K48 linked chains by Ubc7 and Cue1 is mediated by the Ub binding CUE domain

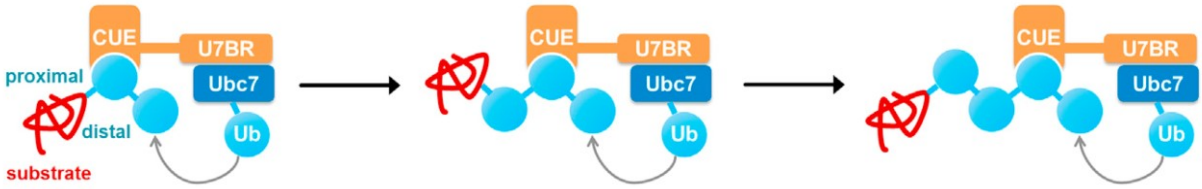

Figure 28: Model of Ubc7 activation by Cue1. The CUE domain of Cue1 binds individual moieties within a Ub chain and Ubc7 is recruited via the U7BR domain. Discharge of donor Ub by Ubc7 is optimally promoted when the CUE domain binds to the penultimate Ub moiety. Additional binding sites facilitate Cue1 recruitment and further accelerate chain elongation. Figure from von Delbrück *et al.*[1]

Ubc7 was previously reported to be recruited and activated through the U7BR domain of its co-factor Cue1.[84] However, how Ub binding by Cue1 could stimulate chain formation remained elusive. In a collaborative effort, we showed through single turnover ubiquitination experiments that interaction of the CUE domain of Cue1 with the penultimate moiety of a K48 chain strongly promotes Ubc7 activity. NMR binding experiments revealed that the CUE domain of Cue1 preferentially associates with Ub molecules, to which another Ub was attached through K48. This facilitates recruitment of Cue1 to K48 chains over other chain types and increases the affinity for K48 chains with increasing length. Intriguingly, we observed higher turnover of $^{48x3}Ub_4$ than $^{48}Ub_2$ in presence of Ubc7/Cue1. In other words, Ub binding by Cue1 prevents self-attenuation of Ub chain elongation and self-accelerates this process (Figure 28).

We found that the interaction between the CUE domain and Ub is well suited for the chain elongation process in several ways. Cross-linking the CUE domain to specific positions in K48

chains provided clear evidence that binding to the penultimate moiety most effectively stimulates elongation reactions with Ubc7. In another line of experiments, the introduction of a R42A amino acid substitution into Ub was exploited to disrupt binding of the CUE domain to defined sites. The substitution elicited the strongest impact when located at the penultimate position of a K48 chain. However, introducing the substitution to more or to other positions also reduced Ubc7 activity. It is therefore possible that the CUE domain promotes Ubc7 activity not only by positioning the E2 enzyme at a specific location but also by increasing the local concentration of the E2 enzyme in proximity to the Ub chain. The CUE domain interacts with the conserved hydrophobic patch in Ub, but we found its binding interface to extend to additional residues in the C-terminus of Ub attached to K48 of another Ub moiety. This was particularly evident for G75 in NMR titration experiments. A prerequisite for this binding mode is the exclusion of K48 from the binding interface, which is involved in the recruitment of, for example, Cue2.[86] This property also minimises the negative effect on reaction rates in conditions under which binding of the CUE domain competes with Ubc7 activity (section 2.1.2). Based on our PELDOR experiments, we showed that the CUE domain associates with and stabilises pre-existing conformations of K48 chains.[2] Binding endogenous conformations with rather low affinity might aid in iterating binding events with high frequency. Possibly this enables the CUE domain to quickly sample different positions within the K48 chain, which increases the chance for a productive alignment of Ubc7 and reduces the dwell time in positions unsuitable for chain elongation.

We observed *de novo* diubiquitin assembly by Ubc7, which putatively requires Ubc7 dimerisation. Chain elongation was more efficient than diubiquitin formation (Figure 10). Nevertheless, this finding was particularly intriguing because Ubc7/Cue1 requires a K48 chain of two or more moieties for efficient chain elongation. In absence of such a K48 chain as scaffold Ubc7 might prime a substrate with diubiquitin to enable subsequent chain elongation. The validity of this finding should be tested through identifying a Ubc7 variant impaired only in diubiquitin formation, but not in chain elongation, and its effects on substrate degradation should be studied *in vivo*.

3.1.3 Assembly of K48/K63 branched ubiquitin chains by Ubc1 is dependent on its Ub binding UBA domain

The UBA domain of Ubc1 was previously reported to facilitate assembly of K48 chains.[126] To assess its role in enzymatic activity, I compared reaction rates in experiments with either Ubc1 or only its UBC domain in presence of different acceptor Ub species. Reactions with the full-length enzyme were compared to only the UBC domain and yielded approximately 25% faster turnover of monoubiquitin and $^{48}Ub_2$. However, this effect was eclipsed by the 6.3 fold increase in reaction rate for $^{63}Ub_2$. This increase is the same order of magnitude as the 12 fold faster turnover of $^{48}Ub_2$ over monoubiquitin by Ubc7/Cue1 under similar reaction conditions.[1] Conversely, turnover of $^{48}Ub_2$ by full-length Ubc1 was 25% slower than turnover of monoubiquitin, which presents a stark contrast to Ubc7/Cue1. Accordingly, NMR binding studies showed that the UBA domain binds better to the distal moiety in $^{48}Ub_2$ than to the proximal one. This is the inverse selectivity as observed for the CUE domain. Moreover, the UBA domain binds worse to K48 chains, which are the enzymatic product of Ubc1, than to K63 chains, which have to this point in time not been linked to Ubc1 activity. These findings conflict with a designated role of the UBA domain in aiding processivity during assembly of K48 chains.

Instead, I observed selective activity towards K63 chains. Amino acid substitutions in $^{63}Ub_2$, which either block the acceptor lysine in Ub (K48R) or interfere with binding of the UBA domain (R42A), revealed that binding of the UBA domain to the distal moiety enables the UBC domain to target K48 in the adjacent proximal moiety. Evidently, the UBA domain of Ubc1 facilitates the rapid modification of K63 chains to form K48/K63 branched chains – an until now little studied chain architecture (Figure 29A). Introducing the K48R substitution into different positions of $^{M1}Ub_2$ revealed the same site specificity as observed for $^{63}Ub_2$. However, the initial reaction rate for turnover of $^{63}Ub_2$ was three times higher than for $^{M1}Ub_2$ despite the strong structural similarity between M1 chains and K63 chains. This emphasises the selectivity of Ubc1 for K63 chains. Importantly, no factors in *S. cerevisiae* are thus far known to assemble M1 chains. Experiments with chimeric Ubc1, in which the UBA domain was replaced with either the CUE domain of Cue1 or the Dsk2 UBA domain, did not allow efficient formation of K48/K63 branched chains. These domains share an equivalent fold and the propensity to associate with the hydrophobic patch in Ub. Therefore, these results point towards unique properties of the Ubc1 UBA domain. Possibly, the binding interface between the UBA domain and the UBC domain is disrupted in the chimeric proteins or the dynamics of the process are disturbed because of an altered binding affinity for Ub.

Unlike the CUE domain, we could not observe a binding preference of the UBA domain for individual moieties within the selectively targeted Ub chain. It could be argued that preferential association with a specific Ub moiety is less important for the formation of branched chains than for chain elongation. The chance to randomly bind the distal Ub in a chain, which is required for chain elongation by Ubc7/Cue1, decreases with increasing chain length. However, to introduce a branching point into a K63 chain, the UBA domain of Ubc1 could associate with any but the proximal moiety. Thus, the chance for a productive binding event increases with growing chain length. Ubc1 recruitment to K63 chains under physiological conditions may benefit from avidity and thereby compensate for the relatively low binding affinity. Conversely, the propensity to bind increasingly long K48 chains is hindered due to the reduced binding affinity between the UBA domain and Ub modified at K48.

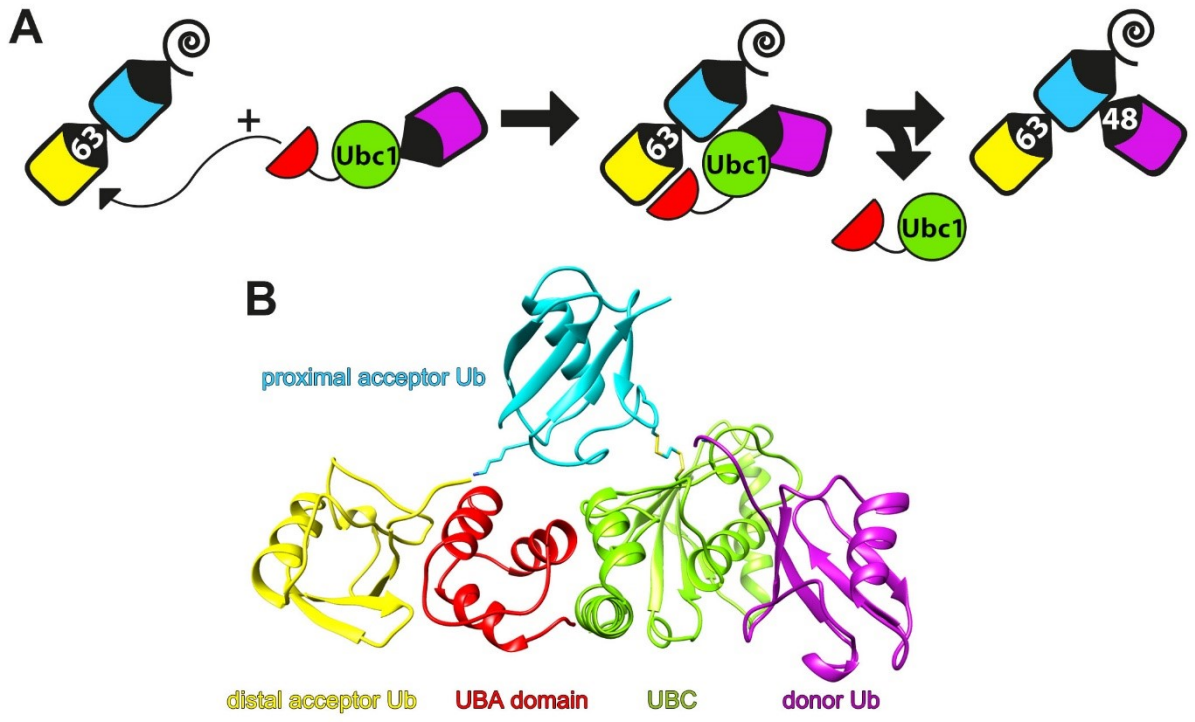

Figure 29: Model of Ubc1 mediated assembly of K48/K63 branched ubiquitin chains. (A) Cartoon model of Ubc1 activity. Ubc1~Ub thioester associates with a K63 chain by binding distal Ub (yellow) via the UBA domain (red). Ubc1 then attaches the donor Ub (purple) to the adjacent proximal moiety (teal), which leads to the generation of a K48/K63 branched chain. (B) Structural model for the transition state of the reaction according to Figure 14F.

3.1.4 Structural insights into Ubc1 activity

Based on existing structural information about Ube2K and my experiments on Ubc1, I propose a structural model for a transition state during branched chain formation (Figure 29B). This transition state relies on three inter-domain interactions. First, the UBA domain binds Ub via a canonical UBA:Ub interface through interaction between helix α1 and α3 of the UBA domain with the hydrophobic patch in Ub. Second, the UBC domain and UBA domain interact through a hydrophobic interface, which was reported in crystal structures of Ube2K. Third, the immediate acceptor Ub aligns with the UBC domain, which most prominently involves D58-Y59-N60 in Ub and S81-S82-T84-D123 in Ubc1. This interaction interface was previously predicted by HADDOCK modelling.[124] The transition state implies that the K63 chain, which is part of the interaction, assumes an open conformation. This indicates that Ubc1 like Ubc7/Cue1 might rely on conformational selection for binding. It would be interesting to experimentally asses how Ubc1 affects the conformational space of $^{63}Ub_2$.

I investigated the interaction between Ubc1 and K63 chains through X-ray crystallography. To this end, I purified and crystallised a complex of Ubc1, which was enzymatically conjugated to a pseudo donor Ub and chemically cross-linked to $^{63}Ub_2$. However, the distal moiety of $^{63}Ub_2$ could not be observed due to a lack of electron-density in the X-ray crystallographic structure. The poor electron density for the distal moiety in $^{63}Ub_2$ could be explained by the inherently high flexibility of K63 chains.[72] Moreover, it appears this Ub unit is not coordinated with any of the other complex components – unlike the proximal unit in $^{63}Ub_2$, which tightly binds to the UBC domain, and unlike Ub_D, which in turn associates with a symmetry related UBA domain. Inter-complex binding or oligomerisation of Ubc1~Ub provide no obvious implication for Ubc1 activity. Although my structural investigation failed to capture a meaningful overall complex architecture, the value of the structure lies in the experimental determination of the binding interfaces between the UBC domain of Ubc1 and acceptor Ub (UBC:Ub_A) as well as the binding interface between the UBA domain and Ub (UBA:Ub). The UBC:Ub_A interface revealed that K63 in Ub_A points towards the helix α4 in Ubc1, where the UBA domain is located.

While Merkley and Shaw[105] report high flexibility in the linker region connecting the UBC domain and the UBA domain in an NMR solution structure of Ubc1, multiple crystal structures of Ube2K show close association between the UBC domain and the UBA domain (PDB IDs: 5DFL, 6IF1, 3E46, 3F92, 3K9O, 3K9P). The significance of this association for enzymatic activity could not directly be inferred from my experimental data. An important observation in this context was the reduced activity of Ubc1 towards M1 chains as compared to K63 chains,

despite their structural similarity. The introduction of Ub(K48R) into $^{M1}Ub_2$ disturbed Ubc1 activity with the same position dependent effect as for $^{63}Ub_2$. However, the reaction rate was three times lower than in reactions with $^{63}Ub_2$. This indicates that the flexibility between UBC domain and UBA domain cannot compensate for the minor structural differences between $^{M1}Ub_2$ and $^{63}Ub_2$. Alternatively, one could speculate about a model, in which the interaction between the UBC domain and the UBA domain is not required to provide an adequate binding interface for $^{63}Ub_2$. Instead, the binding of $^{63}Ub_2$ could bring the UBA domain and the UBC domain in contact, which in turn might facilitate a discharge of Ub_D. In preliminary aminolysis experiments with the UBC domain I could not observe a stimulating effect upon addition of the UBA domain separately (data not shown). However, the exact role of association between the UBC domain and the UBA domain during branched chain formation still needs to be clarified.

3.1.5 Coordination of acceptor ubiquitin is mediated through low affinity interactions

In order to quantify the binding parameters by conventional biophysical methods (*e.g.* ITC, SPR, MST), a ligand typically needs to be employed at concentrations several times higher than the respective K_d value. For very low affinity protein-protein interactions, this might not be feasible. In the MST experiments presented in this study, dissociation constants could not successfully be determined. Although high ligand concentrations were employed, which caused visible viscosity in the Ubc1 stock solution, binding of Ub could not be saturated. Proper quantification might also have failed as thermophoretic mobility of Ub could only be measured at a relatively low pH of 6.2. This might interfere with physiological binding properties of Ubc1. We determined binding affinities to individual Ub moieties in ^{15}N-labelled diubiquitin probes by NMR titration experiments. The K_d values for binding the Ub moiety, which enables Ub transfer, reflected a relatively low affinity with 192 µM and 84 µM for the UBA domain and the CUE domain respectively. Similarly, the K_d value for binding of monoubiquitin by Mms2, which activates the E2 Ubc13, was reported to be 30 µM.[145] Compared to the binding of Ub moieties, which do not enable chain formation, we observed no more than a 2-fold difference in dissociation constants. Despite the low binding affinity and weak preference towards the correct moieties, these interactions play a pivotal role for the activity of the respective E2 enzymes. Ultimately, single turnover ubiquitination experiments provided a clearer picture of chain type preference than binding assays. Binding of Ub might not only be necessary to recruit these E2 enzymes to a specific position, but also to increase the dwell time of the UBC domain in proximity to the correct Ub_A. This might be required to enhance the chance of a productive interaction between enzyme and substrate. The set of acceptor Ub species generated in this

study was used for a first line of experiments on the K48 specific E2 enzyme Ubc3. Similar to Ubc1, Ubc3 – dependent on its C-terminal extension – showed enhanced activity in the presence of $^{63}Ub_2$, but in contrast to Ubc1 not in the presence of $^{M1}Ub_2$. Moreover, Ubc3 preferentially targeted the distal moiety in $^{63}Ub_2$, which is the inverse selectivity observed for Ubc1.

In conclusion, Ub binding interfaces guiding Ub chain assembly may be inherently difficult to discover and characterise. While this study focusses on UBDs, other Ub binding interfaces can be comprised of a single helix[146] or be a small part of an otherwise large protein complex[147]. Low affinity Ub binders might rely on conformational selection as a general pattern. Thus, approaches exploiting simulated docking between the enzymes' surface and known preferential conformations of their cognate Ub chains could provide valuable insights. Moreover, methods which rely on the immobilisation of a bait protein in high density on a surface, could be used to characterise these extremely weak protein-protein interactions. [148] Thereby, the necessity for very high ligand concentrations in traditional methods could be circumvented.

3.2 Biological implications

3.2.1 Modulation of E2 enzyme activity *in vivo*

We found that amino acid substitutions in Cue1, which reduced the binding affinity towards Ub, also impaired its ability to stimulate chain assembly by Ubc7. Moreover, introducing these Cue1 variants into *S. cerevisiae* impaired degradation of the ERAD-substrate Ubc6. This indicates that Ubc7 and Cue1 are fine-tuned machinery, as other factors that modulate the length of existing K48 chains did not override the changes in enzyme kinetics. This includes the UFD pathway which extends K48 chains[47,149] and DUBs. Moreover, ubiquitin receptors in the downstream acting factors – such as Cdc48, which is required for substrate dislocation[150], or the proteasome – could be indifferent towards slightly altered chain length distribution in the substrate. Taken together this highlights that the dynamics in polyubiquitin chain assembly have an impact on a cellular level and, by extension, may affect the entire organism.

While Ubc7 has a well-established role in ERAD, Ubc1 has been implicated in various biological processes and shown to cooperate with multiple different E3 ligases. The role of the UBA domain uniquely contained in Ubc1 and its homologues remains unclear. Ubc1 has been implicated in cell cycle progression[110], in ERAD[21], in nuclear protein quality control[151] and in heat stress tolerance[109,152]. I aimed to replicate reported functions of Ubc1 in several exploratory experiments to assess the impact of the UBA domain. In collaboration with Dr. Janine Kirstein (FMP, Berlin), we identified that depletion of the Ubc1 orthologue ubc-20 in *C. elegans* induced

the aggregation of huntingtin (Htt) with a short polyQ stretch. The human homologue Ube2K or HIP2 ("huntingtin interacting protein 2") has previously been shown to be involved in the formation of Htt aggregates.[117] Interestingly, imbalance of K48 and K63 chains has also been linked to formation of these toxic Htt aggregates[153]. Thus, I reconstituted expression of Htt-GFP in *S. cerevisiae.* I observed the previously reported aggregation propensity in dependence of the length of its polyQ repeats. However, I could not detect an influence of Ubc1 in this context. Despite being a useful system to study the aggregation of Htt, yeast might lack important components which are present in cells endogenously harbouring Htt. Moreover, Htt overexpression might overburden the ubiquitination machinery, resulting in less ubiquitination or a different pattern than under physiological expression levels. To validate a direct effect of Ubc1 and its homologues on polyQ proteins, further experiments should be conducted. A first step could be to quantitatively assess Ub chain types on Htt from *C. elegans* depleted of ubc-20.

The investigation of Ubc1 in *S. cerevisiae* was complicated by poor expression of constructs lacking the UBA domain or harbouring mutations in the sequence coding for the QGF motif (aa179-181), which has previously been reported to be pivotal in Ub binding[130]. The destabilisation of Ubc1 missing the UBA domain has also been observed by others.[123,154] I hypothesised that a correctly folded UBA domain might be necessary to stabilise Ubc1 in the cellular environment through interactions with the UBC domain. Therefore, I tested amino acid substitutions in solvent exposed side chains and I identified the Ubc1-EEAA variant (E211A, E212A) to be expressed at similar levels as wild type Ubc1 (data not shown). Nonetheless, this variant was impaired in Ub binding and branched chain assembly (Figure 16, Figure 20). It could be exploited to identify UBA-domain-dependent processes in established Ubc1 phenotypes. Alternatively, a yeast strain harbouring such a variant could be employed in an unbiased screening approach to identify novel substrates of Ubc1.

3.2.2 Signalling capacity of K48/K63 branched chains

In the pursuit to identify the function of the UBA domain, Ubc1 unexpectedly proved to preferentially assemble K48/K63 branched chains. These unusual Ub signals have only recently been identified in mammalian cells.[58] Ohtake *et al.* show a possible role of such chains in NF-kB-signalling and retargeting of substrates decorated with K63 chains to proteasomal degradation. We were able to show that the assembly of K48/K63 branched chains is conserved in *S. cerevisiae* and thus probably in all eukaryotic organisms. However, their detailed function remains to be explored. As the NF-kB-signalling pathway is not conserved in yeast, Ubc1 and its homologues most likely affect other cellular processes. It will be interesting to see if they

partake in editing of Ub chains to retarget substrates modified with K63 chains for proteasomal degradation or function in other ways. The first step in addressing this question will be to validate the effect of Ubc1 on abundance of K48/K63 branched chains in yeast.

There are indications that Ub binders selective for certain linkages can still bind their cognate chain type, even if it is integrated into branched chains.[60] Alternatively, K48 modification of a K63 chains might disrupt binding of downstream factors due to the proximity of K48 to the hydrophobic patch in Ub. K48/K63 branched chains could also provide a unique interface for selective binders. Future studies could identify such binders by performing pull-down experiments coupled with mass spectrometry[155] using differently linked Ub chains and branched chains as bait. Reversibly, binders specific for branched chains or antibodies engineered for their detection could help to reveal substrates, which are decorated with these signals.

3.3 Concluding remarks

Ubiquitination was discovered as a mechanism for protein degradation in the 1980s. Since then, it emerged as a highly versatile modification governing widespread functions in the eukaryotic cell. Researchers uncovered the different ways in which Ub chains can be assembled, and how post-translational modifications of Ub like phosphorylation and acetylation change its signalling capacity. This led to a much more sophisticated view on protein ubiquitination in cell biological studies. However, there is still much to learn. The different chain types and PTMs of Ub have been metaphorically described as the “words” of the Ubiquitin Code.[156] In extension, we need yet to understand basics about its “grammar”. This entails answering questions such as: What is the interdependence between chains with different linkage types as well as Ub decorated with small chemical groups? Is there a hierarchy in co-occurring modifications? How does chain length and the presence of multiple modifications affect Ub signalling? What role does chain topology play as observed, for example, in mixed and branched chains? Moreover, there is still a significant gap to close between the mechanistic investigation of ubiquitination and its physiological outcomes. Understanding the most complex regulatory network in the eukaryotic cell carries great promise for insights into human development and disease. By providing a functional link between K63 chains and K48 chains as well as Ub chain assembly and the activity of UBDs, this study contributes to the endeavour of achieving an integrated understanding of the Ubiquitin Code.

4. Experimental Procedures

4.1 Materials

4.1.1 Bacterial strains

XL1-blue cells (Aligent Technologies)

BL21 Rosetta 2 cells (Novagen)

DH5a competent *E. coli* (NEB)

4.1.2 Yeast strains

Most yeast strains were derived from DF5[157] (S288C), which has the following genetic background: *MAT a/alpha trp1-1(am) his3-Δ200 ura3-52 lys2-801 leu2-3,-112*.

name	genotype	mat
yWO1	DF5	alpha
yWO2	DF5	a
yWO5	DF5 Δ*ubc1::HIS3*	alpha
yWO6	DF5 Δ*ubc1::HIS3*	a
yTX106	DF5 Δ*ubc7::LEU2*	alpha
yTX105	DF5 Δ*cue1::HIS3*	alpha
Sub328	DF5 *ubil-Δ1::TRP1 ubi2-Δ2::URA3 ubi3Δub-2 ubi4-Δ2::LEU2* +[pUB146] +[pUB100] (Spence *et al.*[23])	a
yLP12	sub328 + pLP048 –[pUB146]	a
yLP13	sub328 + pLP105 –[pUB146]	a
yLP26	sub328 + pLP048 –[pUB146] *Δubc1::URA3*	a
yTX1251	W303 background: *trp1Δ1, his3-11,15, ura3-52, lys2-801, leu2-3,-112*	a
yLP14	yTX1251 *GAL-Htt25Q_p303::HIS3*	a
yLP15	yTX1251 *GAL-Htt103Q_p303::HIS3*	a
yLP16	yTX1251 *Δubc1::URA3*	a
yLP17	yTX1251 *GAL-Htt25Q_p303::HIS3 Δubc1::URA3*	a
yLP18	yTX1251 *GAL-Htt103Q_p303::HIS3 Δubc1::URA3*	a
yLP21	yTX1251 *GAL-Htt25Q_p303::HIS3 Δatg1::kanMX*	a
yLP22	yTX1251 *GAL-Htt25Q_p303::HIS3 Δatg1::kanMX Δubc1::URA3*	a

4.1.3 Plasmid list

name	insert	backbone	origin
GST-tagged Ubc1			
pTX449	GST-Ubc1 (GST cleavable with HRV3C)	pGex-6p1	this study
pTX457	GST-UBC (Ubc1,1-150)	pGex-6p1	this study
pTX432	GST-UBA (Ubc1,151-215)	pGex-6p1	this study
pTX454	GST-Ubc1 LRV (QGF179-181)	pGex-6p1	this study
pTX451	GST-Ubc1 K93R	pGex-6p1	this study
pTX459	GST-UBC K93R	pGex-6p1	this study
pLP034	GST-Ubc1 EEAA (E211,E212)	pGex-6P1	this study
pLP106	GST-Ubc1 K93R, EEAA (E211,E212)	pGex-6P1	this study
pLP099	GST-Ubc1 K93R, T84D	pGex-6p1	this study
pLP101	GST-Ubc1 K93R, E211R	pGex-6p1	this study
pLP102	GST-Ubc1 K93R, R192Q	pGex-6p1	this study
UBC domain of Ubc1(2-149) with UBA domain of Dsk2 or CUE domain of Cue1			
pLP001	GST-Ubc1-3xGS-UBA(Dsk2)	pGex-6p1	this study
pLP002	GST-Ubc1-6xGS-UBA(Dsk2)	pGex-6p1	this study
pLP003	GST-Ubc1-12xGS-UBA(Dsk2)	pGex-6p1	this study
pLP004	GST-Ubc1-3xGS-CUE-GS-6xHis	pGex-6p1	this study
pLP005	GST-Ubc1-6xGS-CUE-GS-6xHis	pGex-6p1	this study
pLP006	GST-Ubc1-12xGS-CUE-GS-6xHis	pGex-6p1	this study
pLP007	GST-Ubc1(K93R)-3xGS-CUE-GS-6xHis	pGex-6p1	this study
pLP008	GST-Ubc1(K93R)-6xGS-CUE-GS-6xHis	pGex-6p1	this study
pLP009	GST-Ubc1(K93R)-12xGS-CUE-GS-6xHis	pGex-6p1	this study
pLP010	GST-Ubc1(K93R)-3xGS-UBA(Dsk2)	pGex-6p1	this study
pLP011	GST-Ubc1(K93R)-6xGS-UBA(Dsk2)	pGex-6p1	this study
pLP012	GST-Ubc1(K93R)-12xGS-UBA(Dsk2)	pGex-6p1	this study
Other enzymes			
pTX475	GST-Ubc4(Δintron)	pGEX-6p1	this study
pLP016	GST-Ubc4(Δintron)-K91R	pGEX-6p1	this study
pMD28	GST-Ubc13	pGEX4T1	Mansour *et al.*[158]
pMD29	GST-Uev1a	pGEX6p1	Mansour *et al.*[158]
pMD27	Ube2K	pET28	gift from Prof. R. Klevit, [159]
pLP054	Ube2K K97R 6His	pET28	this study
pLP061	GST-Ubc20	pGex-6p1	this study
pTX315	Hrd1-RING (325-550)	pGex-6p1	Bagola *et al.*[84]
pTX481	hUbe1-6xHis	pET21d	Berndsen and Wolberger[160]
pTX249	Ubc7	pGEX6p1	Bagola *et al.*[84]
Ubc7-U7BR	Ubc7(FL)-GG-Cue1(147-203, C147S)	pET39b(+)	Kniss *et al.*[2]
pMD26	Cdc34	pGEX6p1	von Delbrück *et al.*[1]
Ub binders			
pSH006	GST-Dsk2-UBA (aa241-374)	pGex-6p1	Bagola *et al.*[84]
gp78-CUE	10xHis-Ub19-TEV-gp78CUE (aa453-503)	pET39b(+)	Kniss *et al.*[2]
OTUB1	His6-GST-3C-OTUB1 C91A (aa1-271)	pOPINK	Kniss *et al.*[2]
Plasmids for structural investigation			
pLP063	6xHis-Smt3-Ubc1	pRSFduett	this study
pLP065	6xHis-Smt3-A-hUb(K48R)	pRSFduett	this study
pLP067	UbK48C,G75*	pET21d	this study

name	insert	backbone	origin
Ubiquitin expression experiments			
pMD10	hUb (human ubiquitin, codon optimised for E. Coli)	pETM60	von Delbrück *et al.*[1]
pMD16	hUb K48R	pETM60	von Delbrück *et al.*[1]
pMD18	hUb K63R	pETM60	von Delbrück *et al.*[1]
pLP109	hUb K48R, K63R	pETM60	this study
pMD14	hUb R42A	pETM60	von Delbrück *et al.*[1]
pLP107	hUb R42A, K48R	pETM60	this study
pMD11	hUb-6xHis	pETM60	von Delbrück *et al.*[1]
pLP090	hUb-6xHis Q62R	pETM60	this study
pMD17	hUb-6xHis K48R	pETM60	von Delbrück *et al.*[1]
pMD15	hUb-6xHis R42A	pETM60	von Delbrück *et al.*[1]
pLP108	hUb-6xHis R54A	pETM60	this study
pLP079	linUb2-6xHis	pRSF Duet	this study
pLP110	linUb2-6xHis K48R(proximal)	pRSF Duet	this study
pLP111	linUb2-6xHis K48R(distal)	pRSF Duet	this study
Ubiquitin for fluorescent labeling (MST assays, *in vitro* ubiquitination)			
pMD12	human ubiquitin S20C (*E. coli* codon optimised	pETM60	von Delbrück *et al.*[1]
pMD13	hUb S20C - 6xHis	PETM60	von Delbrück *et al.*[1]
pLP77	hUb-SGCG-6xHis	pRSF duet	this study
Cue1 costructs for protein expression (NMR titration and activity assays)			
Cue1-CUE	Ub19 – TEV – Cue1 (25-203, C147S) Ub19 – His6	pET39b(+)	von Delbrück *et al.*[1]
pTX410	Cue1 (ΔTM,24-203) pGex-6p1	pGex-6p1	Bagola *et al.*[84]
pMD23	Cue1 E96A	pGex-6p1	von Delbrück *et al.*[1]
pMD24	Cue1 E100A	pGex-6p1	von Delbrück *et al.*[1]
pMD25	Cue1 L103A	pGex-6p1	von Delbrück *et al.*[1]
pTX411	Cue1 RGA (L76,A77,P78)	pGex-6p1	von Delbrück *et al.*[1]
Degradation of Ubc6 in presence of binding deficient Cue1 mutants			
pTX397	Cue1 (bp -450 bis +609)	pRS415	Bagola *et al.*[84]
pLP022	Cue1 E96A	pRS415	von Delbrück *et al.*[1]
pLP023	Cue1 E100A	pRS415	von Delbrück *et al.*[1]
pLP024	Cue1 L103A	pRS415	von Delbrück *et al.*[1]
pTX386	Cue1 RGA	pRS415	Bagola *et al.*[84]
Expression of mutant ubiquitin in yeast			
pUB100	expression of Ubi1 tail	-	Spence *et al.* [23]
pUB146	Ub expression plasmid under GAL promoter (URA3)	-	Spence *et al.* [23]
pGR295	10xHis-Ub	-	Provided by Gwenael Rabut
pLP048	10xHis-Ub R54A	pGR295	this study
pLP105	10xHis-Ub R54A, K63R	pGR295	this study
pLP069	Ubc1(URA) deletion-cassette	pBluescript	this study
Introduction of Htt into *S. cerevisiae*			
Addgene 15576	GAL Htt(Exon1)-25Q+ProGFP-FLAG	p303	Duennwald *et al.*[142]
Addgene 15577	GAL Htt(Exon1)-103Q+ProGFP-FLAG	p303	Duennwald *et al.*[142]

4.1.4 Media and Buffers

4.1.4.1 Media for Yeast cultures

Minimal medium (SD) – 0.67% yeast nitrogen base without amino acids, 2% glucose, 20 mg/l L-histidine, 30 mg/l L-leucine, 30 mg/l L-lysine, 20 mg/l L-tryptophan, 20 mg/l adenine sulfate, 20% uracil

Full medium (YPD) – 2% Bacto™ peptone, 1% Bacto™ yeast extract, 2% glucose, pH5.5 adjusted with HCl

For preparation of growth plates 2% Agar-Agar was included in the respective medium.

4.1.4.2 Media for bacterial growth

Lysogeny broth (LB) – 1% Bacto™ tryptone, 0.5% Bacto™ yeast extract, 1% NaCl

Terrific broth (TB) – 1.2% Bacto™ tryptone, 2.4% Bacto™ yeast extract, 0.4% glycerol, 17 mM KH_2PO_4, 72 mM K_2HPO_4

Super Optimal broth with Catabolite repression (SOC) – 2% Bacto™ tryptone, 0.5% Bacto™ yeast extract, 10 mM NaCl, 2.5 mM KCl, 10 mM $MgCl_2$, 10 mM $MgSO_4$, 0.2% glucose

For preparation of growth plates 2% Agar-Agar was included in LB medium.

Selective antibiotics were used at a final concentrations of 50 µg/ml for Ampicillin or 25 µg/ml for Kanamycin. Plates for blue-white screening contained 1 mM IPTG and 400 µM X-Gal (5-bromo-4-chloro-3-indolyl-β-D-galactopyranoside).

4.1.4.3 Commonly used buffers

10x PBS – 1.37 M NaCl, 27 mM KCl, 101 mM Na_2HPO_4, 18 mM KH_2PO_4 (pH 7.5)

10x TBT – 0.5 M Tris/HCl pH 7.5, 1.5 M NaCl, 1% Tween20

4x SDS sample buffer – 250 mM Tris/HCl pH 6.8, 40% glycerol, 8% SDS, 0.05% bromophenol blue (including 100 mM DTT unless indicated as 'non-reducing')

4x Urea sample buffer – 8 M Urea, 200 mM Tris/HCl pH 6.8, 5% SDS, 0.1 mM EDTA, 0,03% Bromophenol blue (including 50 mM DTT unless indicated as 'non-reducing')

4.1.5 Protein and DNA standards

ColorPlus Prestained Protein Marker, Broad Range (New England Biolabs)

Protein Molecular Weight Marker (Fermentas)

1 kb DNA Ladder (Invitrogen)

4.1.6 Antibodies

Antibody	dilution	source
polyclonal α-Cdc48 antibody	1:10.000	Neuber et al.[161]
polyclonal α-Cue1 antibody	1:1000	Bagola et al.[84]
monoclonal α-GFP antibody	1:1000	Living colors (JL-8)
monoclonal α-Ub antibody	1:5000	Santa Cruz Biotechnology (P4D1)
polyclonal α-Ubc1 antibody	1:10.000	this study
polyclonal α-Ubc6 antibody	1:10.000	Walter et al.[162]
polyclonal α-Ubc7 antibody	1:10.000	Bagola et al.[84]
polyclonal α-Sec61 antibody	1:10.000	Biederer et al. [102]
HRP-conjugated polyclonal α-mouse-IgG (rabbit)	1:10.000	Sigma (A9044)
HRP-conjugated polyclonal α-rabbit-IgG (goat)	1:10.000	Sigma (A0545)

4.1.7 Consumables

Amicon Ultra centrifugal filters (MWCO: 3K/10K/30K) Millipore
BioMax MR Film, Kodak
cOmplete EDTA-free Protease Inhibitor Cocktail (Roche)
electroporation cuvettes (Carl Roth PP39.1, column width 2 mm)
Expand High Fidelity PCR System (Roche)
Falcon® 15mL High Clarity PP Centrifuge Tube (neolab)
Falcon® 50mL High Clarity PP Centrifuge Tube (neolab)
Glass Beads 0.5 mm dia. (BioSpec Products)
JetStar 2.0 Plasmid Purification Midi Kit (Genomed)
JetStar 2.0 Plasmid Purification Mini Kit (Genomed)
NAP-5 prepacked Sephadex G-25 columns (GE Healthcare)
Zeba Spin Desalting Columns (ThermoFisher)
Pfu Ultra HF DNA-Polymerase (Agilent Technologies)
pGEM-T Easy Vector System (Promega)
pH-Fix colour-fixed indicator sticks (Machery-Nagel)
Phusion High-Fidelity DNA Polymerase (NEB)
QIAEX II Gel extraction kit (500) (QIAGEN)
QuikChange Site Directed Mutagenesis Kit (Agilent Technologies)
Sarstedt Inc Cuvette Semimicro 1.6ml
SnakeSkin Dialysis Tubing (ThermoFischer)
Whatman chromatography papers (Carl Roth)
Wizard SV Gel and PCR Clean-Up System (Promega)

4.1.8 Devices

ÄKTA pure protein purification system (GE Healthcare)
- Superdex 75 Increase 10/300 GL
- Superdex 200 Increase 10/300 GL
- HiLoad Superdex 16/600 75p
- HiLoad Superdex 26/600 75p
- HiTrap SP HP cation exchange chromatography column
- HiTrap Q HP anion exchange chromatography column

Capacitance Extender 1652087 (Bio-Rad)
centrifuge 5415D (Eppendorf)
centrifuge 5417R (Eppendorf)
centrifuge 5424 (Eppendorf)
DC1 W13 Heating Water Bath (Haake)
Electrophoresis Migthy Small II (Hoefer)
EmulsiFlex-C5 (Avestin)
Gene Pulser 1652076 (Bio-Rad)
HE 33 Mini Submarine Electrophoresis Unit (Hoefer)
Innova 44 Incubator Shaker (New Brunswick)
IPP 500 Refrigerated Incubator (Memmert)
LI-COR Odyssey imaging system (LI-CORE Biosciences)
LKB MultiTemp II Water Bath (Pharmacia)
Migthy Small Transfer Tank TE22 (Hoefer)
Mini Horizontal Agarose Electrophoresis Unit HE33 (Hoefer)
NanoDrop 2000 spectrophotometer
Optima Max-XP Ultracentrifuge (Beckman Coulter)
pH meter (Schott)
Primus 25 advanced Thermocycler (peQlab)
Pulse Controller 1652098 (Bio-Rad)
RCT basic IKAMAG safety control universal hot plate magnetic stirrer (IKA)
Refrigerated centrifuge Sigma 4K15
Sorvall RC 6 Plus Centrifuge (Thermo Scientific)
Thermomixer Compact (Eppendorf)
Typhoon FLA 9500 laser scanner (GE Healthcare)
Ultrospec 3100 pro UV/Vis spectrophotometer (GE Healthcare/Amersham)
Vibrax VXR basic (IKA Shakers)
Vortex-Genie 2 (Scientific Industries)

4.1.9 Software

ACD/ChemSketch
Adobe Illustrator
Adobe Photoshop
ApE (A plasmid Editor)
Coot 0.8.9 (Crystallographic Object-Oriented Toolkit)
Igor Pro 6 (WaveMetrics)
Image Studio (LI-COR Biosciences)
ImageJ 1.51n
JabRef 4.1
Microsoft Office (Excel, OneNote, PowerPoint, Word)
Phoenix suite 1.13-2998
SnapGene Viewer
UCSF Chimera

4.2 Methods

4.2.1 Molecular Biology

4.2.1.1 Molecular Cloning

4.2.1.1.1 Preparation of plasmid DNA

Electrocompetent XL-1 cells were transformed with the desired vector and grown on agar plates containing selective antibiotics at 37°C. Single colonies were picked, inoculated in LB medium with selective antibiotics and grown at 37°C overnight in a shaking incubator. Plasmid DNA was purified either from 2 ml liquid culture using JetStar 2.0 Plasmid Purification Mini Kit (Genomed) or from 50 ml liquid culture using the JetStar 2.0 Plasmid Purification Midi Kit (Genomed) according to manufacturer's instructions. The precipitated DNA was resuspended in 50 µl ddH_2O. DNA concentration and purity was assessed by measuring absorption at 260 nm and 280 nm using a NanoDrop 2000 spectrophotometer. The plasmids created in the framework of this thesis were validated by analytical restriction digest and by DNA sequencing (LGC genomics).

4.2.1.1.2 Polymerase chain reaction (PCR)

DNA fragments were amplified from a *C. elegans* cDNA preparation provided by Dr. Janine Kirstein (*ubc-20*), from yeast genomic DNA or from plasmids. PCR reactions with 50-200 ng template DNA were performed in a 50 µl reaction volume in aqueous solution containing 1 µl of a 10 mM dNTP stock, 1 µl of a forward and reverse primer solution each (10 µM) as well as buffer and polymerase. When using the Pfu Ultra DNA polymerase from stratagene 5 µl of the 10x buffer supplied by the manufacturer and 1 µl polymerase solution were added. When using the Phusion High-Fidelity DNA polymerase from NEB 10 µl of the 5x buffer supplied by the manufacturer and 1 µl polymerase solution were added. Typically the reaction mix was run through the following PCR program: 5 min at 95°C (DNA denaturation), 25-30 cycles of 45 s at 95°C (denaturation), 45 s at 48-58°C (annealing), 30 sec per 1 kbp at 68°C with the Pfu polymerase or 72°C with the Phusion polymerase respectively (elongation). At the end of the program, a final elongation step was performed for double the time as during cycling before the reaction was cooled to 8°C and stored.

4.2.1.1.3 DNA restriction digest

Plasmids were digested in a total reaction volume of 50 µl with restriction enzymes from NEB and 5 µl 10x CutSmart buffer supplied with the enzymes. For integration of Ubc1-inserts into pGex-6p1 1 µl of SalI-HF and 1 µl BamHI-HF (20,000 units/ml, NEB) were used. The reaction mix was incubated for 2 h at 37°C and the products separated by agarose gel electrophoresis.

4.2.1.1.4 DNA ligation

DNA inserts and linearised vector backbones from restriction digests were purified from agarose gels. They were mixed approximately in a 3 to 1 molar ratio in a total reaction volume of 20 µl and a total DNA amount of 0.5-4 µg. The ligation mix contained 1 µl T4 DNA ligase and 2 µl 10x ligation buffer from the pGEM-T Easy Vector Systems kit (Promega). The mix was incubated over night at 4°C or for 1h at RT before transformation into electrocompetent XL-1 cells.

4.2.1.1.5 Agarose gel electrophoresis for DNA analysis

Agarose gel electrophoresis was performed in order to separate DNA fragments by their molecular weight. Agarose gels were prepared with either 2% agarose for detection of fragments smaller than 1 kbp or otherwise with 1% agarose in 1x TAE buffer (40 mM Tris/HCl pH 8.2, 0.14% acetic acid, 1 mM EDTA). Agarose was melted by microwaving and after cooling down to approximately 50°C mixed with RedSafe (1:30.000), which is required for DNA detection under UV light. Samples were mixed with DNA sample buffer, added to agarose gels in 1x TAE buffer and run for 10-20 min at 100 V. For fragments larger than 500 bp sample buffer was 50% glycerol, 5 mM EDTA and 0.1% (W/V) Bromophenol blue. For fragments of 500 bp and smaller 0.25% Orange G was used instead of Bromophenol blue. Gels were then analysed using a UV-Transilluminator Gel-Doc (peQLab).

4.2.1.1.6 Purification of DNA from agarose gels

To purify DNA from agarose gels, the desired fragments were viewed on a UV-Transilluminator and excised using a scalpel. To separate DNA from agarose the kit Wizard SV Gel and PCR Clean-Up System (Promega) was used according to manufacturer's instructions. In short, the agarose gel pieces were melted in a solution of guanidine isothiocyanate at 50°C and DNA was immobilised on the surface of silica. After multiple wash steps, DNA was eluted from the silica by addition of 10-20 µl ddH_2O and then used for DNA ligation.

4.2.1.1.7 Gibson assembly

Cloning of inserts into pRSFduett and pET21d was achieved by Gibson assembly as described elsewhere.[163] Gibson assembly relies on primers, which amplify the insert and backbone with 30-50 bp complementary overhangs in two separate PCR reactions. Equimolar amounts of reaction products were combined and incubated with a Gibson assembly mix. The mix contained Phusion DNA polymerase ,T5 exonuclease and DNA ligase. The T5 exonuclease removes basepairs from the annealed strands, producing gaps, which are then filled by the polymerase. The DNA ligase seals the nicks between inserts and backbone. Gibson assembly mix was prepared by the biochemical core facility of the MPIB (Martinsried).

4.2.1.1.8 Quickchange PCR

In order to introduce point mutations or delete one to three codons from a plasmid Quickchange Site Directed Mutagenesis kit by Agilent Technologies was used according to manufacturer's instructions. A reaction mix with 5 µl of 10x reaction buffer, 10 ng DNA template, 1 µl of a 10 µM forward primer solution, 1 µl of a 10 µM reverse primer solution, 1 µl dNTP mix, 3 µl DMSO and 1 µl PfuUltra HF DNA polymerase was added to a total reaction volume of 50 µl in ddH_2O and run with the following PCR program: 1 min at 95°C (DNA denaturation), 25-30 cycles of 50 s at 95°C (denaturation), 50 s at 55-65°C (annealing), 1 min per 1 kbp at 68°C. After cycling a final elongation step was performed for double the time before the reaction was cooled to 8°C and stored. 3 µl of the reaction mix were transformed into XL-1 cells and plated onto agar plates with selective antibiotics. Single colonies were picked and inoculated in LB medium with antibiotics for DNA preparation.

4.2.1.1.9 Chromosomal gene modification in *S. Cerevisiae*

In order to delete genes in *S. cerevisiae* and to attach carboxy-terminal epitope tags to proteins of interest methods were applied, which rely on integration of DNA cassettes into the genome through homologous recombination.[164,165] DNA cassettes were generated by PCR-reactions and harboured a selective marker, which either complemented auxotrophy of a specific strain or mediated antibiotic resistance. This enabled selection of transformed cells by growth on selective medium. The cassettes were flanked by sequences of typically 20 to up to 50 bp length, which were homologous to the targeted gene and guide the DNA to the respective loci, where they are integrated through homologous recombination. DNA was transformed into yeast cells by heat shock as described in section 4.2.4.2. Transformed cells were transferred onto selective

agar plates and incubated at 30°C for two days. Successful transformation was validated by analytical PCR reactions and/or SDS-PAGE and immunoblotting.

4.2.1.1.10 Deletion cassette for *ubc1*

All attempts of to delete *ubc1* from yeast strains following standard protocols as described in the previous section failed. I aimed to optimise recombination deletion of *ubc1* in yeast by using longer flanking regions. To this end, I performed a restriction digest at endogenous restriction sites for BamHI 400bp upstream and for XhoI 270bp downstream of the *ubc1* open reading frame and ligated the fragment into pBluescript. A restriction site for PstI within the *ubc1* open reading frame was exploited to introduce the URA selection cassette from pUG72. For *ubc1* deletion 5 µg of the plasmid were digested with BamHI and EcoO109I and run on an agarose gel. The released 689bp was purified and transformed into the desired yeast strain. Successful deletion was confirmed by growth on selective agar plates, immunoblotting for Ubc1 and analytical PCR.

4.2.1.2 Transformation of electrocompetent *E. Coli*

Electro-competent cells were stored in 50 µl aliquots at -80°C and thawed on ice for transformation. 1 µl purified plasmid DNA, 2-3 µl PCR product or 5 µl ligation mix were added to the cells and then transferred to an electroporation cuvette. Cells were pulsed using Bio-Rad Gene Pulser set to 2.5 MV, 25 µF and 200 Ω and incubated for at least 60 min in SOC medium at 37°C. Cells were then plated onto LB agar plates with selective antibiotics and grown overnight at 37°C.

4.2.1.3 Transformation of chemically competent *E. Coli*

Chemically competent *E. coli* cells were transformed by heat shock. Cells were incubated with the desired DNA (either 1 µl purified plasmid DNA or 3 µl from a 50 µl PCR reaction) for 30 min on ice. Then, cells were placed in a heat block at 42°C. After 30 s cells were put back on ice for a few seconds and mixed with 450 µl SOC medium. Subsequently, cells were incubated at 37°C for 1 h and plated onto selective LB agar plates. Single colonies were selected after overnight incubation at 37°C.

4.2.1.4 Expression of recombinant proteins in *E. Coli*

For heterologous protein expression BL21 Rosetta cells were transformed with the desired expression plasmids and transferred onto selective LB Agar plates. Precultures from single colonies were grown over night in LB amp with respective antibiotics in a shaking incubator at

37°C. 10 ml of preculture were added to 1l TB medium and grown while shaking in a large flask (typically 5l) at 37°C to 1 OD_{600}/ml. The cells were the cooled to 18°C unless otherwise indicated and protein expression induced with 500 µM IPTG. Cells were grown over night and harvested by centrifugation at 5000 *x* g for 15 min. Cells were transferred to 50 ml Falcon tubes using the desired lysis buffer and either directly used for purification or flash frozen in liquid nitrogen. Frozen cell pellets were stored at -80°C.

4.2.1.5 Expression of isotope-labelled Ub for NMR

For the expression of ^{15}N labelled Ub monomers with and without 6xHis-tag, cells were grown in minimal medium containing 7.5 g/l Na_2HPO_4, 3 g/l KH_2PO_4, 0.5 g/l NaCl, 2 mM $MgSO_4$, 0.1 mM $CaCl_2$, 10 µM $FeSO_4$, 4 g/l glucose, 1 g/l $^{15}NH_4Cl$, vitamin mix, trace elements mix. Vitamin mix final concentrations were 1 mg/l D-biotin, 500 µg/l choline chloride, 500 µg/l folic acid, 1 mg/l myoinositol, 500 µg/l nicotinamide, 500 µg/l pantothenic acid, 500 µg/l pyridoxal hydrochloride, 50 µg/l riboflavin, 500 µg/l thiamine hydrochloride. Trace element mix final concentrations were 50 mg/l EDTA, 8.3 mg/l $FeCl_3$ x $6H_2O$, 840 µg/l $ZnCl_2$, 0.13 mg/l $CuCl_2x2H_2O$, 100 µg/l $CoCl_2$ x $6H_2O$, 100 µg/l H_3BO_3, 16 µg/l MnCl2 x 6 H_2O.

4.2.2 Biochemistry

4.2.2.1 Cell lysis of *E. Coli*

Cells from 1 l of TB medium were resuspended in 35 ml of the respective lysis buffer. Frozen pellets were thawed on ice. Immediately before lysis 1 mM PMSF was added. High pressure homogenisation was performed by processing the cell suspension twice in a EmulsiFlex-C5 (AVESTIN), which was cooled with ice beforehand. Lysate was cleared by centrifugation at 20.000 *x* g at 4°C for 20 min.

4.2.2.2 Purification of GST-tagged proteins

Lysis buffer for GST-fusion proteins was GST-buffer (50 mM Tris/HCl pH 7.5, 200 mM NaCl and 5 mM DTT) with 1 mM PMSF. Cleared lysate was loaded onto a GSTrap FF Column (GE Healthcare). Alternatively, resin with immobilised GSH was directly added to the cleared lysate. Before binding, resin was equilibrated in GST-buffer. Lysate was incubated with resin for 1 h at 4°C. After binding the resin was washed with 5-10 column volumes of GST-buffer. Proteins were eluted with GST-buffer containing 20 mM reduced glutathione. Alternatively, proteins were released from the resin by digest with PreScission protease (GE) or selfmade GST-tagged 3C protease protease over night. The next day, the supernatant was collected and the resin washed with another column volume of GST-buffer to elute remaining cleaved protein. The

protein solution was further purified by size exclusion chromatography (HiLoad 16/600 Superdex 75pg, GE-Healthcare) in 50 mM HEPES pH 7.5, 200 mM NaCl. Fractions containing the desired protein were identified by UV280 absorbance as well as by SDS-PAGE and Coomassie staining. Peak fractions were united, concentrated using Amicon Ultra concentrators (Millipore), flash frozen in liquid nitrogen and stored at -80°C.

4.2.2.3 Purification of His-tagged proteins

Lysis buffer for 6xHis-tagged proteins was either 1xPBS for Ub, 2x PBS with 2 mM 2-mercapthoethanol for hUbe1 or 50 mM Tris, 200 mM NaCl and 2 mM 2-mercapthoethanol for other proteins. Proteins with a 6xHis-tag were purified from cleared lysate by immobilised metal affinity chromatography. To this end, cleared lysate was applied to a HiTrap Talon affinity column (GE-healthcare). Alternatively, resin with immobilised Co^{2+}-ions (TALON) or Ni^{+}-ions (Ni-NTA) was added to the cleared lysate. Resin was equilibrated with lysis buffer prior to binding and incubated for 1 h at 4°C with the cleared lysate. Subsequently, resin was washed with 5-10 column volumes of lysis buffer. Proteins were eluted with the respective lysis buffer including 300 mM imidazole. To cleave off 6xHis-Smt3, fusion proteins were first eluted and then incubated with Senp2 protease over night at 4°C while dialysing against buffer without imidazole. Typically 1 µg Senp2 protease was used for 50 µg of fusion protein. For dialysis SnakeSkin Dialysis Tubing (ThermoFischer) with an adequate molecular weight cut-off was used. After incubation, the protein solution was incubated with an equal volume of resin as during the initial purification step and incubated for 1 h at 4°C. Untagged proteins were collected from the flow-through. After elution, proteins were concentrated using an Amicon Ultra concentrator (Millipore) and subjected to size exclusion chromatography. hUbe1 was loaded on a HiLoad 16/600 Superdex 200 pg (GE) in 2x PBS, while other proteins were loaded on a HiLoad 16/600 Superdex 75 pg in 50 mM Tris/HCl pH7.5, 200 mM NaCl. Fraction collection and storage as outlined in previous section.

4.2.2.4 Purification of untagged ubiquitin monomers

Purification of untagged Ubiquitin monomers from cleared bacterial cell lysate was performed by acidic precipitation of proteins.[81] Unlike most other proteins Ubiquitin remains soluble at very acidic pH. 70% perchloric acid was added dropwise under stirring to the cleared lysate until a total final concentration of 0.7% was reached. The precipitate was cleared by centrifugation (20.000 *x* g for 20 min at 4°C). The supernatant was removed and 10 M NaOH solution was titrated to adjust the pH to 7-8, which was confirmed using pH paper. Subsequently, monomers were concentrated and further purified by size exclusion

chromatography (HiLoad Superdex 26/600 75p) in 50 mM Tris/HCl pH 8.0. Fraction collection as in section 4.2.2.2.

4.2.2.5 Purification of ubiquitin chains

Ub chains with proximal (*i.e.* C-terminal) hexahistidine-tag (6xHis) were assembled enzymatically *in vitro* typically in a total volume of 3 to 10 ml. Reactions producing K48 chains included 1 µM E1 (hUbe1), 20 µM Cdc34, 900 µM Ub and 600 µM Ub (C-terminal 6xHis) in 20 mM ATP, 0.9 mM DTT, 9 mM $MgCl_2$ and 50 mM Tris/HCl pH 8. Reactions for K63 chain assembly included 1 µM E1 (Ube1), 8 µM Ubc13, 8 µM Uev1a, 1.2 mM Ub and 0.8 mM 6xHis-Ub in 20 mM ATP, 0.9 mM DTT, 9 mM $MgCl_2$ and 50 mM Tris/HCl pH 8. Ub chain formation reactions were incubated at 37 °C for 18 h. 6xHis-tagged chains were removed from the reaction mix with metal affinity chromatography with Talon resin. Ub chains obtained from the eluate were separated by gel filtration (HiLoad 26/600 Superdex 75pg, GE-Healthcare) in PBS, pH 7.5 with a low flow rate (0.3-0.5 ml/min). Fractions containing Ub chains with a specific length were collected and concentrated using Amicon Ultra concentrators (Millipore).

4.2.2.6 SDS-PAGE

Proteins samples were analysed by sodium dodecylsulfate-polyacrylamide gel electrophoresis (SDS-PAGE) using Hoefer gel electrophoresis system (Laemmli1970). Samples were mixed with either urea sample buffer and incubated at RT or with SDS-PAGE sample buffer and incubated at 95°C for 5 min. Seperating gels were cast using 9-18% acrylamide as indicated in the experiment, 0,09% bisacrylamide, 500 mM Tris/HCl pH 8.8, 0.1% SDS, 0.02% TEMED and 0.1% APS and stored at 4°C until usage. Stacking gels were cast using 9% acrylamide, 0,06% bisacrylamide,125 mM Tris/HCl pH 6.8, 0.1% SDS, 0.25% TEMED and 2.5% APS. The gel chamber was filled with SDS-PAGE running buffer containing 0.3 % Tris base, 1.45 % Glycin and 0.1 % SDS. Gels were run at 100V for 10 min and then at 240V until completion. Proteins separated by SDS-PAGE were either analysed by fluorescence scanning, western blotting or Coomassie staining. Fluorescence scans were performed in a Typhoon FLA9500 Biomolecular Imager by GE-Healthcare with an excitation wavelength of 473 nm and a LPB (510LP) filter for detection. Coomassie staining was performed by shortly boiling the gel in Coomassie staining solution (40% MeOH, 10% acetic acid, 0.1% Coomassie Brilliant Blue R-250) and subsequently incubating it for 5 min in the hot staining solution. Afterwards, the gel was transferred to destaining solution (40% MeOH, 10% acetic acid) and also shortly heated in a microwave until clear signals were visible.

4.2.2.7 Immuno blotting (western blotting)

Proteins separated by SDS-PAGE were transferred onto a PVDF membrane in a Hoefer Western Blotting Chamber at 250 mA for 90 min. Transfer buffer was 1.1% glycine, 0.24% Tris base, 25% methanol and 0.01% SDS. The transfer membranes were activated in methanol and assembled with the SDS-PAGE gel between two layers of Whatman-paper from each side. After the transfer membranes were blocked in a 10% skim milk powder (Roth) solution in 1x TBT for 15 min. Primary antibody in its respective dilution was added to a 5% skim milk powder solution in 1x TBT and incubated with the membrane at 4°C over night. The following day the membranes was washed three times with 1x TBT and incubated with secondary antibody in 5% skim milk powder solution in 1x TBT for one hour at RT. Another three wash steps with 1x TBT were performed followed by three wash steps with 1x PBS. Membranes were analysed by adding Western Lightning chemiluminscence solution (Perkin Elmer) and detection either by a LiCor Odyssey imaging device or X-ray films (BioMax MR Film, Kodak).

4.2.2.8 *In vitro* ubiquitination reactions

Depending on the experimental design *in vitro* ubiquitination reactions contained different compositions of hUbe1 (0.1-1 µM), E2 enzymes and ubiquitin variants. Unless otherwise indicated, all reactions contained 4 mM ATP, 4 mM $MgCl_2$, 0.5 mM DTT and 50 mM Tris/HCl pH 7.5. Reactions were started by addition of E2 enzyme. Typically a sample of 15 µl reaction mix was taken at indicated time points and the reaction was stopped by addition of urea sample buffer. Time courses were then analysed by SDS-PAGE and subsequent fluorescence scan or western blotting.

For chain elongation reactions in section 2.2.3.1 the reactions conditions were 10 µM ubiquitin, 0.3 µM hUbe1, 2 µM Ubc7/Ubc4/Ubc1 (as indicated), 2 µM cytosolic fragment of Cue1 in reactions with Ubc7, 2 µM Hrd1-RING-domain, 4 mM ATP, 4 mM $MgCl_2$, 0.5 mM DTT and 50 mM Tris/HCl pH 7.5.

Single turnover *in vitro* ubiquitination reactions contained 1 µM fluorescently labelled (Alexa488) monoubiquitin (Ub-S20C), 10 µM different C-terminally 6xHis-tagged acceptor Ub variants as indicated, 0.2 µM hUbe1 and 2 µM Ubc1. Alternatively, E2 variants were included as indicated. For single turnover ubiquitination reactions with Ubc7-U7BR in presence of ubiquitin binding domains (UBDs), the indicated UBDs were included in the reaction mix at at concentration of 40 µM in reactions with $^{48x3}Ub_4$ and at a concentration of 20 µM with $^{48}Ub_2$. For kinetic analyses reactions were performed in triplicate. Line plots for all lanes in any scan

were extracted using ImageJ. Data was then analysed by using the Multipeak Fitting Package in Igor Pro. Peaks were approximated with Gaussian functions and linear or constant baselines were automatically determined. Product intensity over total intensity per lane was plotted over time and approximated with a line function. Initial reaction rates were determined as slope of the function.

In vitro ubiquitination reactions in section 2.2.3.2 (for *de novo* chain synthesis) contained 12 µM fluorescently labelled (Alexa488) monoubiquitin, 3 µM ^{63x3}Ub1(G76-6xHis) where indicated, 2 µM Ubc1 or variants, 4 mM ATP, 4 mM $MgCl_2$, 0.5 µM DTT, and 50 mM Tris/HCl pH7.5.

Preparative autoubiquitination of Ubc1 for structural analysis was performed with 0.5 µM E1 hUbe1, 100 mM Ubc1, 110 mM Smt3-A-hUb(K48R), 4 mM ATP, 5 mM $MgCl_2$, 0.5 µM β-ME, 50 mM NaCl and 50 mM Bis-Tris propane pH9.5. The reaction mix was incubated for one hour at 4°C.

4.2.2.9 Fluorescent labelling of Ub

Ub(S20C) or Ub with a c-terminal 6xHis-tag and cysteine were fluorescently labelled using Alexa Fluor 488 C5 Maleimide (Life Technologies). Thiole groups were reduced with two-fold molar excess of TCEP in 1x PBS for 10 min at RT. The sample was desalted using NAP5 columns and incubated with the fluorescent dye in 1x PBS for 90 min in the dark. Subsequently, the sample was desalted twice using NAP5 columns equilibrated in 50 mM Tris/HCl ph 8. The sample was concentrated in an Amicon Ultra concentrator (3K MWCO, Millipore). Final protein concentration was determined by a Lowry test. Labelling efficiency was assessed by absorbance measurement at 488 nm.

4.2.2.10 *In vitro* ubiquitin binding assay

To investigate binding properties towards differently linked Ub chains, freshly prepared GST-tagged proteins immobilised on GSH-resin were used after the wash step of the purification protocol and equilibrated to Ub binding buffer (50 mM Tris-HCl pH 7.5, 150 mM NaCl, 1g/l BSA). Amounts of different constructs were adjusted and evaluated by SDS-PAGE and subsequent Coomassie staining. Differently linked Ub chain mixes were diluted to a final concentration of 25 µM monoubiquitin equivalent in Ub binding buffer. 25 µl GSH-resin with immobilised GST-proteins were then incubated with 150 µl of the respective chain mix for 2h at 4°C on a rotating wheel. After the binding step the samples were centrifuged at 800 *x* g for 1 min and the supernatant was removed. The resin was then washed two times in Ub binding

buffer. Urea sample buffer was added to the supernatant and washed resin and heated to 35°C for 5 min. Samples were then analysed by SDS-PAGE, fluorescence scan and Coomassie staining.

4.2.2.11 Chemical cross-linking with ethane-dithiol (EDT)

All steps of protein cross-linking were performed in cross-linking buffer (20 mM HEPES pH7.0, 250 mM NaCl, 5 mM EDTA). Proteins destined for cross-linking were transferred to cross-linking buffer containing 0.5 mM TCEP by SEC during the preceding purification step. Immediately before the procedure, stock solutions of 256 mM 2,2-Dithiodipyridine (AT2) in DMSO and 256 mM 1,2-ethanedithiol (EDT) in DMSO were freshly prepared. Moreover, 5 Zeba Spin Desalting Columns (ThermoFisher) were equilibrated to cross-linking buffer to perform buffer exchange steps. All steps were performed at RT and solutions prewarmed if necessary. 132 mg $^{63}Ub_2$ in 3.65 ml buffer (2.13 mM) were buffer exchanged to cross-linking buffer, added to 100 µl AT2-stock solution and immediately mixed by pipetting up and down. After 10 min incubation, the sample was buffer exchanged and mixed with 100 µl EDT stock solution by pipetting up and down. After 5 min incubation, the sample was buffer exchanged and mixed with 100 µl AT2-stock solution by pipetting up and down. After 10 min incubation, the sample was buffer exchanged. In parallel, 130 mg Ubc1-Ub in 3.92 ml buffer (1.05 mM) was also buffer exchanged and subsequently mixed with the $^{63}Ub_2$ solution. After 90 min incubation the sample was concentrated to 3 ml and 500 µl aliquots were loaded on 6 separate HiLoad 16/600 Superdex 75 pg columns for SEC (0.5 ml/min, 20 mM Tris/HCl pH8, 200 mM NaCl). Fractions most concentrated for the cross-linked complex were united, concentrated to 14.6 mg/ml using Amicon Ultra centrifugal filters (Millipore), aliquoted, snap frozen and stored at -80°C. Side fractions from the SEC run, which contained impurities, were concentrated and prepared for another SEC run.

4.2.3 Biophysical Methods

4.2.3.1 Microscale thermophoresis (MST)

To assess binding affinity between Ubc1 differently linked diubiquitin molecules microscale thermophoresis was performed. Experiments were performed with the NanoTemper Monolith NT115. Method development and measurements were designed according to manufacturer's guidelines. Different conditions for monitoring thermophoresis of the diubiquitin probes were tested, but only one condition was identified to satisfy the quality parameters outlined by the manufacturer: 200nM Ub_2*, 50 mM MES pH 6.2, 200 mM NaCl with coated tubes and

capillaries. Excitation Power was set to 20% and MST power to 60%. The thermophoretic mobility of diubiquitin probes was measured in presence of different concentrations of Ubc1 (3.2 mM to 0.4 µM). Measurements were performed in triplicate. Experiments were designed and carried out under the supervision of Dr. Stefan Übel (Biophysical core facility, MPIB, Martinsried).

4.2.3.2 NMR titration experiments

NMR titration experiments enable identification of surface residues involved in binding[166] as well as determination of dissociation constants[167]. NMR spectra were acquired on Bruker Avance spectrometers operating at proton frequencies ranging from 500 MHz to 950 MHz equipped with 5-mm triple-resonance cryogenic z-axis gradient probes. Samples were measured in salt tolerant NMR tubes in a total volume of 300-400 µl. Chemical shift referencing was performed with 4,4-dimethyl-4-silapentane-1-sulphonate (DSS). Spectra were processed using the TopSpin software provided by Bruker and analysed using SPARKY 3.13 software or NMRFAM-SPARKY.[168] NMR titration experiments with UBDs were performed with either Cue1 (aa45-115) or Ubc1 (aa151-215) in concentrations ranging from 0 to 1.6 mM and diubiquitin probes at a concentration of 0.2 mM at 298K. Diubiquitin probes were either proximally or distally ^{15}N-labelled $^{48}Ub_2$ or $^{63}Ub_2$. Dr. Andreas Kniss from the laboratory of Prof. Dr. Volker Dötsch performed all NMR measurements presented in this study.

4.2.4 Cell biology

4.2.4.1 Yeast cultivation

The cell density of liquid cultures was typically determined by measuring the optical density in a spectral photometer at a wavelength of λ = 600 nm (OD_{600}).

For SILAC labelling cells were grown in SD medium containing 30 mg/l Lys4.

4.2.4.2 Heat-shock transformation of yeast cells

Yeast strains were grown in logarithmic growth phase (OD600 < 1/ml) and an amount of cells equivalent to 1 ml culture at 1 OD_{600}/ml ("1 OD_{600}") were harvested by centrifugation at 3000 *x* g for three minutes. The pellet was first washed with water and then with a solution of 100 mM LiOAc, 10 mM Tris/HCl pH 7.4 and 10 mM EDTA. 200 µl of this buffer were prepared and incubated with 3 µg of the desired DNA and 0.2 µg/µl of denatured Hering sperm DNA for several minutes. After the wash steps the cell pellet was resuspended in this solution and 800 µl of 40% PEG 335, 100 mM LiOAc, 10 mM Tris/HCl pH 7.4 and 10 mM EDTA was added. The

suspension was incubated for 30 minutes at 30°C and subsequently heat shock was performed for 15 minutes at 42°C. Cells were spun down at 3000 *x* g for 1 minute, resuspended in 100 µl water and plated onto selective SD plates. Plates were incubated for 1-3 days at 30°C and then stored at 4°C for no longer than one week.

4.2.4.3 Preparation of genomic DNA from yeast cells

Genomic DNA was prepared from yeast cells as template for PCR reactions. Cells were grown over night in YPD medium cells equivalent to 4-10 OD_{600} were harvested by centrifugation (2000 *x* g, 5 min at RT). Cells were washed with 1 ml ddH_2O, centrifuged as before and resuspended in 200 µl DNA extraction buffer (2% Triton X-100, 100 mM NaCl, 1% SDS, 1 mM EDTA and 10 mM Tris/HCl pH 8.0). Subsequently, 200 µl of a mixture of phenol, chloroform and isoamyl alcohol (25:24:1) was added and mechanical cell lysis was performed. Lysate was transferred to fresh tube with 200 µl TE buffer (pH 8) and centrifuged for 10 min at 10000 *x* g at RT. The samples separated into two phases. The aqueous (upper) phase was removed and added to 1 ml of pure ethanol in order to precipitate DNA on ice by centrifugation (20000 *x* g for 10 min at 4°C). The supernatant was discarded and the precipitated DNA was resuspended in 100 µl ddH_2O.

4.2.4.4 Mechanical lysis of yeast cells

Total yeast cell extract was prepared for SDS-PAGE and western blotting as well as for analytical PCRs. Typically cells were grown to 1.0 OD_{600}/ml and 5-20 ml were harvested by centrifugation at 2000 *x* g for 3 min at RT. The cell pellet was resuspended in 100 µl lysis buffer (50 mM Tric/HCl, 1% SDS, 1 mM PMSF) and transferred to a 2 ml eppendorf tube. Glass beads were added up to the meniscus of the liquid and the suspension was vortexed for 2 min at maximum speed in a Vibrax VXR basic. For direct analysis by SDS-PAGE and western blotting, the lysate was mixed with SDS sample buffer, boiled for 5 min at 95°C, centrifuged for 3 min at 1000 *x* g and the supernatant loaded onto a gel. Alternatively, dilution buffer was added to the lysate for further processing where indicated.

4.2.4.5 Cycloheximide chase assay

Cycloheximide chase experiments were performed with 20 OD_{600} log-phase cells, which were harvested and resuspended in 4.5 ml prewarmed SD medium containing 100 mg/ml cycloheximide. Cell suspensions were incubated at 30°C in a water bath. 1 ml aliquots were taken in 30 min intervals. Degradation was stopped by the addition of 15 mM NaN_3, and total cell lysates were prepared. Samples were analysed by SDS-PAGE and immunoblotting.

4.2.4.6 Detection of Ub linkage types on Htt in *S. Cerevisiae* by mass spectrometry

The respective yeast strains were grown over night in SD medium –LYS and diluted to 0.3 OD_{600}/ml in 400 ml the next morning. After growth until 0.9 OD_{600}/ml at 30°C, 1 mM $CuSO_4$ was added and cells were grown for approximately another 1.5h to 1 OD_{600}/ml. Cells were harvested by centrifugation at 3000 *x* g for 5 minutes, washed twice with ddH_2O and resuspended in 50 ml YP GAL with 0.2 mM $CuSO_4$. Another incubation step was performed for 1h at 30°C. As before cells were harvested by centrigution, washed with ddH_2O and the pellet flash frozen in liquid nitrogen. Pellet was stored at -80°C. Thawing on ice for 30 min was followed by resuspension in 1 ml lysis buffer (8 M Urea, 50 mM HEPES pH7.6, 5 mM chloroacetamide) in a 15 ml Falcon tube. Glass beads were added to a total volume of ~3.5 ml for mechanical lysis at maximal speed for 5 minutes by Vibrax VXR basic. Subsequently 8 ml dilution buffer (50 mM HEPES pH7.6) were added, followed by centrifugation for 5 min at 800 *x* g after inverting the tube several times. Supernatant was transferred to a fresh 15 ml Falcon tube and 40 µl M2 FLAG-affinity gel (Sigma A2220) was added, which was previously washed with dilution buffer. After incubation for 3h at 4°C on a rolling incubator, resin was centrifuged and washed three times with 1 ml dilution buffer. Supernatant was completely removed with a Hamilton pipette. 50 µl elution buffer (8 M Urea, 50 mM HEPES pH7.6) was added and incubated at 30°C for 1h in a heating block. The eluate was transferred to a fresh tube using a Hamilton pipette and protein amount adjusted as assessed by BCA assay. Samples were flash frozen and stored at -20°C until further processing. Subsequent steps were performed by Dr. Oliver Popp from the mass spectrometric core facility under the supervision of Dr. Philipp Mertins (MDC, Berlin).

After thawing, the eluate was subjected to reduction, alkylation and in-solution digest with 50 ng LysC and 50 ng trypsin in a consecutive manner. After desalting, half of the samples have been acquired in a data-dependent mode by LC-MS on a Q Exactive Plus mass spectrometer using a 2 h gradient. The other half was spiked with 200 fmol heavy labelled internal standard peptide of the respective ubiquitin linkage type marker peptides (SpikeTides TQL, JPT) as an internal reference and subjected to parallel reaction monitoring (PRM) analysis on a Q Exactive Plus mass spectrometer. Data obtained from the discovery-experiment was analysed using the MaxQuant software package[169] version 1.5.2.8., PRM data was analysed using Skyline[170]. Data visualisation was achieved using R.

4.2.4.7 Sample preparation for mass spectrometric detection of K48/K63 branched chains from yeast lysate

To investigate the abundance of K48/K63 branched chains in dependence of Ubc1 expression in *S. cerevisiae*, yeasts strains expressing 10xHis-Ub(R54A) and no other Ub gene were grown in either unlabelled or Lys4-labelled media. Precultures were diluted to 0.03 OD_{600}/ml and then grown to 1.1 OD_{600}/ml. To compare two conditions, equal amounts (400 ml) of cells grown in unlabelled media from one strain were combined with cell grown in Lys4-labelled media from the other strain and reverse. The combined cells were centrifuged for 10 min at 2000 *x* g, resuspended in 3 ml lysis buffer (8 M urea, 1% SDS, 50 mM HEPES pH 8.0, 1 mM PMSF), transferred to a 15 ml Falcon tube, flash frozen in liquid nitrogen and stored at -80°C overnight. Pellets were thawed on ice and 3 ml glass beads were added for subsequent mechanical lysis at RT by Vibrax VXR basic at maximum speed for 3 min. After lysis, 6 ml equilibration buffer were added (EB, 8 M Urea, 50 mM HEPES pH 8.0), inverted several times and centrifuged at 5000 *x* g for 5 min at RT. Supernatant was removed and centrifuged again at 20000 *x* g for 20 min at RT. Subsequent steps were carried out with LC-MS grade reagents and under the fume hood. Per sample 150 µl Talon-resin was washed in EB, added to the cleared supernatant and incubated for 3h at 4°C on a rotating wheel. Resin was removed from the solution by centrifugation for 1 min at 800 *x* g, washed six times with EB and one time in 150 µl denaturation buffer (DB, 6 M urea, 2 M thiourea, 10 mM HEPES pH 8.0). Resin was then resuspended in 50 µl DB, reduced with 0.8 mM DTT for 30 min at RT and alkylated with 1 mM 2-Chloroacetamide for 20 min at RT in darkness. Samples were kept in darkness from here on. Then, 3 µg LysC protease were added and incubated for 3h at RT under shaking. 200 µl 50 mM ammonium bicarbonate buffer were added to dilute the sample, before adding 3 µg trypsin for digest at RT overnight. After a final centrifugation at 800 *x* g for 1 min the supernatant was removed and acidified with 25 µl 10% trifluoroacetic acid. Samples were then given to Dr. Henrik Zauber from the laboratory of Prof. Matthias Selbach for analysis by Parallel Reaction Monitoring (PRM).

4.2.4.8 Mass spectrometric analysis of K48/K63 branched chains

A spectral library for K48/K63 branched chains was obtained from a Ub trimer, which was prepared as outlined in section 2.2.4.1. The Ub trimer was incubated with trypsin in a mass ratio of 50:1 and incubated over night at RT. Tryptic peptides were separated by reverse phase chromatography (200 min gradient) and analysed by mass spectrometry on a Q-Exactive Plus (Thermo Fisher Scientific). Settings in brief were: 70000 MS1 resolution, 120 ms MS1 MaxIT,

300-1700 m/z scan range, 17500 MS2 resolution, 2.0 Da isolation window, 26 normalised collision energy, MS2 AGC target 5e2, 60 ms MS2 MaxIT.

Samples obtained from yeast lysate as described in the previous section were subjected to LC-MS/MS analysis. To this end, peptides were separated by reverse phase chromatography on a 130 min gradient, with increasing concentrations of Buffer B (80 % acetonitrile, 0.1 % formic acid) from 2 to 90 % and analysed on a Q-Exactive Plus (Thermo Fisher Scientific). The PRM settings were: 35000 resolution, 2e5 AGC target, 2 m/z isolation window, 120 ms max ion injection time. Precursors have been selected based on a report from Ohtake *et al.*[58] The DDA (top3) settings were: 17500 MS1 resolution, 60 ms MaxIT, 17500 MS2 resolution, 60 ms MaxIT, 2 Da isolation window.

PRM data was analysed using the open source Skyline analysis tool.[170] Peaks were manually assigned and validated based on the DotProduct. Exported fragment intensities were analysed using R. To identify other peptides from the top3 acquisition part of the data, raw-files were analysed with MaxQuant (1.5.2.8) with standard settings and setting complexity to 2 for analysis of SILAC ratios. Shifts in the log2 ratio distribution were used to correct the log2 ratios of corresponding fragments from the PRM analysis and plotted against the fragment intensities.

4.2.5 Crystallography

4.2.5.1 Crystallisation conditions and data collection

Initial protein crystallisation trials were performed in a 96-well sitting drop format at 4°C. Commercial screening kits (Hampton Research Index, Molecular Dimensions JCSG-plus, Qiagen pHClear 2) and “Complex 1” screen (made by the crystallisation core facility at MPIB, Martinsried) were used in. Per well 0.1 µl protein solution (15 mg/ml) was dispensed in 0.1 µl reservoir solution using a nanoliter crystallisation robot (Phoenix). During initial screenings, the complex formed protein crystals in form of needle-stacks within a week in 15% PEG 6000, 0.1 M magnesium acetate and 0.1 M sodium cacodylate (pH 6.5) as well as in 8% PEG 6000, 0.1 M magnesium chloride and 0.1 M MES (pH 6.0). Crystallisation conditions were optimised by Dr. Jérôme Basquin in 24 well format using sitting drops with 0.4 µl protein solution and 0.4 µl reservoir solution. Optimisation was achieved by microseeding in combination with variation of precipitant and salt concentrations as well as pH. The final crystallisation conditions were 10°C in 6.5% PEG 6000, 100 mM $MgCl_2$, 100 mM HEPES pH 7.0. The protein complex crystallised as needles. A diffraction dataset was recorded by Dr. Basquin at PXII beam line,

Swiss Light Source (SLS) Villingen, Switzerland. Data was recorded at 0.5 degree rotation intervals using PILATUS detector.

4.2.5.2 Phasing and model building

Data was indexed, integrated and scaled using XDS package[171] to a resolution limit of 3.2 Å. Initial analysis revealed two molecules per asymmetric unit with a matthews coefficient of 1.96 and 37% solvent content. Phases were determined by Dr. Rajan Prabu (MPIB, Martinsried) using molecular replacement based on previously published PDB structures using PHASER software implemented in the PHENIX software suite.[172] I improved the model by interactive model building using coot[173] and reciprocal space refinement using phenix.refine[172]. We used a twin law (h, -k, -l) during refinement to compensate for the lattice twinning. 5% of reflections were kept aside to evaluate the model. The final refined structure had an R-factor of 20.2 % and R_{free} of 23.2 %. For final data collection and refinement statistics, which were obtained using MolProbity[174], refer to Table 1 (page 91). Molecular graphics and analyses were performed with UCSF Chimera.[175]

5. Supplementary data

5.1 Summary of data collection and refinement statistics

Table 1 Summary of data collection and refinement statistics.

Ubc1	
Resolution range (Å)	76.77 - 3.11 (3.22 - 3.11)*
Space group	C 1 2 1
Unit cell dimensions	
a, b, c (Å)	57.85, 132.69, 153.55
α, β, ɣ (°)	90, 90.12, 90
Total reflections	42476 (13928)
Unique reflections	20859 (589)
Multiplicity	6.8 (6.6)
Completeness (%)	84.46 (27.86)
Mean I/sigma(I)	8.89 (0.95)
Wilson B-factor	80.1
R-merge	0.201 (2.132)
R-meas	0.2179 (2.317)
R-pim	0.08314 (0.8966)
CC1/2	0.995 (0.543)
CC*	0.999 (0.839)
Reflections used in refinement	17701 (589)
Reflections used for R-free	870 (21)
R-work	0.2023 (0.5420)
R-free	0.2322 (0.7652)
CC(work)	0.878 (0.456)
CC(free)	0.821 (0.104)
Number of non-hydrogen atoms	5223
RMS(bonds) (Å)	0.006
RMS(angles) (°)	1.14
Ramachandran favored (%)	98.13
Ramachandran allowed (%)	1.87
Ramachandran outliers (%)	0
Rotamer outliers (%)	0
Clashscore	11.67
Average B-factor	63.73

*Values in parenthesis are for highest resolution shell.

5.2 Electron density map of the crystallised Ubc1 complex

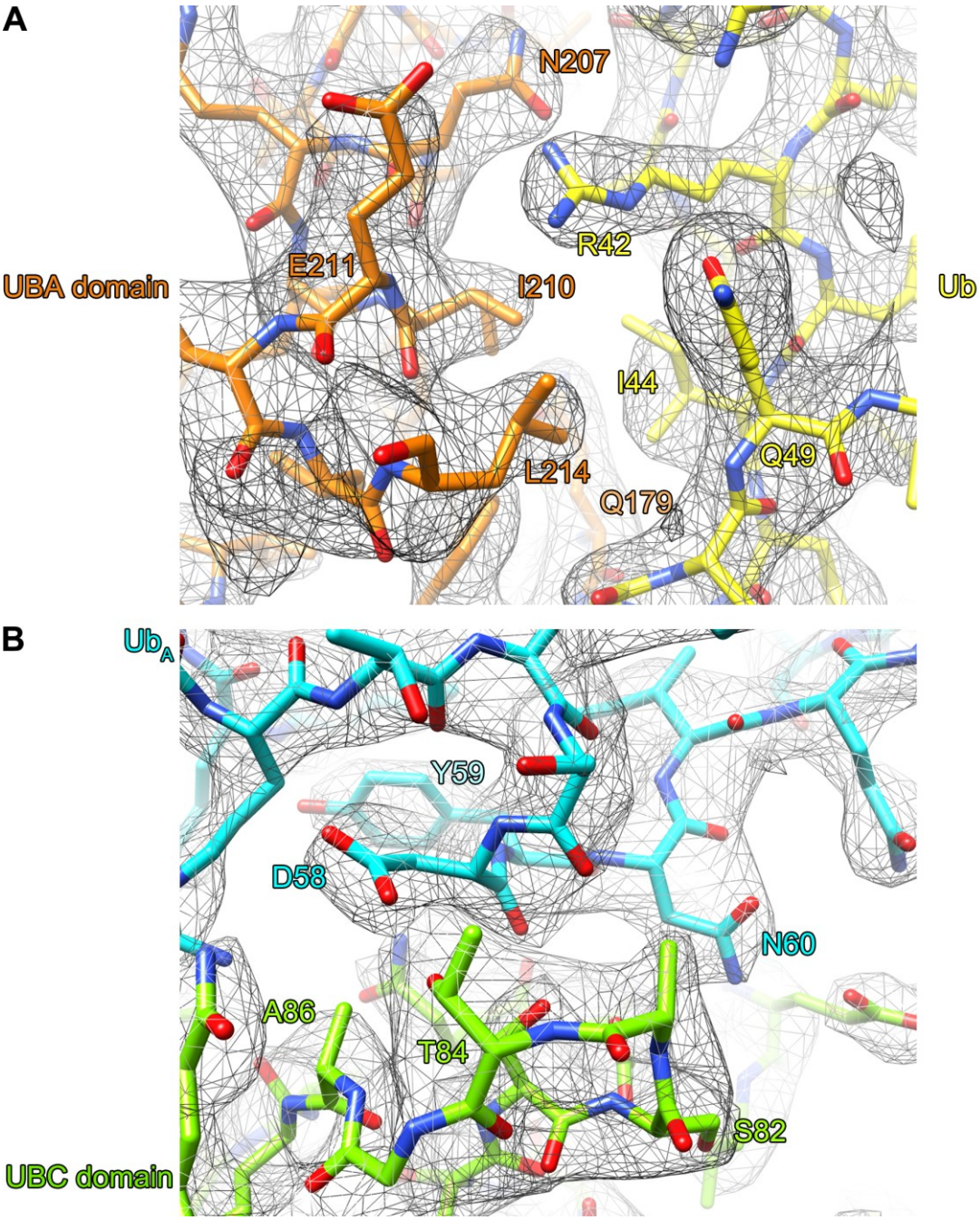

Figure 30: Representative images for the electron density map obtained for Ubc1-Ub-X-^{63}Ub$_2$. The $2F_o - F_c$ electron density map (grey mesh) was contoured at 1.1σ (grey mesh). (A) Critical residues in the interface between UBA domain and Ub are shown as sticks. (B) Interface between UBC domain and Ub_A in stick representation.

5.3 Supplementary fluorescence scans for section 2.2.3.2

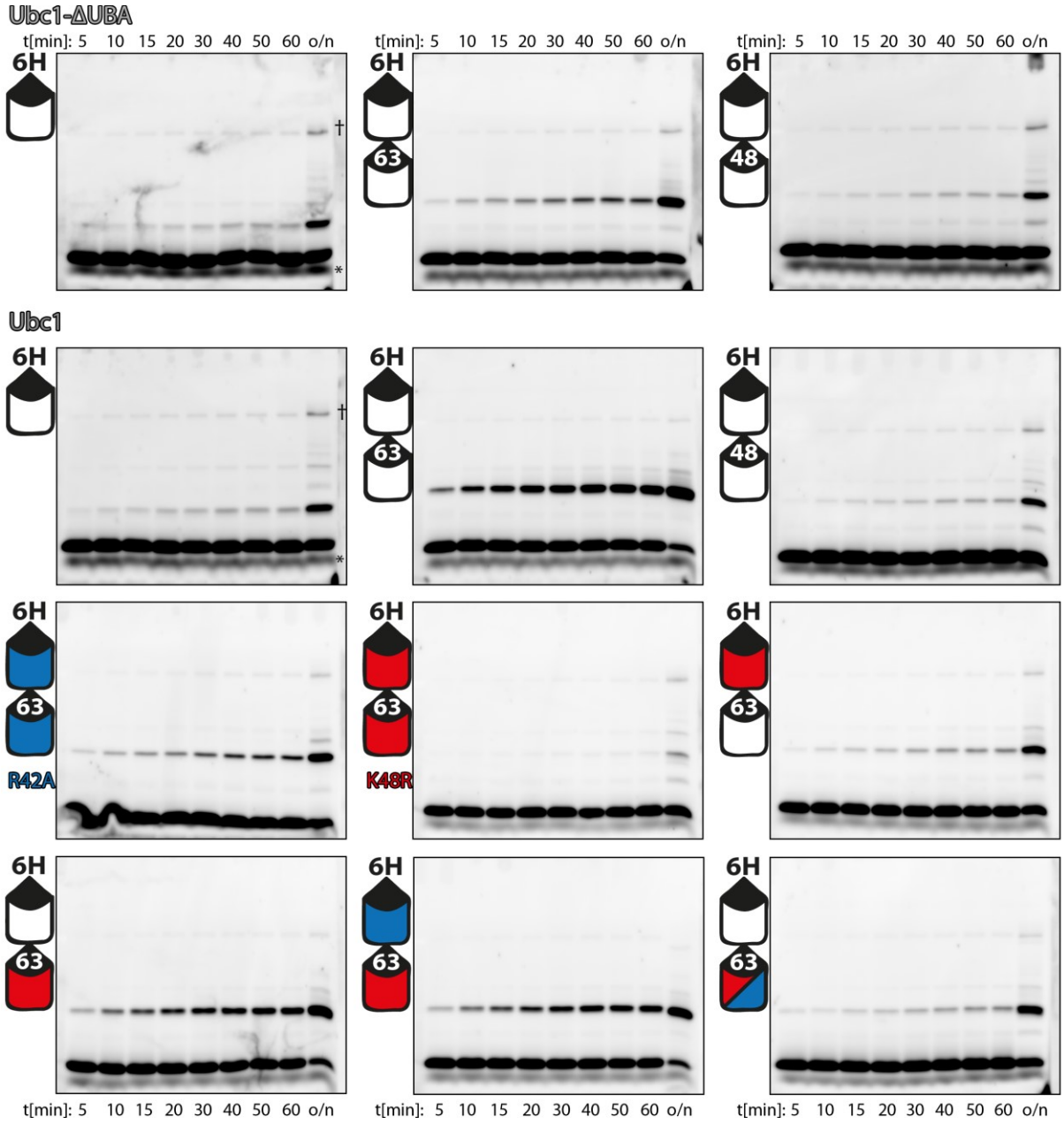

Figure 31: Representative fluorescence scans of single turnover ubiquitination experiments for kinetic analysis described in section 2.2.3.2. Top row shows reactions with the UBC domain of Ubc1(K93R), while the other reactions were performed in presence of full-length Ubc1 (K93R). Acceptor Ub as in Figure 20. Asterisk (*) indicates signal from free dye. Cross (†) indicates E1 modified with fluorescent Ub.

6. References

[1] M. von Delbrück, A. Kniss, V. V. Rogov, L. Pluska, K. Bagola, F. Löhr, P. Güntert, T. Sommer and V. Dötsch, "The CUE Domain of Cue1 Aligns Growing Ubiquitin Chains with Ubc7 for Rapid Elongation.", *Mol Cell,* vol. 62, pp. 918-928, 2016.

[2] A. Kniss, D. Schuetz, S. Kazemi, L. Pluska, P. E. Spindler, V. V. Rogov, K. Husnjak, I. Dikic, P. Güntert, T. Sommer, T. F. Prisner and V. Dötsch, "Chain Assembly and Disassembly Processes Differently Affect the Conformational Space of Ubiquitin Chains.", *Structure*, vol. 26, pp. 249-258, 2018.

[3] A. Ciechanover, A. Hershko and I. Rose, "Nobel Prize 2004 in Chemistry for the discovery of ubiquitin-mediated protein degradation," *Nobel Media AB,* 2004.

[4] D. Komander and M. Rape, "The ubiquitin code.", *Annu Rev Biochem,* vol. 81, pp. 203-229, 2012.

[5] R. Yau and M. Rape, "The increasing complexity of the ubiquitin code.", *Nature cell biology,* vol. 18, no. 6, pp. 579-586, 2016.

[6] V. K. Chaugule and H. Walden, "Specificity and disease in the ubiquitin system.", *Biochemical Society transactions,* vol. 44, no. 1, pp. 212-227, 2016.

[7] S. Fulda, K. Rajalingam and I. Dikic, "Ubiquitylation in immune disorders and cancer: from molecular mechanisms to therapeutic implications.", *EMBO Mol Med,* vol. 4, pp. 545-556, 2012.

[8] Y. Ye and M. Rape, "Building ubiquitin chains: E2 enzymes at work.", *Nat Rev Mol Cell Biol,* vol. 10, pp. 755-764, 2009.

[9] D. Finley, H. D. Ulrich, T. Sommer and P. Kaiser, "The ubiquitin-proteasome system of *Saccharomyces cerevisiae*.", *Genetics,* vol. 192, pp. 319-360, 2012.

[10] D. Komander, M. J. Clague and S. Urbé, "Breaking the chains: structure and function of the deubiquitinases.", *Nature reviews. Molecular cell biology,* vol. 10, no. 8, pp. 550-563, 2009.

[11] S. M. B. Nijman, M. P. A. Luna-Vargas, A. Velds, T. R. Brummelkamp, A. M. G. Dirac, T. K. Sixma and R. Bernards, "A genomic and functional inventory of deubiquitinating enzymes.", *Cell,* vol. 123, no. 5, pp. 773-786, 2005.

[12] M. J. Clague, I. Barsukov, J. M. Coulson, H. Liu, D. J. Rigden and S. Urbé, "Deubiquitylases from genes to organism.", *Physiological reviews,* vol. 93, no. 3, pp. 1289-1315, 2013.

[13] S. A. Abdul Rehman, Y. A. Kristariyanto, S.-Y. Choi, P. J. Nkosi, S. Weidlich, K. Labib, K. Hofmann and Y. Kulathu, "MINDY-1 Is a Member of an Evolutionarily Conserved and Structurally Distinct New Family of Deubiquitinating Enzymes.", *Molecular cell,* vol. 63, no. 1, pp. 146-155, 2016.

[14] L. Bedford, J. Lowe, L. R. Dick, R. J. Mayer and J. E. Brownell, "Ubiquitin-like protein conjugation and the ubiquitin-proteasome system as drug targets.", *Nat Rev Drug Discov,* vol. 10, pp. 29-46, 2011.

[15] J. Peng, D. Schwartz, J. E. Elias, C. C. Thoreen, D. Cheng, G. Marsischky, J. Roelofs, D. Finley and S. P. Gygi, "A proteomics approach to understanding protein ubiquitination.", *Nature biotechnology,* vol. 21, no. 8, pp. 921-926, 2003.

[16] M. L. Matsumoto, K. E. Wickliffe, K. C. Dong, C. Yu, I. Bosanac, D. Bustos, L. Phu, D. S. Kirkpatrick, S. G. Hymowitz, M. Rape, R. F. Kelley and V. M. Dixit, "K11-linked polyubiquitination in cell cycle control revealed by a K11 linkage-specific antibody.", *Molecular cell,* vol. 39, no. 3, pp. 477-484, 2010.

[17] G. M. Silva, D. Finley and C. Vogel, "K63 polyubiquitination is a new modulator of the oxidative stress response.", *Nat Struct Mol Biol,* vol. 22, no. 2, pp. 116-123, 2015.

[18] J. S. Thrower, L. Hoffman, M. Rechsteiner and C. M. Pickart, "Recognition of the polyubiquitin proteolytic signal.", *The EMBO journal,* vol. 19, no. 1, pp. 94-102, 2000.

[19] D. Finley, S. Sadis, B. P. Monia, P. Boucher, D. J. Ecker, S. T. Crooke and V. Chau, "Inhibition of proteolysis and cell cycle progression in a multiubiquitination-deficient yeast mutant.", *Mol Cell Biol,* vol. 14, pp. 5501-5509, 1994.

[20] T. Sommer and D. H. Wolf, "Endoplasmic reticulum degradation: reverse protein flow of no return.", *FASEB journal: official publication of the Federation of American Societies for Experimental Biology,* vol. 11, no. 14, pp. 1227-1233, 1997.

[21] R. Friedlander, E. Jarosch, J. Urban, C. Volkwein and T. Sommer, "A regulatory link between ER-associated protein degradation and the unfolded-protein response.", *Nat Cell Biol,* vol. 2, pp. 379-384, 2000.

[22] L. Chang and D. Barford, "Insights into the anaphase-promoting complex: a molecular machine that regulates mitosis.", *Current opinion in structural biology,* vol. 29, pp. 1-9, 2014.

[23] J. Spence, S. Sadis, A. L. Haas and D. Finley, "A ubiquitin mutant with specific defects in DNA repair and multiubiquitination.", *Molecular and cellular biology,* vol. 15, no. 3, pp. 1265-1273, 1995.

[24] I. Ziv, Y. Matiuhin, D. S. Kirkpatrick, Z. Erpapazoglou, S. Leon, M. Pantazopoulou, W. Kim, S. P. Gygi, R. Haguenauer-Tsapis, N. Reis, M. H. Glickman and O. Kleifeld, "A perturbed ubiquitin landscape distinguishes between ubiquitin in trafficking and in proteolysis.", *Molecular & cellular proteomics: MCP,* vol. 10, no. 5, p. M111.009753, 2011.

[25] P. Liu, W. Gan, S. Su, A. V. Hauenstein, T.-M. Fu, B. Brasher, C. Schwerdtfeger, A. C. Liang, M. Xu and W. Wei, "K63-linked polyubiquitin chains bind to DNA to facilitate DNA damage repair.", *Science signaling,* vol. 11, no. 533, 2018.

[26] C. Wang, L. Deng, M. Hong, G. R. Akkaraju, J. Inoue and Z. J. Chen, "TAK1 is a ubiquitin-dependent kinase of MKK and IKK.", *Nature,* vol. 412, no. 6844, pp. 346-351, 2001.

[27] M. Xu, B. Skaug, W. Zeng and Z. J. Chen, "A ubiquitin replacement strategy in human cells reveals distinct mechanisms of IKK activation by TNFalpha and IL-1beta.", *Molecular cell,* vol. 36, no. 2, pp. 302-314, 2009.

[28] M. U. Gack, Y. C. Shin, C.-H. Joo, T. Urano, C. Liang, L. Sun, O. Takeuchi, S. Akira, Z. Chen, S. Inoue and J. U. Jung, "TRIM25 RING-finger E3 ubiquitin ligase is essential for RIG-I-mediated antiviral activity.", *Nature,* vol. 446, no. 7138, pp. 916-920, 2007.

[29] J. M. Galan and R. Haguenauer-Tsapis, "Ubiquitin lys63 is involved in ubiquitination of a yeast plasma membrane protein.", *The EMBO journal,* vol. 16, no. 19, pp. 5847-5854, 1997.

[30] J. M. Boname, M. Thomas, H. R. Stagg, P. Xu, J. Peng and P. J. Lehner, "Efficient internalization of MHC I requires lysine-11 and lysine-63 mixed linkage polyubiquitin chains.", *Traffic (Copenhagen, Denmark),* vol. 11, no. 2, pp. 210-220, 2010.

[31] R. Gulia, R. Sharma and S. Bhattacharyya, "A Critical Role for Ubiquitination in the Endocytosis of Glutamate Receptors.", *The Journal of biological chemistry,* vol. 292, no. 4, pp. 1426-1437, 2017.

[32] E. Lauwers, C. Jacob and B. André, "K63-linked ubiquitin chains as a specific signal for protein sorting into the multivesicular body pathway.", *The Journal of cell biology,* vol. 185, no. 3, pp. 493-502, 2009.

[33] E. Lauwers, Z. Erpapazoglou, R. Haguenauer-Tsapis and B. André, "The ubiquitin code of yeast permease trafficking.", *Trends in cell biology,* vol. 20, no. 4, pp. 196-204, 2010.

[34] Z.-P. Xia, L. Sun, X. Chen, G. Pineda, X. Jiang, A. Adhikari, W. Zeng and Z. J. Chen, "Direct activation of protein kinases by unanchored polyubiquitin chains.", *Nature,* vol. 461, no. 7260, pp. 114-119, 2009.

[35] W. Zeng, L. Sun, X. Jiang, X. Chen, F. Hou, A. Adhikari, M. Xu and Z. J. Chen, "Reconstitution of the RIG-I pathway reveals a signaling role of unanchored polyubiquitin chains in innate immunity.", *Cell,* vol. 141, pp. 315-330, 2010.

[36] A. Ordureau, J.-M. Heo, D. M. Duda, J. A. Paulo, J. L. Olszewski, D. Yanishevski, J. Rinehart, B. A. Schulman and J. W. Harper, "Defining roles of PARKIN and ubiquitin phosphorylation by PINK1 in mitochondrial quality control using a ubiquitin replacement strategy.", *Proceedings of the National Academy of Sciences of the United States of America,* vol. 112, no. 21, pp. 6637-6642, 2015.

[37] C. N. Cunningham, J. M. Baughman, L. Phu, J. S. Tea, C. Yu, M. Coons, D. S. Kirkpatrick, B. Bingol and J. E. Corn, "USP30 and parkin homeostatically regulate atypical ubiquitin chains on mitochondria.", *Nature cell biology,* vol. 17, no. 2, pp. 160-169, 2015.

[38] R. M. Hofmann and C. M. Pickart, "Noncanonical MMS2-encoded ubiquitin-conjugating enzyme functions in assembly of novel polyubiquitin chains for DNA repair.", *Cell,* vol. 96, no. 5, pp. 645-653, 1999.

[39] J. Brusky, Y. Zhu and W. Xiao, "UBC13, a DNA-damage-inducible gene, is a member of the error-free postreplication repair pathway in Saccharomyces cerevisiae.", *Current genetics,* vol. 37, no. 3, pp. 168-174, 2000.

[40] H. D. Ulrich and S. Jentsch, "Two RING finger proteins mediate cooperation between ubiquitin-conjugating enzymes in DNA repair.", *The EMBO journal,* vol. 19, no. 13, pp. 3388-3397, 2000.

[41] B. Gerlach, S. M. Cordier, A. C. Schmukle, C. H. Emmerich, E. Rieser, T. L. Haas, A. I. Webb, J. A. Rickard, H. Anderton, W. W.-L. Wong, U. Nachbur, L. Gangoda, U. Warnken, A. W. Purcell, J. Silke and H. Walczak, "Linear ubiquitination prevents inflammation and regulates immune signalling.", *Nature,* vol. 471, pp. 591-596, 2011.

[42] F. Ikeda, Y. L. Deribe, S. S. Skånland, B. Stieglitz, C. Grabbe, M. Franz-Wachtel, S. J. L. Wijk, P. Goswami, V. Nagy, J. Terzic, F. Tokunaga, A. Androulidaki, T. Nakagawa, M. Pasparakis, K. Iwai, J. P. Sundberg, L. Schaefer, K. Rittinger, B. Macek and I. Dikic, "SHARPIN forms a linear ubiquitin ligase complex regulating NF-κB activity and apoptosis.", *Nature,* vol. 471, no. 7340, pp. 637-641, 2011.

[43] L. Jin, A. Williamson, S. Banerjee, I. Philipp and M. Rape, "Mechanism of ubiquitin-chain formation by the human anaphase-promoting complex.", *Cell,* vol. 133, no. 4, pp. 653-665, 2008.

[44] K. E. Wickliffe, A. Williamson, H.-J. Meyer, A. Kelly and M. Rape, "K11-linked ubiquitin chains as novel regulators of cell division.", *Trends in cell biology,* vol. 21, no. 11, pp. 656-663, 2011.

[45] M. Gatti, S. Pinato, A. Maiolica, F. Rocchio, M. G. Prato, R. Aebersold and L. Penengo, "RNF168 promotes noncanonical K27 ubiquitination to signal DNA damage.", *Cell reports,* vol. 10, no. 2, pp. 226-238, 2015.

[46] J. Liu, C. Han, B. Xie, Y. Wu, S. Liu, K. Chen, M. Xia, Y. Zhang, L. Song, Z. Li, T. Zhang, F. Ma, Q. Wang, J. Wang, K. Deng, Y. Zhuang, X. Wu, Y. Yu, T. Xu and X. Cao, "Rhbdd3 controls autoimmunity by suppressing the production of IL-6 by dendritic cells via K27-linked ubiquitination of the regulator NEMO.", *Nature immunology,* vol. 15, no. 7, pp. 612-622, 2014.

[47] E. S. Johnson, P. C. Ma, I. M. Ota and A. Varshavsky, "A proteolytic pathway that recognizes ubiquitin as a degradation signal.", *The Journal of biological chemistry,* vol. 270, no. 29, pp. 17442-17456, 1995.

[48] F. C. Nucifora, L. G. Nucifora, C.-H. Ng, N. Arbez, Y. Guo, E. Roby, V. Shani, S. Engelender, D. Wei, X.-F. Wang, T. Li, D. J. Moore, O. Pletnikova, J. C. Troncoso, A. Sawa, T. M. Dawson, W. Smith, K.-L. Lim and C. A. Ross, "Ubiqutination via K27 and K29 chains signals aggregation and neuronal protection of LRRK2 by WSB1.", *Nature communications,* vol. 7, p. 11792, 2016.

[49] W.-C. Yuan, Y.-R. Lee, S.-Y. Lin, L.-Y. Chang, Y. P. Tan, C.-C. Hung, J.-C. Kuo, C.-H. Liu, M.-Y. Lin, M. Xu, Z. J. Chen and R.-H. Chen, "K33-Linked Polyubiquitination of Coronin 7 by Cul3-KLHL20 Ubiquitin E3 Ligase Regulates Protein Trafficking.", *Molecular cell,* vol. 54, no. 4, pp. 586-600, 2014.

[50] A. Ordureau, S. A. Sarraf, D. M. Duda, J.-M. Heo, M. P. Jedrychowski, V. O. Sviderskiy, J. L. Olszewski, J. T. Koerber, T. Xie, S. A. Beausoleil, J. A. Wells, S. P. Gygi, B. A. Schulman and J. W. Harper, "Quantitative proteomics reveal a feedforward mechanism for mitochondrial PARKIN translocation and ubiquitin chain synthesis.", *Molecular cell,* vol. 56, no. 3, pp. 360-375, 2014.

6. References

[51] S. A. Sarraf, M. Raman, V. Guarani-Pereira, M. E. Sowa, E. L. Huttlin, S. P. Gygi and J. W. Harper, "Landscape of the PARKIN-dependent ubiquitylome in response to mitochondrial depolarization.", *Nature,* vol. 496, no. 7445, pp. 372-376, 2013.

[52] N. Shabek, Y. Herman-Bachinsky, S. Buchsbaum, O. Lewinson, M. Haj-Yahya, M. Hejjaoui, H. A. Lashuel, T. Sommer, A. Brik and A. Ciechanover, "The size of the proteasomal substrate determines whether its degradation will be mediated by mono- or polyubiquitylation.", *Mol Cell,* vol. 48, pp. 87-97, 2012.

[53] O. Braten, I. Livneh, T. Ziv, A. Admon, I. Kehat, L. H. Caspi, H. Gonen, B. Bercovich, A. Godzik, S. Jahandideh, L. Jaroszewski, T. Sommer, Y. T. Kwon, M. Guharoy, P. Tompa and A. Ciechanover, "Numerous proteins with unique characteristics are degraded by the 26S proteasome following monoubiquitination.", *Proceedings of the National Academy of Sciences of the United States of America,* vol. 113, no. 32, pp. E4639-E4647, 2016.

[54] H. Tsuchiya, D. Burana, F. Ohtake, N. Arai, A. Kaiho, M. Komada, K. Tanaka and Y. Saeki, "Ub-ProT reveals global length and composition of protein ubiquitylation in cells.", *Nature communications,* vol. 9, no. 1, p. 524, 2018.

[55] C. H. Emmerich, A. Ordureau, S. Strickson, J. S. C. Arthur, P. G. A. Pedrioli, D. Komander and P. Cohen, "Activation of the canonical IKK complex by K63/M1-linked hybrid ubiquitin chains.", *Proceedings of the National Academy of Sciences of the United States of America,* vol. 110, no. 38, pp. 15247-15252, 2013.

[56] I. E. Wertz, K. Newton, D. Seshasayee, S. Kusam, C. Lam, J. Zhang, N. Popovych, E. Helgason, A. Schoeffler, S. Jeet, N. Ramamoorthi, L. Kategaya, R. J. Newman, K. Horikawa, D. Dugger, W. Sandoval, S. Mukund, A. Zindal, F. Martin, C. Quan, J. Tom, W. J. Fairbrother, M. Townsend, S. Warming, J. DeVoss, J. Liu, E. Dueber, P. Caplazi, W. P. Lee, C. C. Goodnow, M. Balazs, K. Yu, G. Kolumam and V. M. Dixit, "Phosphorylation and linear ubiquitin direct A20 inhibition of inflammation.", *Nature,* vol. 528, no. 7582, pp. 370-375, 2015.

[57] H.-J. Meyer and M. Rape, "Enhanced protein degradation by branched ubiquitin chains.", *Cell,* vol. 157, pp. 910-921, 2014.

[58] F. Ohtake, Y. Saeki, S. Ishido, J. Kanno and K. Tanaka, "The K48-K63 Branched Ubiquitin Chain Regulates NF-kB Signaling.", *Mol Cell,* vol. 64, no. 2, pp. 251-266, 2016.

[59] F. Ohtake, H. Tsuchiya, Y. Saeki and K. Tanaka, "K63 ubiquitylation triggers proteasomal degradation by seeding branched ubiquitin chains.", *Proceedings of the National Academy of Sciences of the United States of America,* vol. 115, no. 7, pp. E1401-E1408, 2018.

[60] M. A. Nakasone, N. Livnat-Levanon, M. H. Glickman, R. E. Cohen and D. Fushman, "Mixed-linkage ubiquitin chains send mixed messages.", *Structure,* vol. 21, pp. 727-740, 2013.

[61] K. E. Sloper-Mould, J. C. Jemc, C. M. Pickart and L. Hicke, "Distinct functional surface regions on ubiquitin.", *The Journal of biological chemistry,* vol. 276, no. 32, pp. 30483-30489, 2001.

[62] S. Vijay-Kumar, C. E. Bugg and W. J. Cook, "Structure of ubiquitin refined at 1.8 A resolution.", *Journal of molecular biology,* vol. 194, no. 3, pp. 531-544, 1987.

[63] J. T. Biel, M. C. Thompson, C. N. Cunningham, J. E. Corn and J. S. Fraser, "Flexibility and Design: Conformational Heterogeneity along the Evolutionary Trajectory of a Redesigned Ubiquitin.", *Structure (London, England: 1993),* vol. 25, no. 5, pp. 739-749, 2017.

[64] O. F. Lange, N.-A. Lakomek, C. Farès, G. F. Schröder, K. F. A. Walter, S. Becker, J. Meiler, H. Grubmüller, C. Griesinger and B. L. Groot, "Recognition dynamics up to microseconds revealed from an RDC-derived ubiquitin ensemble in solution.", *Science (New York, N.Y.),* vol. 320, no. 5882, pp. 1471-1475, 2008.

[65] C. A. Castañeda, E. K. Dixon, O. Walker, A. Chaturvedi, M. A. Nakasone, J. E. Curtis, M. R. Reed, S. Krueger, T. A. Cropp and D. Fushman, "Linkage via K27 Bestows Ubiquitin Chains with Unique Properties among Polyubiquitins.", *Structure (London, England: 1993),* vol. 24, no. 3, pp. 423-436, 2016.

[66] W. J. Cook, L. C. Jeffrey, M. Carson, Z. Chen and C. M. Pickart, “Structure of a diubiquitin conjugate and a model for interaction with ubiquitin conjugating enzyme (E2).”, *The Journal of biological chemistry,* vol. 267, no. 23, pp. 16467-16471, 1992.

[67] A. Bremm, S. M. V. Freund and D. Komander, “Lys11-linked ubiquitin chains adopt compact conformations and are preferentially hydrolyzed by the deubiquitinase Cezanne.”, *Nature structural & molecular biology,* vol. 17, no. 8, pp. 939-947, 2010.

[68] M. K. Hospenthal, S. M. V. Freund and D. Komander, "Assembly, analysis and architecture of atypical ubiquitin chains.," *Nat Struct Mol Biol,* vol. 20, pp. 555-565, 2013.

[69] M. A. Michel, P. R. Elliott, K. N. Swatek, M. Simicek, J. N. Pruneda, J. L. Wagstaff, S. M. V. Freund and D. Komander, “Assembly and Specific Recognition of K29- and K33-Linked Polyubiquitin.”, *Mol Cell,* vol. 58, no. 1, pp. 95-109, 2015.

[70] T. Hirano, O. Serve, M. Yagi-Utsumi, E. Takemoto, T. Hiromoto, T. Satoh, T. Mizushima and K. Kato, “Conformational dynamics of wild-type Lys-48-linked diubiquitin in solution.”, *The Journal of biological chemistry,* vol. 286, no. 43, pp. 37496-37502, 2011.

[71] Y. Ye, G. Blaser, M. H. Horrocks, M. J. Ruedas-Rama, S. Ibrahim, A. A. Zhukov, A. Orte, D. Klenerman, S. E. Jackson and D. Komander, “Ubiquitin chain conformation regulates recognition and activity of interacting proteins.”, *Nature,* vol. 492, no. 7428, pp. 266-270, 2012.

[72] Y. Wang, C. Tang, E. Wang and J. Wang, “PolyUbiquitin chain linkage topology selects the functions from the underlying binding landscape.”, *PLoS Comput Biol,* vol. 10, p. e1003691, 2014.

[73] A. M. Weissman, “Themes and variations on ubiquitylation.”, *Nature reviews. Molecular cell biology,* vol. 2, no. 3, pp. 169-178, 2001.

[74] I. Dikic, S. Wakatsuki and K. J. Walters, “Ubiquitin-binding domains - from structures to functions.”, *Nat Rev Mol Cell Biol,* vol. 10, pp. 659-671, 2009.

[75] J. M. Winget and T. Mayor, “The diversity of ubiquitin recognition: hot spots and varied specificity.”, *Molecular cell,* vol. 38, no. 5, pp. 627-635, 2010.

[76] X. Ren and J. H. Hurley, “VHS domains of ESCRT-0 cooperate in high-avidity binding to polyubiquitinated cargo.”, *The EMBO journal,* vol. 29, no. 6, pp. 1045-1054, 2010.

[77] A. Cohen, E. Rosenthal and J. M. Shifman, “Analysis of Structural Features Contributing to Weak Affinities of Ubiquitin/Protein Interactions.”, *Journal of molecular biology,* vol. 429, no. 22, pp. 3353-3362, 2017.

[78] L. Hicke, H. L. Schubert and C. P. Hill, “Ubiquitin-binding domains.”, *Nature reviews. Molecular cell biology,* vol. 6, no. 8, pp. 610-621, 2005.

[79] J. J. Sims, A. Haririnia, B. C. Dickinson, D. Fushman and R. E. Cohen, “Avid interactions underlie the Lys63-linked polyubiquitin binding specificities observed for UBA domains.”, *Nat Struct Mol Biol,* vol. 16, pp. 883-889, 2009.

[80] T. Wang, L. Yin, E. M. Cooper, M.-Y. Lai, S. Dickey, C. M. Pickart, D. Fushman, K. D. Wilkinson, R. E. Cohen and C. Wolberger, “Evidence for bidentate substrate binding as the basis for the K48 linkage specificity of otubain 1.”, *J Mol Biol,* vol. 386, pp. 1011-1023, 2009.

[81] S. Raasi, R. Varadan, D. Fushman and C. M. Pickart, “Diverse polyubiquitin interaction properties of ubiquitin-associated domains.”, *Nat Struct Mol Biol,* vol. 12, pp. 708-714, 2005.

[82] L. Pastushok, T. F. Moraes, M. J. Ellison and W. Xiao, “A single Mms2 "key" residue insertion into a Ubc13 pocket determines the interface specificity of a human Lys63 ubiquitin conjugation complex.”, *The Journal of biological chemistry,* vol. 280, no. 18, pp. 17891-17900, 2005.

[83] Y.-S. Choi, K. Wu, K. Jeong, D. Lee, Y. H. Jeon, B.-S. Choi, Z.-Q. Pan, K.-S. Ryu and C. Cheong, “The human Cdc34 carboxyl terminus contains a non-covalent ubiquitin binding activity that contributes to SCF-dependent ubiquitination.”, *J Biol Chem,* vol. 285, pp. 17754-17762, 2010.

[84] K. Bagola, M. von Delbrück, G. Dittmar, M. Scheffner, I. Ziv, M. H. Glickman, A. Ciechanover and T. Sommer, "Ubiquitin binding by a CUE domain regulates ubiquitin chain formation by ERAD E3 ligases.", *Mol Cell,* vol. 50, pp. 528-539, 2013.

[85] K. A. Swanson, L. Hicke and I. Radhakrishnan, "Structural basis for monoubiquitin recognition by the Ede1 UBA domain.", *Journal of molecular biology,* vol. 358, no. 3, pp. 713-724, 2006.

[86] R. S. Kang, C. M. Daniels, S. A. Francis, S. C. Shih, W. J. Salerno, L. Hicke and I. Radhakrishnan, "Solution structure of a CUE-ubiquitin complex reveals a conserved mode of ubiquitin binding.", *Cell,* vol. 113, no. 5, pp. 621-630, 2003.

[87] I. Lee and H. Schindelin, "Structural insights into E1-catalyzed ubiquitin activation and transfer to conjugating enzymes.", *Cell,* vol. 134, no. 2, pp. 268-278, 2008.

[88] D. Rotin and S. Kumar, "Physiological functions of the HECT family of ubiquitin ligases.", *Nature reviews. Molecular cell biology,* vol. 10, no. 6, pp. 398-409, 2009.

[89] D. M. Wenzel, A. Lissounov, P. S. Brzovic and R. E. Klevit, "UBCH7 reactivity profile reveals parkin and HHARI to be RING/HECT hybrids.", *Nature,* vol. 474, no. 7349, pp. 105-108, 2011.

[90] R. J. Deshaies and C. A. P. Joazeiro, "RING domain E3 ubiquitin ligases.", *Annual review of biochemistry,* vol. 78, pp. 399-434, 2009.

[91] A. Weber, I. Cohen, O. Popp, G. Dittmar, Y. Reiss, T. Sommer, T. Ravid and E. Jarosch, "Sequential Poly-ubiquitylation by Specialized Conjugating Enzymes Expands the Versatility of a Quality Control Ubiquitin Ligase.", *Molecular cell,* vol. 63, no. 5, pp. 827-839, 2016.

[92] K.-C. Pao, N. T. Wood, A. Knebel, K. Rafie, M. Stanley, P. D. Mabbitt, R. Sundaramoorthy, K. Hofmann, D. M. F. Aalten and S. Virdee, "Activity-based E3 ligase profiling uncovers an E3 ligase with esterification activity.", *Nature,* vol. 556, no. 7701, pp. 381-385, 2018.

[93] M. D. Stewart, T. Ritterhoff, R. E. Klevit and P. S. Brzovic, "E2 enzymes: more than just middle men.", *Cell Res*, vol. 26, no. 4, pp. 423-440 2016.

[94] B. Sarcevic, A. Mawson, R. T. Baker and R. L. Sutherland, "Regulation of the ubiquitin-conjugating enzyme hHR6A by CDK-mediated phosphorylation.", *The EMBO journal,* vol. 21, no. 8, pp. 2009-2018, 2002.

[95] A. Plechanovová, E. G. Jaffray, M. H. Tatham, J. H. Naismith and R. T. Hay, "Structure of a RING E3 ligase and ubiquitin-loaded E2 primed for catalysis.", *Nature,* vol. 489, no. 7414, pp. 115-120, 2012.

[96] I. Valimberti, M. Tiberti, M. Lambrughi, B. Sarcevic and E. Papaleo, "E2 superfamily of ubiquitin-conjugating enzymes: constitutively active or activated through phosphorylation in the catalytic cleft.", *Scientific reports,* vol. 5, p. 14849, 2015.

[97] J. N. Pruneda, K. E. Stoll, L. J. Bolton, P. S. Brzovic and R. E. Klevit, "Ubiquitin in motion: structural studies of the ubiquitin-conjugating enzyme∼ubiquitin conjugate.", *Biochemistry,* vol. 50, no. 10, pp. 1624-1633, 2011.

[98] J. N. Pruneda, P. J. Littlefield, S. E. Soss, K. A. Nordquist, W. J. Chazin, P. S. Brzovic and R. E. Klevit, "Structure of an E3:E2 Ub complex reveals an allosteric mechanism shared among RING/U-box ligases.", *Molecular cell,* vol. 47, no. 6, pp. 933-942, 2012.

[99] K. E. Wickliffe, S. Lorenz, D. E. Wemmer, J. Kuriyan and M. Rape, "The mechanism of linkage-specific ubiquitin chain elongation by a single-subunit E2.," *Cell,* vol. 144, pp. 769-781, 2011.

[100] R. M. Hofmann and C. M. Pickart, "*In vitro* assembly and recognition of Lys-63 polyubiquitin chains.", *The Journal of biological chemistry,* vol. 276, no. 30, pp. 27936-27943, 2001.

[101] T. Ravid and M. Hochstrasser, "Autoregulation of an E2 enzyme by ubiquitin-chain assembly on its catalytic residue.", *Nature cell biology,* vol. 9, no. 4, pp. 422-427, 2007.

[102] T. Biederer, C. Volkwein and T. Sommer, “Role of Cue1p in ubiquitination and degradation at the ER surface.”, *Science (New York, N.Y.),* vol. 278, no. 5344, pp. 1806-1809, 1997.

[103] Z. Kostova, J. Mariano, S. Scholz, C. Koenig and A. M. Weissman, “A Ubc7p-binding domain in Cue1p activates ER-associated protein degradation.”, *Journal of cell science,* vol. 122, no. 9, pp. 1374-1381, 2009.

[104] R. Das, J. Mariano, Y. C. Tsai, R. C. Kalathur, Z. Kostova, J. Li, S. G. Tarasov, R. L. McFeeters, A. S. Altieri, X. Ji, R. A. Byrd and A. M. Weissman, “Allosteric activation of E2-RING finger-mediated ubiquitylation by a structurally defined specific E2-binding region of gp78.”, *Molecular cell,* vol. 34, no. 6, pp. 674-685, 2009.

[105] N. Merkley and G. S. Shaw, “Solution structure of the flexible class II ubiquitin-conjugating enzyme Ubc1 provides insights for polyubiquitin chain assembly.”, *J Biol Chem,* vol. 279, pp. 47139-47147, 2004.

[106] B. M. Kus, C. E. Caldon, R. Andorn-Broza and A. M. Edwards, “Functional interaction of yeast SCF complexes with a set of yeast E2 enzymes *in vitro*.”, *Proteins,* vol. 54, pp. 455-467, 2004.

[107] W. Seufert, J. P. McGrath and S. Jentsch, “UBC1 encodes a novel member of an essential subfamily of yeast ubiquitin-conjugating enzymes involved in protein degradation.”, *EMBO J,* vol. 9, pp. 4535-4541, 1990.

[108] R. Hodgins, C. Gwozd, T. Arnason, M. Cummings and M. J. Ellison, “The tail of a ubiquitin-conjugating enzyme redirects multi-ubiquitin chain synthesis from the lysine 48-linked configuration to a novel nonlysine-linked form.”, *J Biol Chem,* vol. 271, pp. 28766-28771, 1996.

[109] R. C. Meena, S. Thakur, S. Nath and A. Chakrabarti, “Tolerance to thermal and reductive stress in Saccharomyces cerevisiae is amenable to regulation by phosphorylation-dephosphorylation of ubiquitin conjugating enzyme 1 (Ubc1) S97 and S115.”, *Yeast,* vol. 28, pp. 783-793, 2011.

[110] M. C. Rodrigo-Brenni and D. O. Morgan, “Sequential E2s drive polyubiquitin chain assembly on APC targets.”, *Cell,* vol. 130, pp. 127-139, 2007.

[111] K. E. Stoll, P. S. Brzovic, T. N. Davis and R. E. Klevit, “The essential Ubc4/Ubc5 function in yeast is HECT E3-dependent, and RING E3-dependent pathways require only monoubiquitin transfer by Ubc4.”, *J Biol Chem,* vol. 286, pp. 15165-15170, 2011.

[112] J. Lim and Z. Yue, “Neuronal aggregates: formation, clearance, and spreading.”, *Developmental cell,* vol. 32, no. 4, pp. 491-501, 2015.

[113] Z. Ortega and J. J. Lucas, “Ubiquitin-proteasome system involvement in Huntington's disease.”, *Frontiers in molecular neuroscience,* vol. 7, p. 77, 2014.

[114] D. D. O. Martin, S. Ladha, D. E. Ehrnhoefer and M. R. Hayden, “Autophagy in Huntington disease and huntingtin in autophagy.”, *Trends in neurosciences,* vol. 38, no. 1, pp. 26-35, 2015.

[115] Y. Bae, S. H. Jung, G.-Y. Kim, H. Rhim and S. Kang, “Hip2 ubiquitin-conjugating enzyme overcomes radiation-induced G2/M arrest.”, *Biochimica et biophysica acta,* vol. 1833, no. 12, pp. 2911-2921, 2013.

[116] M. A. Kalchman, R. K. Graham, G. Xia, H. B. Koide, J. G. Hodgson, K. C. Graham, Y. P. Goldberg, R. D. Gietz, C. M. Pickart and M. R. Hayden, “Huntingtin is ubiquitinated and interacts with a specific ubiquitin-conjugating enzyme.”, *The Journal of biological chemistry,* vol. 271, no. 32, pp. 19385-19394, 1996.

[117] R. Pril, D. F. Fischer, R. A. C. Roos and F. W. Leeuwen, “Ubiquitin-conjugating enzyme E2-25K increases aggregate formation and cell death in polyglutamine diseases,” *Molecular and Cellular Neuroscience,* vol. 34, pp. 10-19, 2007.

[118] A. Yu, Y. Shibata, B. Shah, B. Calamini, D. C. Lo and R. I. Morimoto, “Protein aggregation can inhibit clathrin-mediated endocytosis by chaperone competition.”, *Proceedings of the National Academy of Sciences of the United States of America,* vol. 111, no. 15, pp. E1481-E1490, 2014.

[119] C. Hetz, “The unfolded protein response: controlling cell fate decisions under ER stress and beyond.”, *Nature reviews. Molecular cell biology,* vol. 13, no. 2, pp. 89-102, 2012.

[120] C. Hetz and B. Mollereau, “Disturbance of endoplasmic reticulum proteostasis in neurodegenerative diseases.”, *Nature reviews. Neuroscience,* vol. 15, no. 4, pp. 233-249, 2014.

[121] J. W. Brewer and J. A. Diehl, “PERK mediates cell-cycle exit during the mammalian unfolded protein response.”, *Proceedings of the National Academy of Sciences of the United States of America,* vol. 97, no. 23, pp. 12625-12630, 2000.

[122] M. K. Rout, B. L. Lee, A. Lin, W. Xiao and L. Spyracopoulos, “Active Site Gate Dynamics Modulate the Catalytic Activity of the Ubiquitination Enzyme E2-25K.”, *Scientific reports,* vol. 8, no. 1, p. 7002, 2018.

[123] M. C. Rodrigo-Brenni, S. A. Foster and D. O. Morgan, “Catalysis of lysine 48-specific ubiquitin chain assembly by residues in E2 and ubiquitin.”, *Mol Cell,* vol. 39, pp. 548-559, 2010.

[124] A. J. Middleton and C. L. Day, “The molecular basis of lysine 48 ubiquitin chain synthesis by Ube2K.”, *Scientific reports,* vol. 5, p. 16793, 2015.

[125] N. Merkley, K. R. Barber and G. S. Shaw, “Ubiquitin manipulation by an E2 conjugating enzyme using a novel covalent intermediate.”, *J Biol Chem,* vol. 280, pp. 31732-31738, 2005.

[126] R. C. Wilson, S. P. Edmondson, J. W. Flatt, K. Helms and P. D. Twigg, “The E2-25K ubiquitin-associated (UBA) domain aids in polyubiquitin chain synthesis and linkage specificity.”, *Biochemical and biophysical research communications,* vol. 405, no. 4, pp. 662-666, 2011.

[127] J. R. Girard, J. L. Tenthorey and D. O. Morgan, “An E2 Accessory Domain Increases Affinity for the Anaphase-Promoting Complex and Ensures E2 Competition.”, *J Biol Chem,* vol. 290, no. 40, pp. 24614-24625, 2015.

[128] S. Liu, Y. Chen, J. Li, T. Huang, S. Tarasov, A. King, A. M. Weissman, R. A. Byrd and R. Das, “Promiscuous interactions of gp78 E3 ligase CUE domain with polyubiquitin chains.”, *Structure (London, England: 1993),* vol. 20, no. 12, pp. 2138-2150, 2012.

[129] R. C. Wilson, R. C. Hughes, J. W. Flatt, E. J. Meehan, J. D. Ng and P. D. Twigg, “Structure of full-length ubiquitin-conjugating enzyme E2-25K (huntingtin-interacting protein 2).”, *Acta crystallographica. Section F, Structural biology and crystallization communications,* vol. 65, no. 5, pp. 440-444, 2009.

[130] S. Ko, G. B. Kang, S. M. Song, J.-G. Lee, D. Y. Shin, J.-H. Yun, Y. Sheng, C. Cheong, Y. H. Jeon, Y.-K. Jung, C. H. Arrowsmith, G. V. Avvakumov, S. Dhe-Paganon, Y. J. Yoo, S. H. Eom and W. Lee, “Structural basis of E2-25K/UBB+1 interaction leading to proteasome inhibition and neurotoxicity.”, *The Journal of biological chemistry,* vol. 285, no. 46, pp. 36070-36080, 2010.

[131] J.-G. Lee, H.-S. Youn, J. Y. Kang, S.-Y. Park, A. Kidera, Y. J. Yoo and S. H. Eom, “Crystal structure of the Ube2K/E2-25K and K48-linked di-ubiquitin complex provides structural insight into the mechanism of K48-specific ubiquitin chain synthesis.”, *Biochemical and biophysical research communications,* vol. 506, no. 1, pp. 102-107, 2018.

[132] G. Kozlov, L. Nguyen, T. Lin, G. De Crescenzo, M. Park and K. Gehring, “Structural basis of ubiquitin recognition by the ubiquitin-associated (UBA) domain of the ubiquitin ligase EDD.”, *The Journal of biological chemistry,* vol. 282, no. 49, pp. 35787-35795, 2007.

[133] S. Michielssens, J. H. Peters, D. Ban, S. Pratihar, D. Seeliger, M. Sharma, K. Giller, T. M. Sabo, S. Becker, D. Lee, C. Griesinger and B. L. Groot, “A designed conformational shift to control protein binding specificity.”, *Angewandte Chemie (International ed. in English),* vol. 53, no. 39, pp. 10367-10371, 2014.

[134] M. V. Shapovalov and R. L. Dunbrack, “A smoothed backbone-dependent rotamer library for proteins derived from adaptive kernel density estimates and regressions.”, *Structure (London, England: 1993),* vol. 19, no. 6, pp. 844-858, 2011.

[135] F. C. Streich Jr and C. D. Lima, “Capturing a substrate in an activated RING E3/E2--SUMO complex,” *Nature,* vol. 536, pp. 304-308, 2016.

[136] M. A. Michel, D. Komander and P. R. Elliott, “Enzymatic Assembly of Ubiquitin Chains.”, *Methods in molecular biology (Clifton, N.J.),* vol. 1844, pp. 73-84, 2018.

[137] K. S. Hamilton, M. J. Ellison, K. R. Barber, R. S. Williams, J. T. Huzil, S. McKenna, C. Ptak, M. Glover and G. S. Shaw, “Structure of a conjugating enzyme-ubiquitin thiolester intermediate reveals a novel role for the ubiquitin tail.”, *Structure (London, England: 1993),* vol. 9, no. 10, pp. 897-904, 2001.

[138] P. Beaudette, O. Popp and G. Dittmar, “Proteomic techniques to probe the ubiquitin landscape.”, *Proteomics,* vol. 16, no. 2, pp. 273-287, 2016.

[139] F. Ohtake and H. Tsuchiya, “The emerging complexity of ubiquitin architecture.”, *Journal of biochemistry,* vol. 161, no. 2, pp. 125-133, 2017.

[140] U. H. Toprak, L. C. Gillet, A. Maiolica, P. Navarro, A. Leitner and R. Aebersold, “Conserved peptide fragmentation as a benchmarking tool for mass spectrometers and a discriminating feature for targeted proteomics.”, *Molecular & cellular proteomics: MCP,* vol. 13, no. 8, pp. 2056-2071, 2014.

[141] M. Chen and P. G. Wolynes, “Aggregation landscapes of Huntingtin exon 1 protein fragments and the critical repeat length for the onset of Huntington's disease.”, *Proceedings of the National Academy of Sciences of the United States of America,* vol. 114, no. 17, pp. 4406-4411, 2017.

[142] M. L. Duennwald, S. Jagadish, P. J. Muchowski and S. Lindquist, “Flanking sequences profoundly alter polyglutamine toxicity in yeast.”, *Proceedings of the National Academy of Sciences of the United States of America,* vol. 103, no. 29, pp. 11045-11050, 2006.

[143] E. Branigan, A. Plechanovová, E. G. Jaffray, J. H. Naismith and R. T. Hay, “Structural basis for the RING-catalyzed synthesis of K63-linked ubiquitin chains.”, *Nat Struct Mol Biol,* vol. 22, no. 8, pp. 597-602, 2015.

[144] N. G. Brown, E. R. Watson, F. Weissmann, M. A. Jarvis, R. VanderLinden, C. R. R. Grace, J. J. Frye, R. Qiao, P. Dube, G. Petzold, S. E. Cho, O. Alsharif, J. Bao, I. F. Davidson, J. J. Zheng, A. Nourse, I. Kurinov, J.-M. Peters, H. Stark and B. A. Schulman, "Mechanism of Polyubiquitination by Human Anaphase-Promoting Complex: RING Repurposing for Ubiquitin Chain Assembly.," *Mol Cell,* vol. 56, pp. 246-260, 2014.

[145] S. McKenna, J. Hu, T. Moraes, W. Xiao, M. J. Ellison and L. Spyracopoulos, “Energetics and specificity of interactions within Ub.Uev.Ubc13 human ubiquitin conjugation complexes.”, *Biochemistry,* vol. 42, no. 26, pp. 7922-7930, 2003.

[146] N. Sekiyama, J. Jee, S. Isogai, K.-I. Akagi, T.-H. Huang, M. Ariyoshi, H. Tochio and M. Shirakawa, “NMR analysis of Lys63-linked polyubiquitin recognition by the tandem ubiquitin-interacting motifs of Rap80.”, *Journal of biomolecular NMR,* vol. 52, no. 4, pp. 339-350, 2012.

[147] A. Kelly, K. E. Wickliffe, L. Song, I. Fedrigo and M. Rape, “Ubiquitin chain elongation requires e3-dependent tracking of the emerging conjugate.”, *Mol Cell,* vol. 56, pp. 232-245, 2014.

[148] J. Yoo, T.-S. Lee, B. Choi, M. J. Shon and T.-Y. Yoon, “Observing Extremely Weak Protein-Protein Interactions with Conventional Single-Molecule Fluorescence Microscopy.”, *Journal of the American Chemical Society,* vol. 138, no. 43, pp. 14238-14241, 2016.

[149] Y. Saeki, Y. Tayama, A. Toh-e and H. Yokosawa, “Definitive evidence for Ufd2-catalyzed elongation of the ubiquitin chain through Lys48 linkage.”, *Biochemical and biophysical research communications,* vol. 320, no. 3, pp. 840-845, 2004.

[150] E. Jarosch, C. Taxis, C. Volkwein, J. Bordallo, D. Finley, D. H. Wolf and T. Sommer, "Protein dislocation from the ER requires polyubiquitination and the AAA-ATPase Cdc48.," *Nat Cell Biol,* vol. 4, pp. 134-139, 2002.

[151] R. Ibarra, D. Sandoval, E. K. Fredrickson, R. G. Gardner and G. Kleiger, "The San1 ubiquitin ligase functions preferentially with ubiquitin-conjugating enzyme Ubc1 during protein quality control.," *J Biol Chem,* 2016.

[152] H. Hiraishi, M. Mochizuki and H. Takagi, "Enhancement of stress tolerance in Saccharomyces cerevisiae by overexpression of ubiquitin ligase Rsp5 and ubiquitin-conjugating enzymes.," *Biosci Biotechnol Biochem,* vol. 70, pp. 2762-2765, 2006.

[153] K. P. Bhat, S. Yan, C.-E. Wang, S. Li and X.-J. Li, “Differential ubiquitination and degradation of huntingtin fragments modulated by ubiquitin-protein ligase E3A.”, *Proceedings of the National Academy of Sciences of the United States of America,* vol. 111, no. 15, pp. 5706-5711, 2014.

[154] V. A. Van Voorhis and D. O. Morgan, "Activation of the APC/C Ubiquitin Ligase by Enhanced E2 Efficiency.," *Curr Biol,* vol. 24, no. 13, pp. 1556-1562, 2014.

[155] X. Zhang, A. H. Smits, G. B. A. Tilburg, P. W. T. C. Jansen, M. M. Makowski, H. Ovaa and M. Vermeulen, “An Interaction Landscape of Ubiquitin Signaling.”, *Molecular cell,* vol. 65, no. 5, pp. 941-955, 2017.

[156] K. N. Swatek and D. Komander, “Ubiquitin modifications.”, *Cell research,* vol. 26, no. 4, pp. 399-422, 2016.

[157] D. Finley, E. Ozkaynak and A. Varshavsky, “The yeast polyubiquitin gene is essential for resistance to high temperatures, starvation, and other stresses.”, *Cell,* vol. 48, no. 6, pp. 1035-1046, 1987.

[158] W. Mansour, M. A. Nakasone, M. Delbrück, Z. Yu, D. Krutauz, N. Reis, O. Kleifeld, T. Sommer, D. Fushman and M. H. Glickman, “Disassembly of Lys11 and mixed linkage polyubiquitin conjugates provides insights into function of proteasomal deubiquitinases Rpn11 and Ubp6.”, *The Journal of biological chemistry,* vol. 290, no. 8, pp. 4688-4704, 2015.

[159] D. E. Christensen, P. S. Brzovic and R. E. Klevit, “E2-BRCA1 RING interactions dictate synthesis of mono- or specific polyubiquitin chain linkages.”, *Nature structural \& molecular biology,* vol. 14, no. 10, pp. 941-948, 2007.

[160] C. E. Berndsen and C. Wolberger, “A spectrophotometric assay for conjugation of ubiquitin and ubiquitin-like proteins.”, *Analytical biochemistry,* vol. 418, no. 1, pp. 102-110, 2011.

[161] O. Neuber, E. Jarosch, C. Volkwein, J. Walter and T. Sommer, “Ubx2 links the Cdc48 complex to ER-associated protein degradation.”, *Nature cell biology,* vol. 7, no. 10, pp. 993-998, 2005.

[162] J. Walter, J. Urban, C. Volkwein and T. Sommer, “Sec61p-independent degradation of the tail-anchored ER membrane protein Ubc6p.”, *The EMBO journal,* vol. 20, no. 12, pp. 3124-3131, 2001.

[163] D. G. Gibson, L. Young, R.-Y. Chuang, J. C. Venter, C. A. Hutchison and H. O. Smith, “Enzymatic assembly of DNA molecules up to several hundred kilobases.”, *Nature methods,* vol. 6, no. 5, pp. 343-345, 2009.

[164] M. S. Longtine, A. McKenzie, D. J. Demarini, N. G. Shah, A. Wach, A. Brachat, P. Philippsen and J. R. Pringle, “Additional modules for versatile and economical PCR-based gene deletion and modification in Saccharomyces cerevisiae.”, *Yeast,* vol. 14, pp. 953-961, 1998.

[165] U. Gueldener, J. Heinisch, G. J. Koehler, D. Voss and J. H. Hegemann, “A second set of loxP marker cassettes for Cre-mediated multiple gene knockouts in budding yeast.”, *Nucleic Acids Res,* vol. 30, p. e23, 2002.

[166] E. R. P. Zuiderweg, “Mapping protein-protein interactions in solution by NMR spectroscopy.”, *Biochemistry,* vol. 41, no. 1, pp. 1-7, 2002.

[167] L. Fielding, “NMR methods for the determination of protein-ligand dissociation constants.”, *Current topics in medicinal chemistry,* vol. 3, no. 1, pp. 39-53, 2003.

[168] W. Lee, M. Tonelli and J. L. Markley, “NMRFAM-SPARKY: enhanced software for biomolecular NMR spectroscopy.”, *Bioinformatics (Oxford, England),* vol. 31, no. 8, pp. 1325-1327, 2015.

[169] J. Cox and M. Mann, “MaxQuant enables high peptide identification rates, individualized p.p.b.-range mass accuracies and proteome-wide protein quantification.”, *Nature biotechnology,* vol. 26, no. 12, pp. 1367-1372, 2008.

[170] B. MacLean, D. M. Tomazela, N. Shulman, M. Chambers, G. L. Finney, B. Frewen, R. Kern, D. L. Tabb, D. C. Liebler and M. J. MacCoss, “Skyline: an open source document editor for creating and analyzing targeted proteomics experiments.”, *Bioinformatics (Oxford, England),* vol. 26, no. 7, pp. 966-968, 2010.

6. References

[171] W. Kabsch, “XDS.”, *Acta crystallographica. Section D, Biological crystallography,* vol. 66, no. 2, pp. 125-132, 2010.

[172] P. V. Afonine, R. W. Grosse-Kunstleve, N. Echols, J. J. Headd, N. W. Moriarty, M. Mustyakimov, T. C. Terwilliger, A. Urzhumtsev, P. H. Zwart and P. D. Adams, “Towards automated crystallographic structure refinement with phenix.refine.”, *Acta crystallographica. Section D, Biological crystallography,* vol. 68, no. 4, pp. 352-367, 2012.

[173] P. Emsley, B. Lohkamp, W. G. Scott and K. Cowtan, “Features and development of Coot.”, *Acta crystallographica. Section D, Biological crystallography,* vol. 66, no. 4, pp. 486-501, 2010.

[174] I. W. Davis, A. Leaver-Fay, V. B. Chen, J. N. Block, G. J. Kapral, X. Wang, L. W. Murray, W. B. Arendall, J. Snoeyink, J. S. Richardson and D. C. Richardson, “MolProbity: all-atom contacts and structure validation for proteins and nucleic acids.”, *Nucleic acids research,* vol. 35, Web Server issue, pp. W375-W383, 2007.

[175] E. F. Pettersen, T. D. Goddard, C. C. Huang, G. S. Couch, D. M. Greenblatt, E. C. Meng and T. E. Ferrin, “UCSF Chimera--a visualization system for exploratory research and analysis.”, *Journal of computational chemistry,* vol. 25, no. 13, pp. 1605-1612, 2004.

[176] K. Bagola, M. Mehnert, E. Jarosch and T. Sommer, “Protein dislocation from the ER.”, *Biochim Biophys Acta,* vol. 1808, pp. 925-936, 2011.

[177] D. Komander, F. Reyes-Turcu, J. D. F. Licchesi, P. Odenwaelder, K. D. Wilkinson and D. Barford, “Molecular discrimination of structurally equivalent Lys 63-linked and linear polyubiquitin chains.”, *EMBO reports,* vol. 10, no. 5, pp. 466-473, 2009.

7. Appendix

7.1 Publications and presentations

A. Kniss, D. Schuetz, S. Kazemi, **L. Pluska**, P. E. Spindler, V. V. Rogov, K. Husnjak, I. Dikic, P. Güntert, T. Sommer, T. F. Prisner and V. Dötsch, "Chain Assembly and Disassembly Processes Differently Affect the Conformational Space of Ubiquitin Chains.," *Structure*, vol 26, pp. 249-258, 1 2018.

M. von Delbrück, A. Kniss, V. V. Rogov, **L. Pluska**, K. Bagola, F. Löhr, P. Güntert, T. Sommer and V. Dötsch, "The CUE Domain of Cue1 Aligns Growing Ubiquitin Chains with Ubc7 for Rapid Elongation.," Mol Cell, vol. 62, pp. 918-928, 6 2016.

EMBO Conference on Ubiquitin and SUMO: From molecular mechanisms to system-wide responses (15 – 19 Sept 2017 in Cavtat, Croatia), poster presentation

SignGene Symposium "Ubiquitin: One Traveler, Two Roads", invited speaker

7.2 Selbständigkeitserklärung

Hiermit erkläre ich, die Dissertation selbstständig und nur unter Verwendung der angegebenen Hilfen und Hilfsmittel angefertigt zu haben. Ich habe mich anderwärts nicht um einen Doktorgrad beworben und besitze keinen entsprechenden Doktorgrad. Ich erkläre, dass ich die Dissertation oder Teile davon nicht bereits bei einer anderen wissenschaftlichen Einrichtung eingereicht habe und dass sie dort weder angenommen noch abgelehnt wurde. Ich erkläre die Kenntnisnahme der dem Verfahren zugrunde liegenden Promotionsordnung der Mathematisch-Naturwissenschaftlichen Fakultät I der Humboldt-Universität zu Berlin vom 27. Juni 2012. Weiterhin erkläre ich, dass keine Zusammenarbeit mit gewerblichen Promotionsberaterinnen/Promotionsberatern stattgefunden hat und dass die Grundsätze der Humboldt-Universität zu Berlin zur Sicherung guter wissenschaftlicher Praxis eingehalten wurden.

Berlin, den 07.08.2020

Lukas Pluska

7.3 Acknowledgements

First of all, I would like to express my gratitude to my supervisor Thomas Sommer, who enabled me to conduct my doctoral research, and provided excellent guidance, encouragement and advice.

My thanks also go to Ernst Jarosch for inspiring discussions, ideas as well as teachings and help with yeast genetics. I am particularly grateful for preliminary data on Ubc1 by Katrin Bagola and for providing fantastic initial training. I thank Maximilian von Delbrück for great discussions, sharing of expertise on *in vitro* ubiquitination assays and the fruitful collaboration in joint projects.

Corinna Volkwein and Mandy Mustroph provided excellent technical support, which was greatly appreaciated. I also want to thank all other current and former members of the Sommer lab for creating an exceptionally supportive and friendly work environment. Conducting research can be frustrating and arduous at times and all of you made it so much easier. Thank you, Tim Abel, Maren Berger, Holger Brendebach, Alba Ferri Blazquez, Susanne Fichtner, Sara Knape, Anett Köhler, Christian Lips, Martin Mehnert, Suzuka Nakagawa, Marcel Nowak, Benjamin Sünkel, Anita Waltho, Annika Weber, Robert Welke and Angelika Wittstruck,

Moreover, I would like to express my great appreciation for Brenda Schulman, who invited me to work at the Max Planck Institute in Martinsried, where I spent a very productive and instructive time. To all the members of the Schulman lab, who made my stay so enjoyable – thank you, I really appreciated it.

I would like to offer special thanks to Volker Dötsch, Andreas Kniss, Matthias Selbach, Henrik Zauber, Janine Kirstein and David Krist for great work in collaborative projects.

I thank Alexander Pluska for helping me with his mathematical aptitude in formulating the ubiquitin nomenclature presented in this work, for being a great brother and for always appreciating me. I thank my parents Stefania Kuczera-Pluska and Czarek Pluska for never getting tired of questions, for their efforts and sacrifices in bringing me up and for being an invaluable constant in my life.

I thank my partner Finja Höwe for her love, for her support, for enduring my oddities and for reminding me of light-heartedness, when I occasionally forget about it.